PFC/RR-86-11 DOE/ET-51013-180

Poloidal Field Coil System Design for the Compact Ignition Tokamak, (CIT)

Status Report April 15, 1986

R.J. Thome, Editor

Contributors

Massachusetts Institute of Technology

H.D. Becker
E.S. Bobrov
L. Bromberg
B. Lipschultz
W.R. Mann
D.B. Montgomery
R.D. Pillsbury, Jr.
J.H. Schultz
J.E.C. Williams

Fusion Engineering Design Center

T. Brown
S. Kalsi
J. Mayhall
D. Strickler

Princeton Plasma Physics Laboratory

R. Izzo
S. Jardin
N. Pomphrey

Plasma Fusion Center
Massachusetts Institute of Technology
Cambridge, Massachusetts

Table of Contents

1.0 Introduction

MIT has had the primary responsibility for the PF coil system (WBS G) during the CIT conceptual design. The purpose of this report is to summarize the status of that subsystem design as of April 15, 1986.

Coil locations and currents have been defined in a manner consistent with physics requirements (as of February 21, 1986) and system code selections of radial build dimensions, volt-second, and pulse time requirements (February 12, 1986). Plasma equilibria have been determined for limiter and divertor cases and have driven the design. A design summary is given in Section 2.0 while more detailed discussions are contained in Sections 3.0 through 6.0.

The poloidal field magnet system provides the equilibrium, control and shaping fields for the plasma as well as the flux change which induces plasma current and ohmic heating. In CIT, all of the main coils play an active part in all of these functions. This combined function system consists of ten coaxial coils which are external to the TF coils and symmetrically located with respect to the z=0 plane. Two coils (i.e., PF1 and PF2) comprise the central solenoid stack which is close to the machine axis and six other coils (three pairs: PF3, PF4, and PF5) are located around the TF coil set. PF3-5 are called "ring" coils because their cross-sectional dimensions are relatively small compared with their diameter.

The current scenarios for the coils can be programmed to provide the field null, low fields, and loop voltage pulse required for plasma start-up then the higher fields and flux swing for plasma growth to either a limiter or double null divertor shape and burn.

The coils are liquid nitrogen cooled between pulses and experience a temperature rise during a pulse under essentially adiabatic conditions. They are excited in independently controlled pairs and require peak power and energies per pulse consistent with capabilities at PPPL.

In addition to the main coils external to the TF coils, the PF system also includes six coils (in 3 pairs symmetric wrt z=0) internal to the TF coils for active stabilization and control purposes. These coils can be used to trim the position of the separatrix in a diverted plasma or provide minor adjustments to shape. They are also necessary to provide a radial field to control the natural vertical instability associated with an elongated plasma. In this regard, the vacuum vessel has been determined to be sufficiently well-coupled to the plasma to restrain the vertical motion to the 15 ms time scale. This is sufficiently long

to allow the active coil system to come into play at a reasonable power level.

The electromagnetic loads on all coils are nontrivial, but they are particularly severe for PF1 and PF2, the coils in the solenoid stack near the machine axis. The maximum fields in this coil set are 23.6 T and 21.7 T for the limiter and divertor cases, respectively. These coils are formed from pancakes, each of which is cut from a single laminated plate of Inconel-copper-Inconel. Stress and temperature considerations require that the cross section be about 50% copper, 40% Inconel, and 10% insulation. At the inner turn, the Inconel is at 70-80% of yield, however it is below two-thirds of yield when averaged over the radial build. These levels are within the guidelines accepted for this phase of the conceptual design based on preliminary analyses and experimental data on laminates of this type. It is clear, however, that an extensive program is necessary to verify that operation at these levels is consistent with the desired machine lifetime. These stress levels could be reduced with a modest increase in the central solenoid outer diameter.

Temperature rise in each coil is the other critical design allowable. This is intimately linked to the total cross section and fraction of copper in each coil and was chosen after iterating on likely current profile scenarios for the system to evaluate temperatures, power and energy requirements. For each coil, structural analyses have been performed to show feasibility of the winding and support concepts and interface conditions have been evaluated to determine likely paths for leads and coolant lines.

The compact nature of this machine has forced the use of highly loaded configurations and high design allowables. This, coupled with the natural complexity of a tokamak leads to the requirement for a considerable R and D effort. An outline of the effort is given in Appendix A. It includes tests of winding components, leads, joints, and prototypes for both the central solenoid and a typical ring coil.

In view of recent discussions on possible changes in machine requirements, the impact of selected changes in machine characteristics have been estimated with a parametric code. Results are given in Appendix B and imply that:

1. Changing from a TF coil design with a press to one with a self-supported TF system requires a major radius increase of about 14 cm.

2. Central solenoid stresses can be decreased by 10% or 20% with a net major radius change of about 3 cm or 5 cm, respectively.

3. Additional volt seconds (beyond the change required for increased plasma inductive

V·s) of 1.1 and 2.3 V·s can be achieved with a net major radius change of 3 cm and 5 cm, respectively (note: no change in solenoid stress).

4. Pulse length flattop times can be increased by 1.4, 3.3, and 5 s with an increase in major radius of about 3, 5, and 9 cm, respectively.

2.0 Design Summary

2.1 Functional Requirements

The poloidal field magnet system provides the equilibrium, control and shaping fields for the plasma as well as the flux change which induces plasma current and ohmic heating. In CIT, all of the main coils play an active part in all of these functions. This combined function system consists of ten coaxial coils which are external to the TF coils and symmetrically located with respect to the z=0 plane. They are illustrated in the partial elevation view of the machine in Figure 2.1-1. Two coils (i.e., PF1 and PF2) comprise the central solenoid stack which is close to the machine axis and six other coils (three pairs: PF3, PF4, and PF5) are located around the TF coil set.

In addition to the main coils external to the TF coils, the PF system also includes six coils (in 3 pairs symmetric wrt z=0) internal to the TF coils for active plasma stabilization and control purposes. These coils are labeled I1, I2 and I3 in Figure 2.1-1 and can be used to trim the position of the separatrix in a diverted plasma or provide minor adjustments to shape. They are also necessary to provide a radial field to control the natural vertical instability associated with an elongated plasma.

The current scenarios for the coils can be programmed to provide the field null, low fields, and loop voltage pulse required for plasma start-up and then the higher fields and flux swing for plasma growth to either a limiter or double null divertor shape and burn. The plasma characteristics for these cases are summarized in Table 2.1-1.

Figures 2.1-2 and 2.1-3 show the high beta equilibria for the plasmas in the limiter and divertor cases respectively. In the divertor case the plasma characteristics (e.g., elongation and triangularity) were defined using the 96% flux surface in accordance with guidance from the physics group. The outer surfaces of these plasmas are superimposed in Figure 2.1-4 which also shows the location of the divertor plate profiles and the inner surface of the TF coil.

Figure 2.1-1
Elevation of Core of Machine Showing Poloidal Field Coils 1 – 5 and Internal Coils I1 – I3, [FEDC]

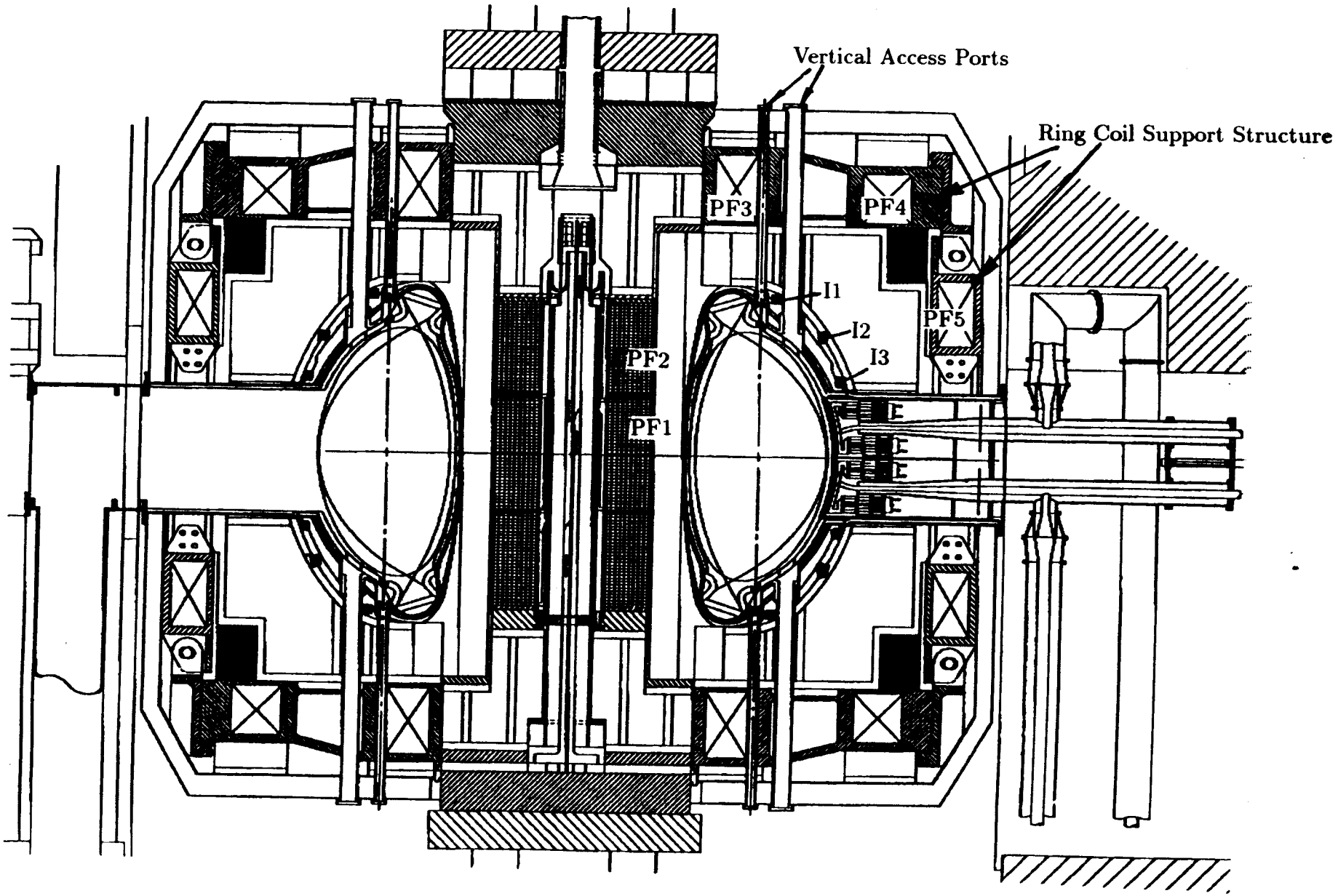

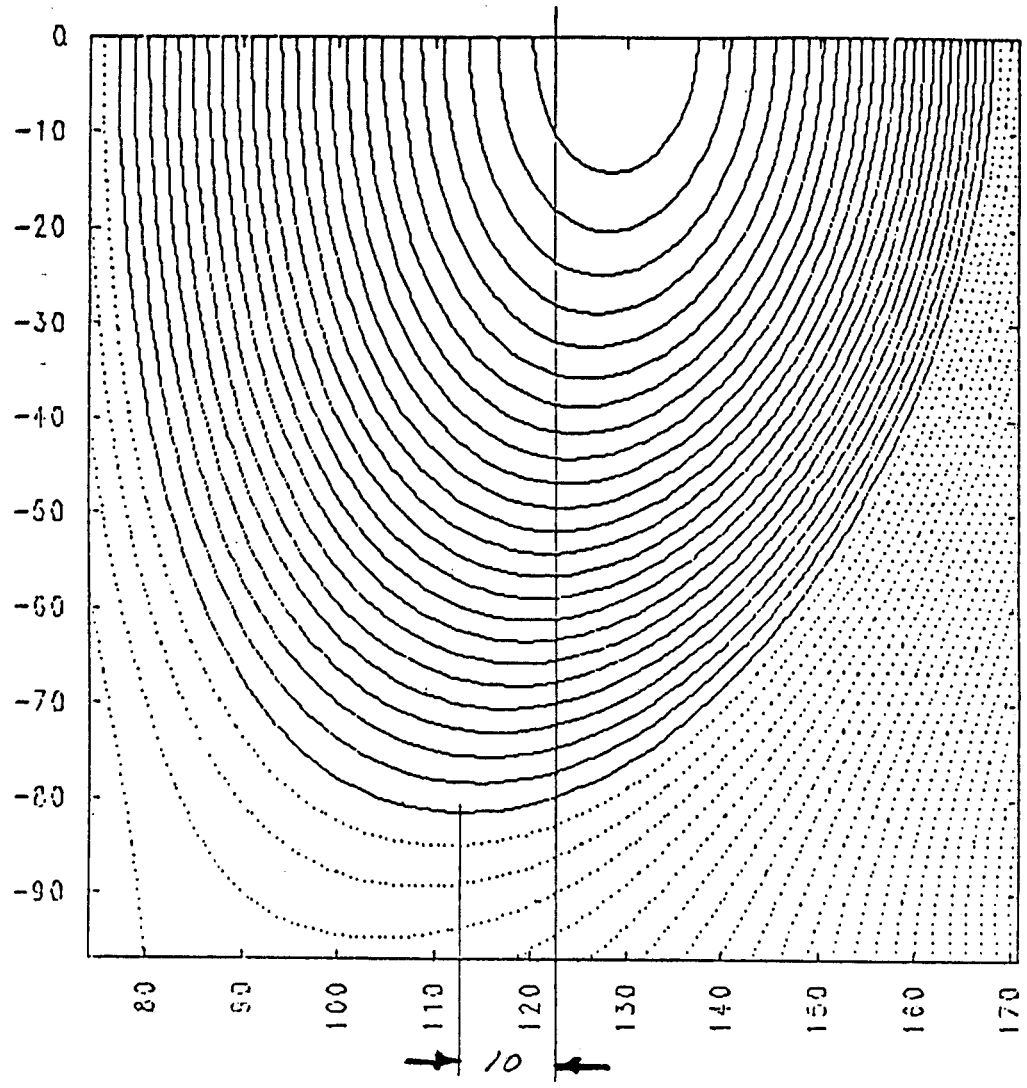

2a=91

b=82

$\frac{b}{a} = \frac{(82)2}{91} = 1.86$

$\delta = \frac{(10)2}{91} = 0.22$

Figure 2.1-2
CIT Limited Plasma (MIT 0306L)

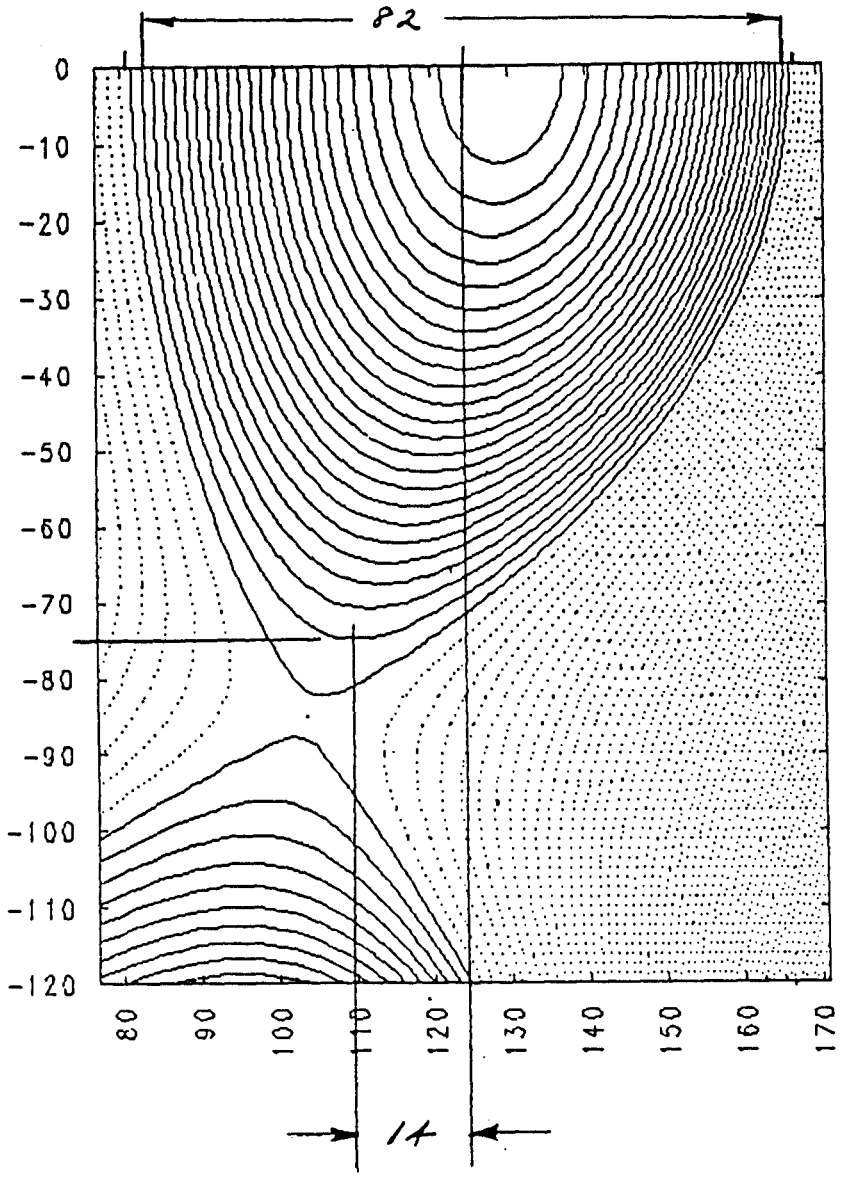

96% Surface:
2a=82
b=75
$\kappa = \frac{b}{a} = 1.83$
$\delta = 0.34$

Figure 2.1-3
CIT Diverted Plasma (MIT 0306D)

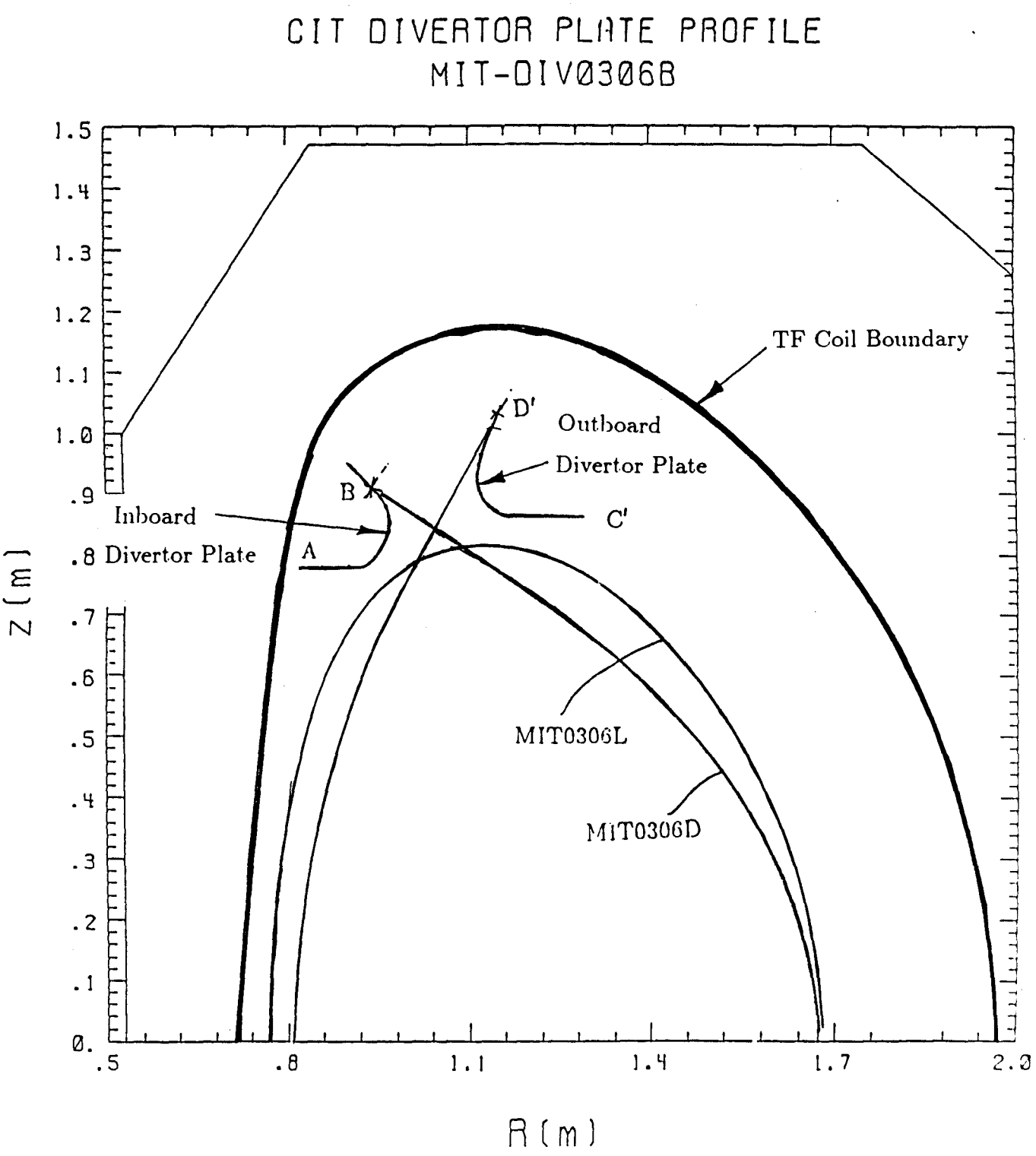

Figure 2.1-4

Superposed Figures of Limited and Diverted Plasma Outer Flux Surfaces with Divertor Plate Profiles (A – B and C′ – D′) and TF Coil Inner Boundary

Table 2.1-1 Plasma Characteristics

	limiter	divertor
major radius, m	1.226	1.241
minor radius, m	0.455	0.41*
plasma current, MA	10	9
elongation	1.8	1.83*
triangularity	0.22	0.34*
B, toroidal, T	10.4	10.3
q, edge	2.68	2.6*
avg beta, %	6.35	6.35
volt-sec reqd.	26.2	24.7
volt-sec available	26.2	25.2

*=evaluated at 96% plasma flux surface

2.2 PF System Characteristics

The coils are liquid-nitrogen cooled between pulses and experience a temperature rise during a pulse under essentially adiabatic conditions. Table 2.2-1 summarizes the location of the main PF coils. It also gives the ampere-turn requirements in each coil to provide the field null at start-up when the system is "fully-cocked" at one end of the required flux-swing. The next two columns give the ampere-turn distribution for the end-of-flattop when the coils are at the other end of the flux-swing and also provide the field distribution for the high beta plasma equilibrium. A comparison of these two columns shows a significant difference for operation in the limiter *vs* the divertor mode.

The coil weights given in the table do not include structure external to the winding pack and indicate a total coil weight of about 67 tonnes. The last three columns provide the estimated liquid-nitrogen requirements for this coil set. As indicated, about 60,000 liters are needed for the initial cooldown from room temperature. A subsequent pulse requires about 6000 liters for the limiter mode and about 11,000 liters for the divertor mode. This implies the more energetic needs for the PF coil set for a divertor pulse which will also be evident from the power supply standpoint.

The coils are excited in independently controlled pairs and require the peak power and energies per pulse outlined in Table 2.2-2.

Table 2.2-1
PF Coil Characteristics

COIL	R_1 (m)	R_2 (m)	Z_1 (m)	Z_2 (m)	START-UP MAT	LIMITER END-OF-BURN MAT	DIVERTOR END-OF-BURN MAT	COIL WEIGHT kG	LN_2 REQUIREMENTS INITIAL COOLDOWN (10^3 ℓ)	LIMITER PULSE (10^3 ℓ)	DIVERTOR PULSE (10^3 ℓ)
PF1	0.259	0.507	0	0.368	- 5.86	7.00	6.03	1760	0.82	0.72	0.43
PF2	0.259	0.507	0.368	1.000	-12.6	9.46	11.8	3020	1.41	0.80	1.41
PF3	0.910	1.189	1.518	1.979	- 7.66	2.46	-10.7	6420	5.00	0.14	2.22
PF4	1.887	2.213	1.517	1.843	2.47	-4.22	7.79	10360	12.70	0.22	1.48
PF5	2.351	2.670	0.795	1.115	- 0.92	7.10	2.62	12180	9.84	1.17	0.10
							10 Coil Total	67480	59.5	6.10	11.3

Table 2.2-2 PF Coil System Peak Power and Energy Requirements

	Limiter	Divertor
Energy, MJ		
Max Magnetic	520	801
Total Joule Losses	990	1830
Max Required	1280	2170
Power, MW		
Positive	429	497
Negative	-1200	-860

The maximum magnetic energy stored occurs during flattop and the maximum energy required is the sum of magnetic energy and joule losses at the end of flattop. Figure 2.2-1 shows the energy flow to the individual coils and to the PF system during a divertor pulse. Note the peak at end of flattop and the fact that PF3 is the largest energy dissipator. This is partly due to the high ampere-turn requirement at this location to form the diverted shape and partly due to the severe space restrictions at this location because of the vertical access port (see Figure 2.1-1).

The power supplied to the system during a divertor pulse is shown in Figure 2.2-2. The large negative spike occurs when the plasma initiation voltage (about 30 V) is provided by a sudden (20 ms) change in flux. This is accomplished by temporarily dissipating stored energy in resistors and is not a load on line power (see section 3.2.1). The figure also shows the instantaneous flow of real and reactive power in the PF system. Requirements for a limiter pulse are somewhat less severe, and are also discussed in a later section.

2.3 Summary of Coil Characteristics

The electromagnetic loads on all coils are nontrivial, but they are particularly severe for PF1 and PF2, the coils in the solenoid stack near the machine axis. The maximum fields in this coil set are 23.6 T and 21.7 T for the limiter and divertor cases, respectively. These coils are illustrated in the elevation view in Figure 2.3 -1. Even though they are excited as two coil sets, three pairs of leads are used for these coils to allow for differences in vertical deflections under load and thermal expansion effects. The lead sections are an integral part of the central stack subassembly and run to the top of the coil set where they mate with leads within a supporting tube which then run to the bottom of the machine to the power supply bus work as shown in Figure 2.1-1.

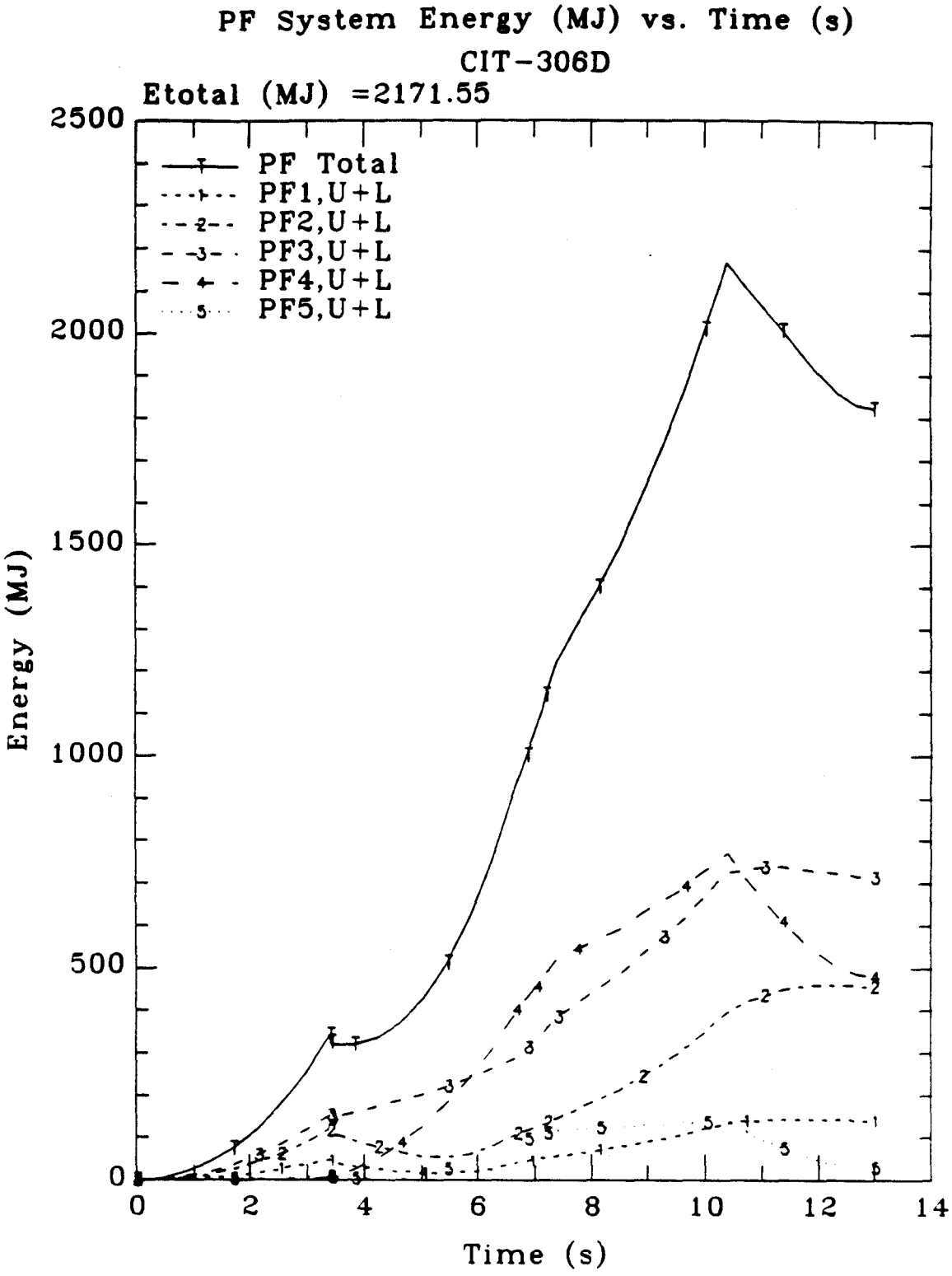

Figure 2.2-1
Energy Flow to the PF Coils for a Divertor Discharge

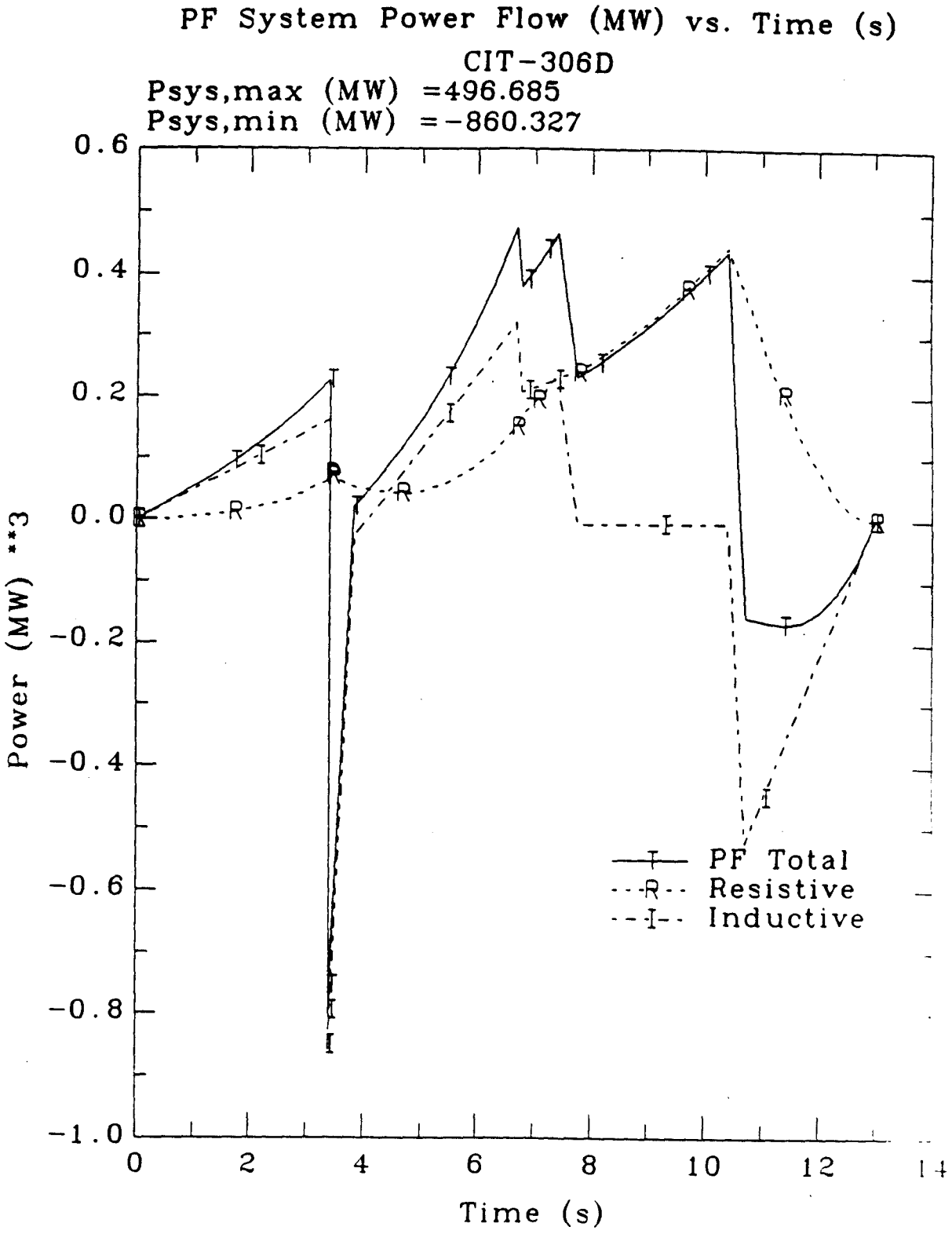

Figure 2.2-2
Power Flow to the PF System During a Divertor Pulse
(R = Resistive; I = Reactive; T = Total)

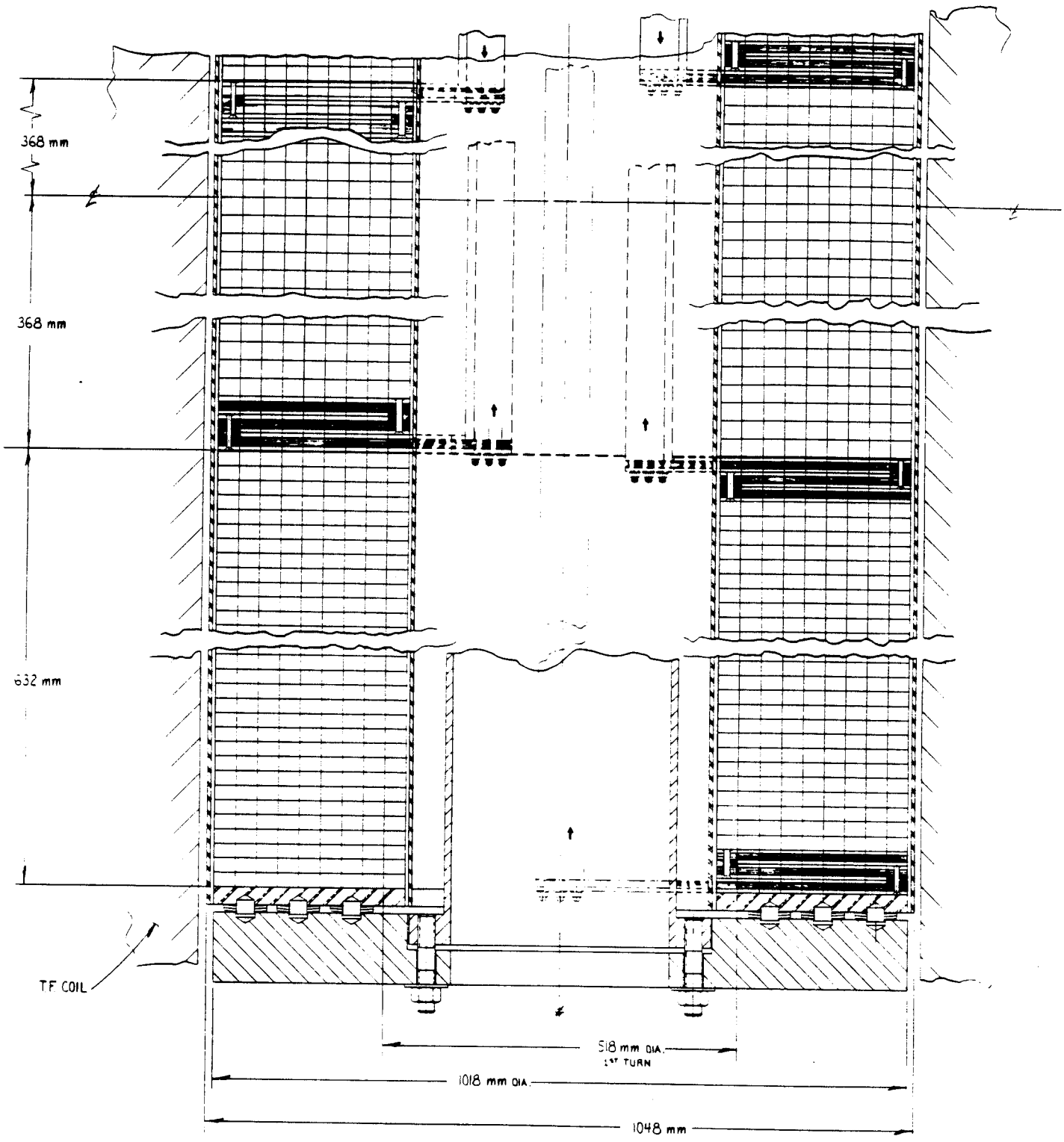

Figure 2.3-1
Central Solenoid Assembly, Cross-Sectional View

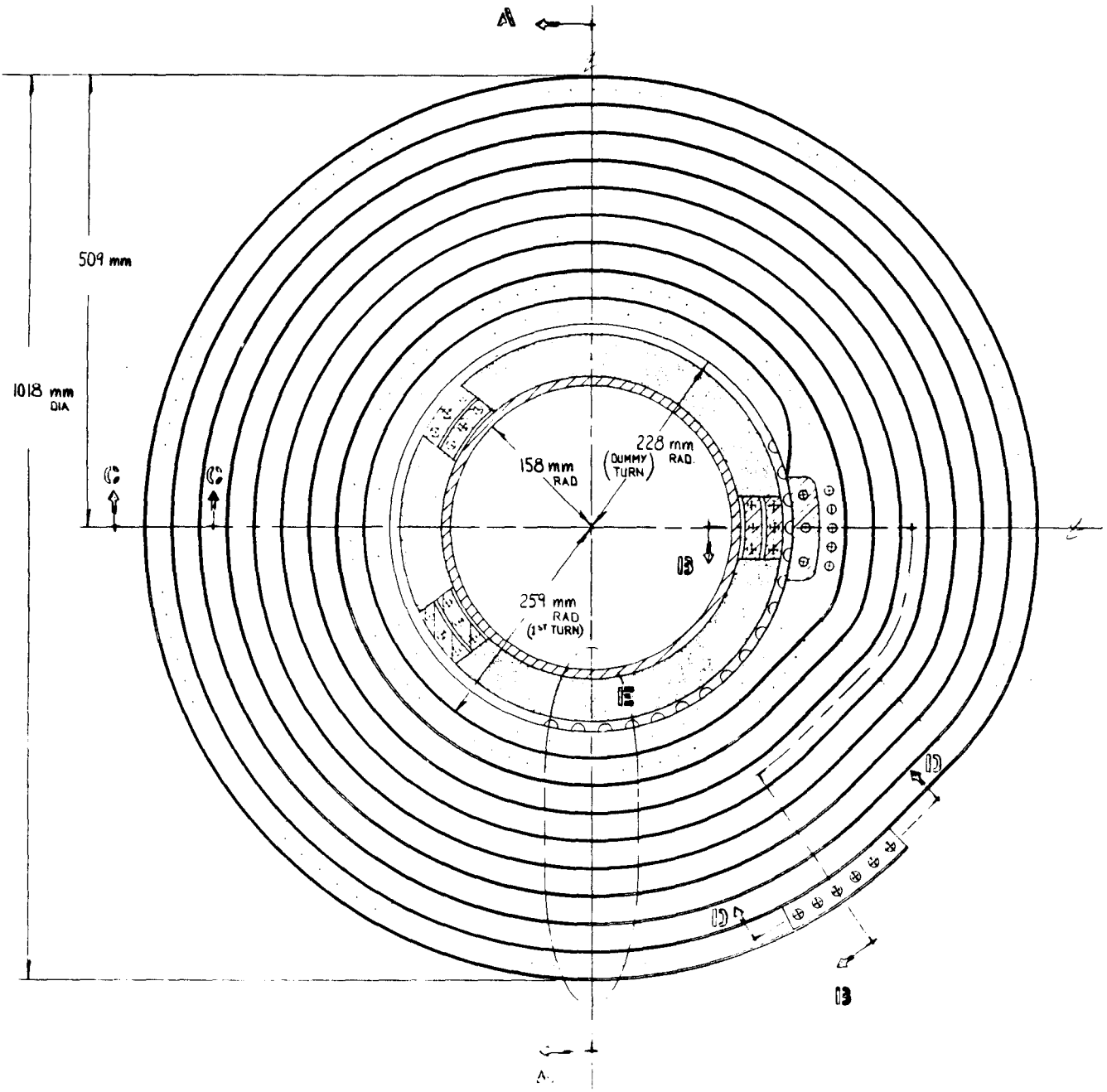

Figure 2.3-2
Pancake Coil – PF1 or PF2

Each pancake in PF1 and PF2 is cut from a single laminated plate of Inconel-copper-Inconel as shown in Figure 2.3-2. Stress and temperature considerations require that the cross section be about 50% copper, 40% Inconel, and 10% insulation. Shear loads at the inside and outside joints are taken in pins. Heat is conducted from inner turns to the inside and to the outside surfaces by copper heat conduits between layers. The outer boundary of the coil is a grooved insulating layer which provides channels for axial liquid nitrogen flow and electrical insulation for the voltage relative to the TF system. There is a one centimeter radial gap between the outside of this layer and the TF coil surface.

A typical ring coil cross section is shown in Figure 2.3-3. Each coil is a double pancake of wide, relatively thin copper conductor with a b-stage epoxy insulation between turns which is cured after winding. A solid insulation sheet exists between the pancakes. Grooved insulation plates, together with a periodically spaced wrap of epoxy-glass, provide ground insulation relative to the case and cooling passages on the coil surface. Liquid nitrogen enters through one manifold, edge cools the conductor in one layer, passes along the outer surface between coil and case to the other layer, and edge cools the second layer before exiting into the other manifold.

The PF coil locations and currents have been determined to satisfy the physics specifications and use high design allowables in areas which have a direct impact on machine size. The central solenoid stack is one example and contains about 40% Inconel so as to be self-supporting. One part of the design procedure involved biasing the flux level for the required volt-second swing so that the solenoid stresses at start-up and at end-of-burn were at approximately the same level.

The PF3 ring coil is copper and is able to carry its in-plane loads without internal reinforcement. PF4 and PF5, on the other hand, are heavily loaded and require a substantial structure for support of their in-plane loads. This is provided by the external steel structure indicated in Figure 2.1-1. This structure is also integrated with the cases for all the ring coils and the TF coil structure to also provide support for the out-of-plane loads on the PF ring coils. The latter are nontrivial and are summarized in Table 2.3-1 which gives the extreme values of the loads on each coil. The time loading of this force component on each coil is also shown and indicates a considerable load cancellation between adjacent coils.

The temperature rise in each coil is the other critical design allowable. This is intimately linked with the total cross section and fraction of copper in each coil and was chosen after iterating on likely current profile scenarios for the system to evaluate temperatures, power and energy requirements. Table 2.3-2 summarizes the temperature in each

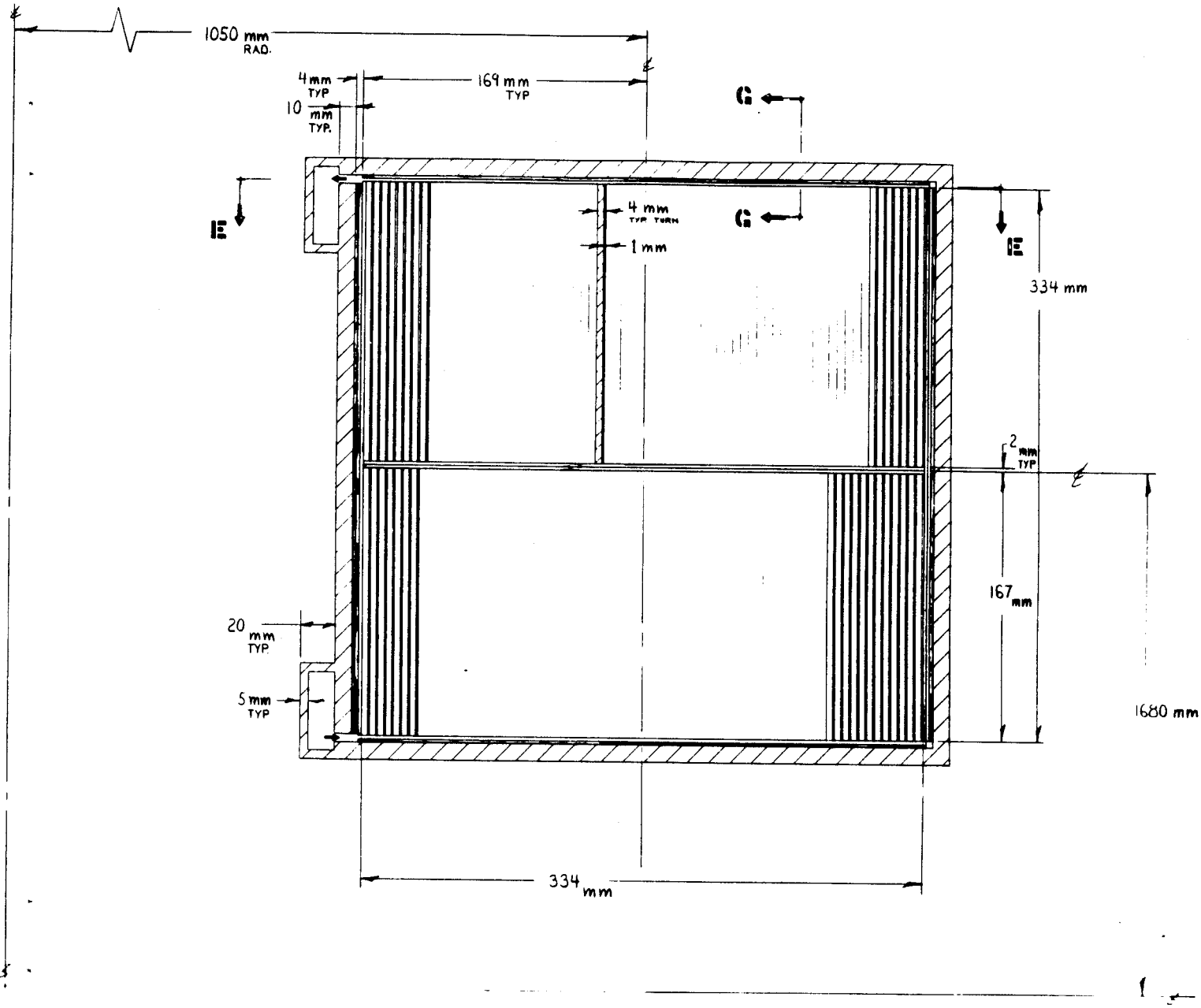

Figure 2.3-3
Section of PF3

Table 2.3-1

PF Vertical Force Summary

(extreme loads during cycle)

	limiter		divertor		
	$+F_z\|_{max}$	$F_z\|_{min}$	$+F_z\|_{max}$	$F_z\|_{min}$	
PF3	~0	-22	+21	-19	MN
PF4	+72	~0	+8	-56	
PF5	~0	-83	+37	-4	

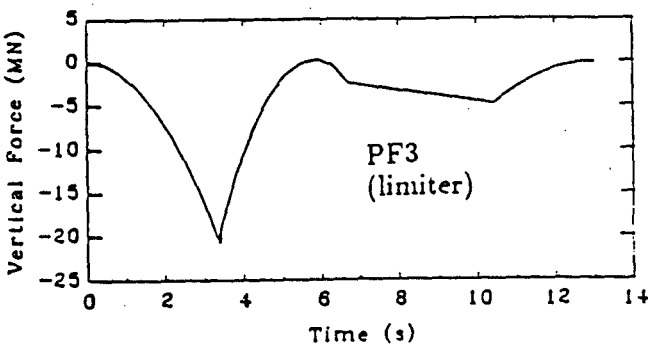

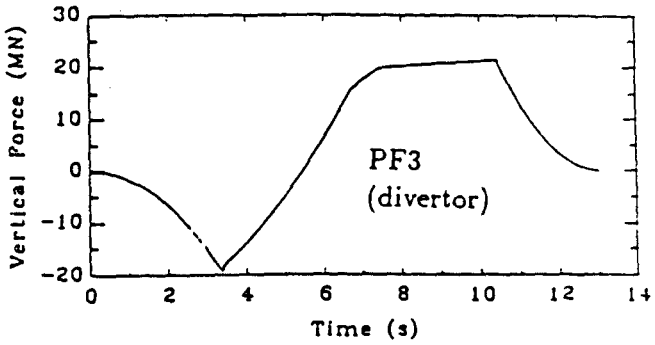

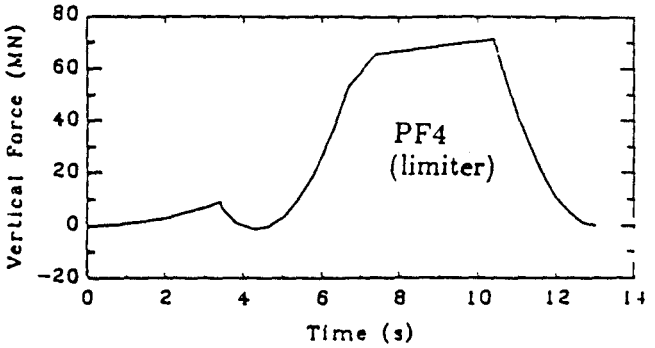

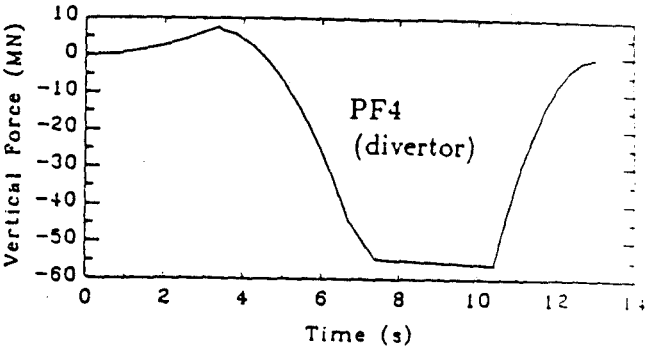

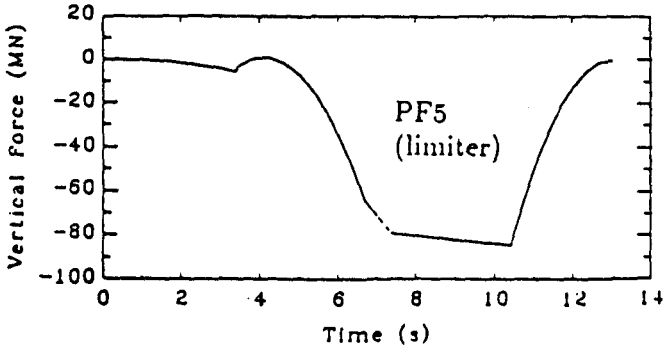

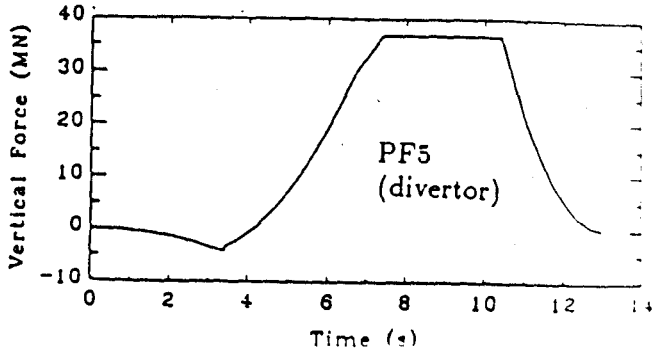

Table 2.3-2
PF Coil Maximum Current Densities and Temperatures

	Limiter		Divertor	
	(MA/m^2)	(K)	(MA/m^2)	(K)
PF1	76.71	292	66.1	221
PF2	80.4	229	79.4	317
PF3	59.6	96	88.8	254
PF4	39.7	96	75.4	163
PF5	69.8	140	25.7	86

coil following a limiter or divertor pulse together with the maximum current densities in the coils during a pulse.

For each of the PF coils, structural analyses have been performed to show feasibility of the winding and support concepts and interface conditions have been evaluated to determine likely paths for leads and coolant lines. Alternate designs for the windings for both the ring and central solenoid stack have been developed in less detail as a backup position. For the solenoids, the alternate is a wound design with steel behind copper conductor. For the ring coils, the backup is a fully impregnated, hollow conductor design, wound several turns in-hand to shorten the cooling passage length. Each concept is considered feasible.

2.4 Next Iteration Design Issues

Thus far, several design areas have been addressed and show system feasibility. Literally hundreds of details require consideration before final design, however, several issues appear to be particularly important over the near term. These are outlined in this section.

2.4.1 Plasma Scenario

Thus far, coils have been designed and interface system requirements (e.g., power and energy) have been determined by choosing approximate current profiles for the evolution of plasma shape and current during start-up, burn, and shut-down. They have been based on matching plasma requirements at start-up (field null) and end of flattop then interpolating between these points. Further work with more static equilibrium code "snapshots" throughout the pulse is required to allow coil current profiles to be selected in more detail. This is critical in view of the lack of margin in stress and temperature in many of the

present cases. Parallel work with the more advanced transient codes for plasma shape development (e.g., Jardin)* is also essential. This will allow a better specification to be formulated for the dynamic field and flux profile requirements for the PF system and for the overall requirements such as total volt-seconds.

2.4.2 Material Lifetime Verification

The desire for a minimum machine size has forced the use of high design allowables, particularly in the central solenoid stack. The high loads on this coil set have led to the use of Inconel-copper-Inconel laminate. Samples of this material have been produced by explosive bonding methods and material property tests to date have been promising.

The expected Tresca stresses at the worst point in the central solenoid imply that the copper operates beyond yield and the Inconel is at about 75% of yield. If the loads are averaged over the winding build in the worst z-plane, then the copper is still at yield and the Inconel is below two-thirds of yield. These results are consistent with the design allowables selected for this phase of the design. However, it is clear that a substantial analytical and experimental program is required to assure adequate performance for the lifetime of the machine. Some relief in this area could be achieved with a modest increase in solenoid outside diameter, provided the physics requirements (e.g., total volt-seconds or pulse length) are not correspondingly increased.

2.4.3 PF3 Interface

The location of PF3 has a particularly strong influence on the diverted plasma shape and separatrix location. Its ampere-turn requirements are very sensitive to its distance from the plasma and its size is restricted by the need for the adjacent vertical access port. Its integration with the surrounding structures and the port must be addressed in more detail because of the potentially strong effect on the PF3 energy requirements which are already quite large.

2.4.4 PF4 and PF5 Interfaces

PF4 is subjected to particularly high in-plane loads. These will be supported by the adjacent steel structure which also couples to the other ring coils for out-of-plane support. A workable, size-efficient concept must be developed to allow separate coil fabrication and enclosure in a cryogenic vessel with subsequent insertion in the heavy structure. The result

* S.C. Jardin,*et al.*, Dynamic Modeling of Transport and Positioning Control of Tokamaks, PPPL Report No. 2258, Oct. 1985.

must provide adequate means for load transmittal from the coil to the structure with due consideration of thermal effects. A similar concept must be generated for PF5; however, its in-plane loading is not as severe.

2.4.5 Lead, Joint and Cooling Details

Viable concepts have been developed for the leads, joints and cooling paths for the PF coils. These must be subjected to the next level of analysis to assure allocation of adequate space and routes through the machine. Interface with machine elements for support against electromagnetic loads with consideration of thermal effects also requires attention.

2.4.6 Power Supply Interface

Coil current scenarios and circuits require further consideration to arrive at a more detailed specification of the power and energy supply systems in view of the equipment already available at the site. This is also necessary to freeze the impedance level (i.e., number of turns) in each coil and allow another iteration to be performed on stress analysis and concepts for joints and terminations.

2.4.7 Separatrix and Vertical Stability Control

Studies thus far have barely begun relative to separatrix control. Current changes of the order of 100 kA in one of the internal coils (i.e., I1) have been shown to shift the separatrix by about two centimeters, thus implying control with a reasonble amount of power and ampere-turns. However, the requirements in this area need better definition followed by a detailed study to position coils for this function.

The elongated plasma and the applied field distribution necessary to produce it result in a natural vertical instability for the plasma. The unstabilized growth rate is on the microsecond time scale, but can be controlled by a combined active and passive stabilization system. In this regard, the vacuum vessel has been determined to be sufficiently well-coupled to the plasma to restrain the vertical displacement growth rate to the 15 ms time scale. This is sufficiently long to allow the active coil system to come into play at a reasonable power level. Estimates to date imply that the internal coils (i.e., I1) are adequately positioned to provide this function. More detailed studies over a wider range of plasma parameters are required to assure that adequate space is provided for these coils and their electrical and coolant lines.

3.0 Coil System Selection

3.1 Trade Studies

3.1.1 Volt-second Swing Bias

The bias of the central solenoids involves a number of trade-offs, including the peak solenoid stress, energy and power consumption and peak temperature specifications. An optimal trade is frequently found in the vicinity of zero biasing, in which the PF currents at the beginning of initiation provide a number of volt seconds which are equal in magnitude, but opposite in sign to that at the end of burn. However, recent studies with high current ignition plasmas have shown that the plasma is usually strongly demagnetizing at the end of burn and that stresses in the solenoid tend to be considerably higher at the beginning of initiation with zero biasing. This is partially counterbalanced by the fact that the coil temperatures are higher in inertially cooled magnets at the end of a pulse than at the beginning and, therefore, the allowable stresses are also lower at the end of burn.

A method for comparing many of the PF cost and feasibility parameters as a function of flux swing bias has been developed by Pillsbury and Thome, in order to get a good first choice of the central solenoid biasing [PI85A].* The trade-off in cost parameters is shown in Table 3.1-1. In general, a high bias at initiation drives the value of cost parameters up at initiation and down at the end of burn. Optimal cost parameters for a complete scenario are selected graphically by finding the intersection of cost parameter curves at initiation and the end-of-burn. This is illustrated for the important central solenoid hoop stress parameter J $\times$ B in Figure 3.1-1. There is a moderate amount of variation (2.7 V·s) in the optimum bias for various parameters. Of the different parameters, only hoop stress in the PF2 solenoid has presented a system feasibility problem. Thus, a bias of +9.5 V·s to -16.5 V·s was selected, in order to optimize this parameter.

* [see reference list at end of Section 3.0.]

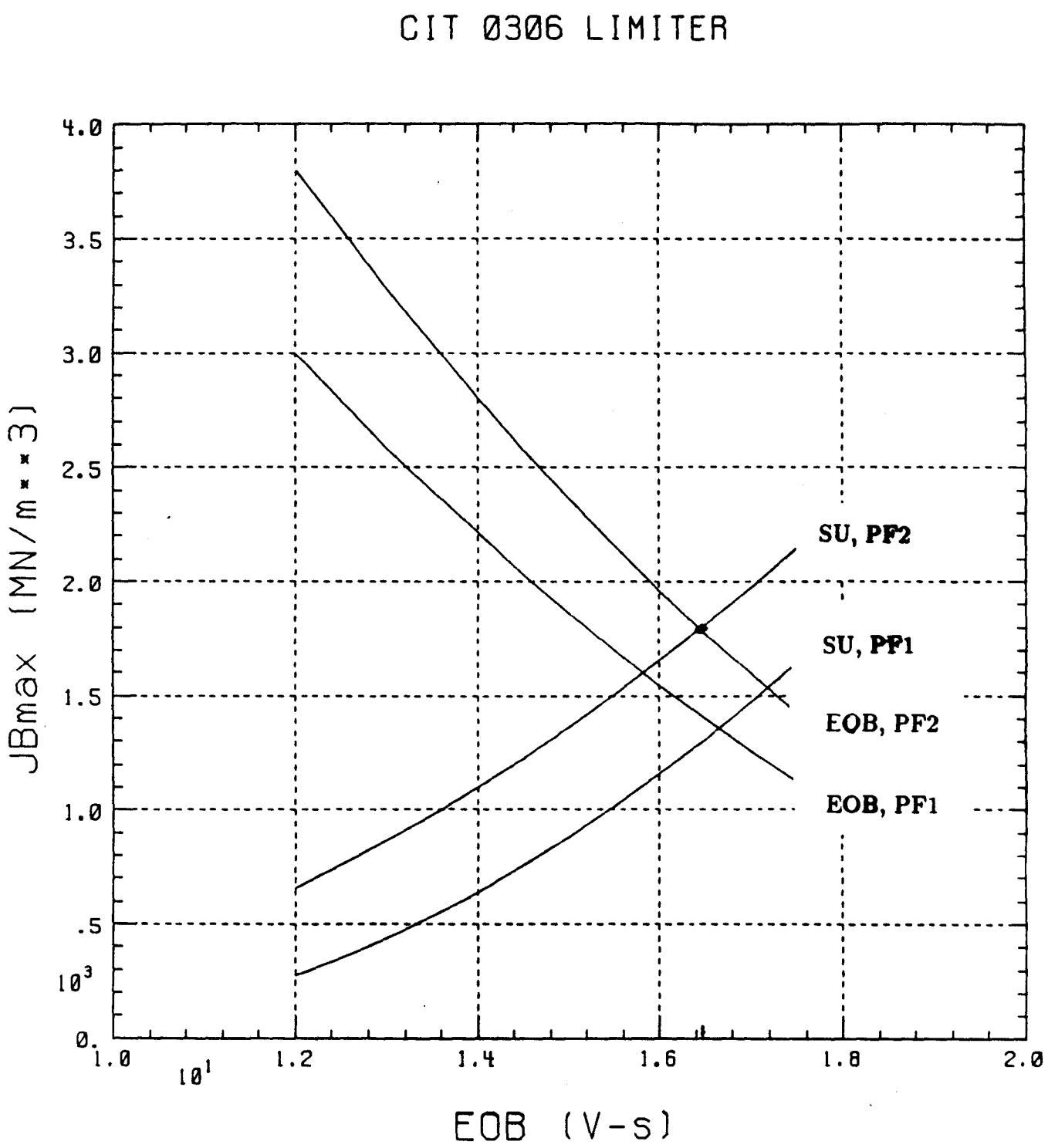

Figure 3.1-1
Hoop Stress Parameter J×B vs End-of-Burn, V·s

Table 3.1-1
PF Cost Parameters as a Function of Biasing

Parameter	Units	Optimal Vs_{swing}	Minimum
PF Stored Energy	(MJ)	(+11.9 to -14.1)	500
PF Ampere-turns	(MAT)	(+9.5 to -16.5)	59
PF Ampere-meters	(MAm)	(+12.2 to -13.8)	360
JB_{max}	(MN/m^3)	(+9.5 to -16.5)	180

3.1.2 Central Solenoid Temperature/Stress Trade-off

The feasibility of the central solenoid is typically marginal for compact ignition devices, because the cost advantages of making the machine as small as possible tend to push this solenoid to the limits of its stress and temperature allowables. Within the dimensions of a difficult-to-achieve performance envelope, the approach to the allowable limits can be optimized by selecting the best ratios of copper, reinforcing steel and electrical insulation. The basic trade-off is that the solenoid will be stronger but hotter when more steel is added to a fixed envelope.

The trade-off in temperature and energy is relatively straightforward. Of the two scenarios developed, the divertor scenario leads to slightly higher temperature and energy requirements for the central solenoid. The central solenoid has been split into two independently controllable segments. The segment farther from the equatorial plane, designated as PF2, has the higher stresses and temperatures in both the limiter and divertor scenarios. The PF scenario analysis code [SC86] was run several times with different fractions of steel and copper in PF2 to determine the thermal limitations on steel reinforcement. The results of a series of simulations, all with 10% insulation packing factor, are shown in Table 3.1-2. The energy requirements shown are the peak, instantaneous integrated energies, including magnetic and dissipated, in the upper and lower mirror image coils. Two specifications that must be satisfied are that the local temperature is not permitted to rise above 370 K, in order to avoid damage to the insulation or annealing of copper and that the energy requirements must be compatible with the TFTR pulsed motor-generator set. An evaluation of available energy, after reserving some of the pulsed energy for the TF magnet system, estimated that at least 2,300 MJ remained to be allocated to the PF system. (See Section 3.2.2) This energy is available without "superpulsing" the generator to lower speed or drawing any power directly from the line. Either of these strategies could individually add an additional 1000 MJ. Exclusive of PF2, the peak energy required by the PF system is 1710 MJ for the divertor scenario, which is the more severe, leaving at least

590 MJ available for PF2. For a steel fraction of 0.4, the peak temperature in the copper would be 317 K, while the peak energy requirement would be 458 MJ, both of which are within allowables. For a steel fraction of 0.45, the peak temperature in the copper would be 371 K, while the peak energy requirement for PF2 would be 582 MJ. These are both marginal. The temperature specification is actually considerably more severe than the energy specification, because of the possibilities of superpulsing the generator or drawing power from the line. Furthermore, the circuit model used to calculate temperatures did not take into account the lag time in transferring heat from copper to the adjacent steel. A 50 % steel fraction cannot satisfy allowables. These results are shown in Table 3.1-2. Attention was focused on finding a solution with 40 % steel or less.

Table 3.1-2
Temperature and Energy Requirements for PF2 in the Divertor Scenario for Different Fractions(f_{ss}) of Reinforcing Steel

f_{cu}	f_{ss}	T_{peak} (K)	E_{max} (MJ)
0.7	0.2	208	234
0.6	0.3	249	312
0.5	0.4	317	458
0.45	0.45	371	582
0.4	0.5	448	766

When the scenario emulator had identified the time points and coils that were highly stressed, detailed analysis of the stresses was done through the use of the Bobrov three-dimensional shell code [BO84]. This code is more flexible and accurate than other closed-form solutions for the stress in a solenoid, because it can accept arbitrary magnetic field patterns. Two-dimensional closed-form solutions typically assume the self-field of a solenoid, but this will not give the correct answers in applications where a large fraction of the field in a solenoid is from external solenoids. The Bobrov code is itself limited for the analysis of the PF2 coil above, because its use and interpretation are straightforward only in the elastic regime. As discussed below in the section on structural design, an elastic-plastic design was selected. This section discusses the trade study that made the need for an elastic-plastic design clear, while section 4 discusses the design criteria, elastic-plastic stress analysis and the design solution.

Since the thermal design criteria indicated that the fraction of steel should not be much higher than 0.4, a structural analysis was made of PF2 at the beginning of initiation for the limiter scenario case, which is the highest stress point for either scenario. Figure 3.1-2

shows the hoop and axial stresses in a homogeneous, anisotropic, composite structure that has the same force-displacement characteristics in three dimensions as the actual steel-copper-insulation composite. The local peak in hoop stress occurs on the inside of the coil and is about 1.5 times higher than than the average hoop stress in the coil. There is smaller radial variation in the axial stress, which peaks slightly above the bottom of the coil. Thus, the maximum compressive stress within the solenoid is higher than that predicted by the circuit model, which calculated the total downward force on PF2. These composite stresses can be decomposed into Tresca stresses in copper and steel. A postprocessor that assumed elastic behavior shows the implications in Figure 3.1-3. However, as can be seen from the figure, approximately 3/4 of the copper would have to operate at Tresca stresses above the yield of copper. Since the average stress on the copper is only 100 MPa above yield, while the steel is everywhere at least 200 MPa below its yield, and there is almost as much steel as copper, it is reasonable to expect that the copper can be allowed to yield and transfer its calculated elastic stresses to the steel, without driving the steel past its allowables. This has been confirmed in the detailed analysis reported in chapter 4. However, it would obviously be more conservative and desirable if yield in the copper could be avoided altogether. The results of a second analysis, using a steel fraction of 0.5 and a copper fraction of 0.4 is shown in Figure 3.1-4. Now, instead of most of the copper being locally in yield, it appears that something less than half would be yielded. However, a steel fraction of 0.5 already gives peak temperatures of 450 K as shown in Table 3.1-2. Since this is above the temperature allowables and the peak local stress in the copper is still above yield, it is clearly not possible to prevent local yielding in the copper with the dimensional and operational constraints for this system.

3.2 PF Scenarios and Power Supply Requirements

3.2.1 Power/Energy Flow Scenarios

Complete PF coil current scenarios have been developed for both the divertor and limiter cases, using the reference set of PF envelopes. The scenarios are based on specific MHD equilibria, volt-second requirements, initiation loop voltage and plasma current ramp rates and flattop time [PI85B]. These scenarios have then been used to match power supplies and insulation requirements in order to select the number of turns in each PF coil. The poloidal field systems and the number of turns selected for each coil are listed in Table 3.2-1. Energy requirements, peak powers and final temperatures are listed in Tables 3.2-2 and 3.2-3 for the limiter, and then the divertor scenarios. For both the limiter and divertor scenarios, the highest current density occurs in the central solenoids, because of

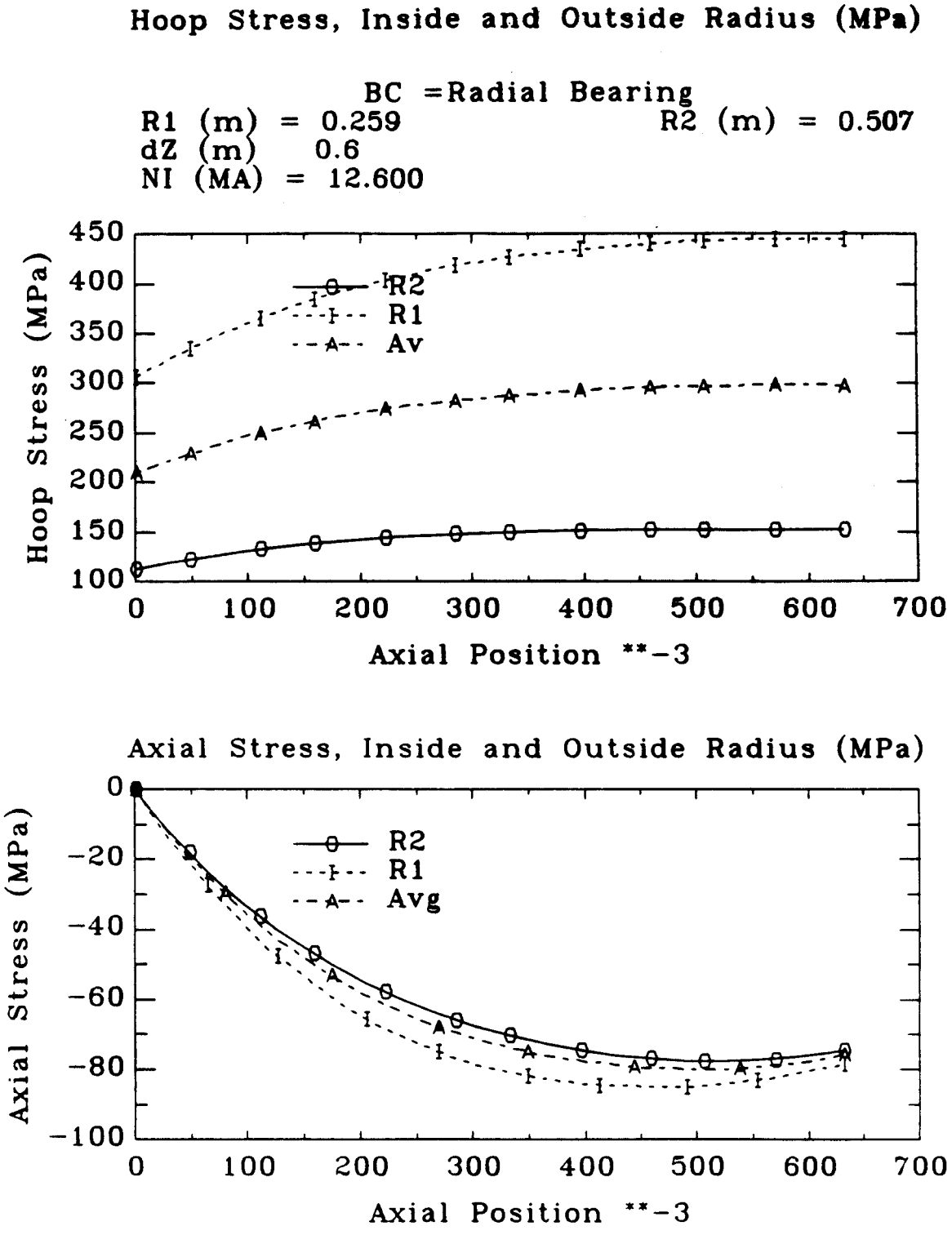

Figure 3.1-2
Hoop and Axial Stresses on PF2 at Initiation
Modeled as a Homogeneous, Anisotropic Composite

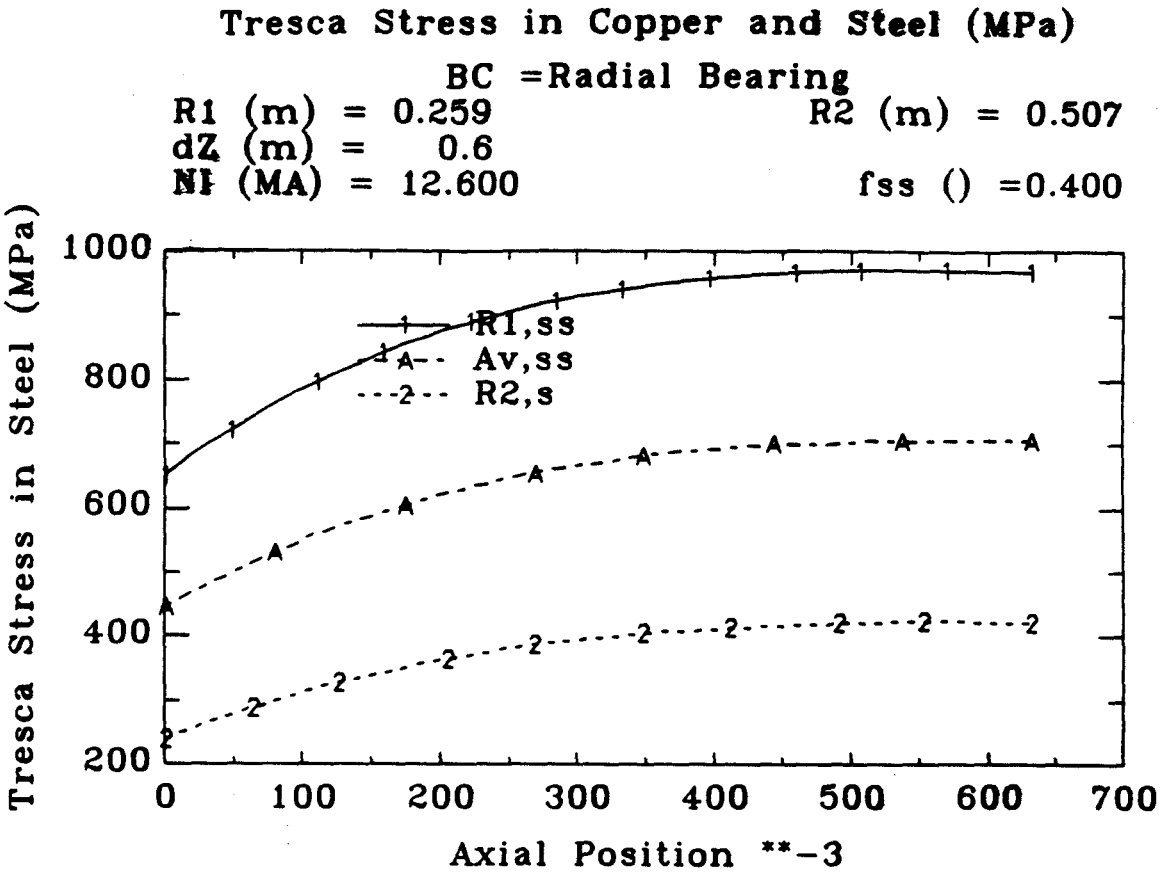

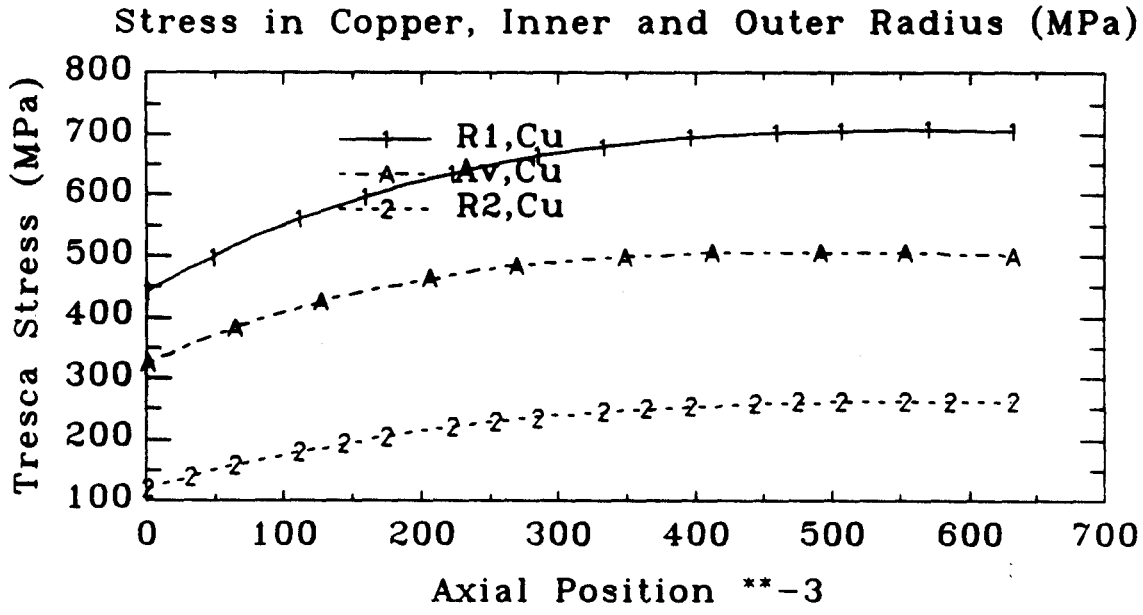

Figure 3.1-3
Local Tresca Stress in PF2 at Initiation
with 40% Steel, Elastic Analysis

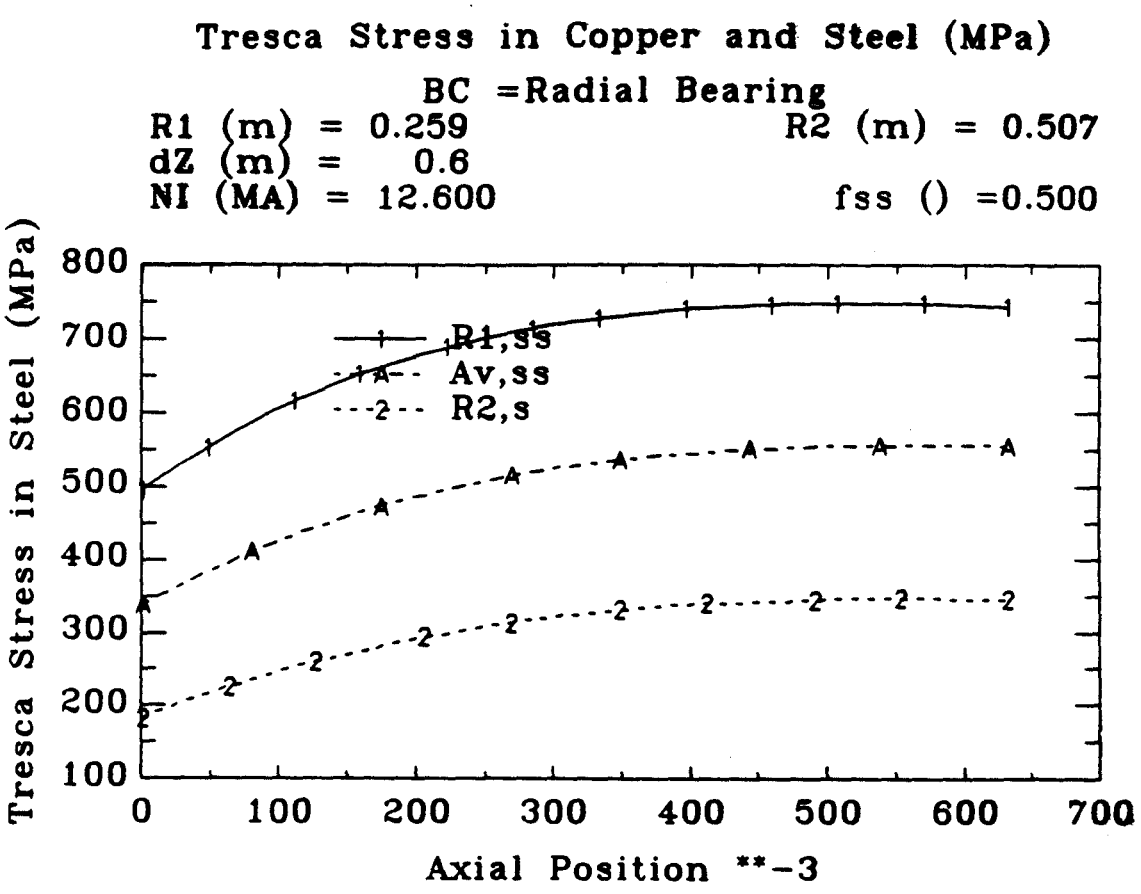

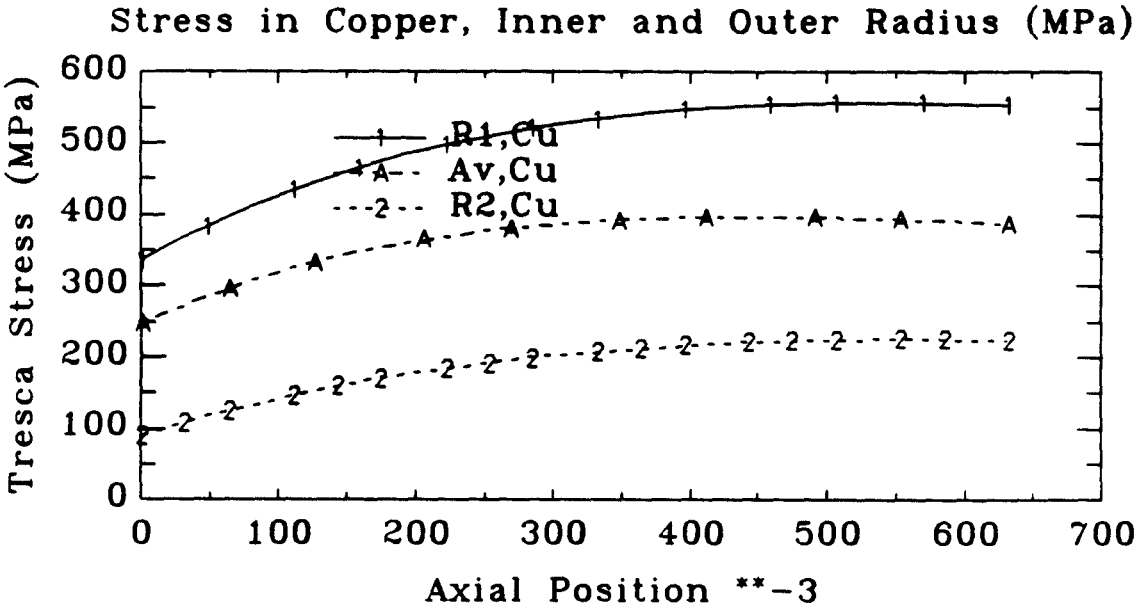

Figure 3.1-4
Local Tresca Stresses in PF2 at Initiation
with 50% Steel, Elastic Analysis

Table 3.2-1
PF System Winding Pack Dimensions

Coil	R (m)	Z (m)	R_1 (m)	R_2 (m)	Z_1 (m) (m)	Z_2 (MAT)	NI_{max} ()	n_{turns}
PF1,U	0.383	0.184	0.259	0.507	0.000	0.368	7.000	200.0
PF2,U	0.383	0.684	0.259	0.507	0.368	1.000	13.100	160.0
PF3,U	1.050	1.748	0.910	1.189	1.518	1.979	10.7	300.0
PF4,U	2.050	1.680	1.887	2.213	1.517	1.843	8.37	112.0
PF5,U	2.510	0.955	2.351	2.670	0.795	1.115	7.1	160.0

Table 3.2-2
Energy, Power and Temperature for the Limiter Discharge

Coil	$J_{env,pk}$ (MA/m^2)	T_{max} (K)	$E_{pk,req}$ (MJ)	P_{max} (MW)
PF1,U	76.7	292	117	35
PF2,U	80.4	229	131	45
PF3,U	59.6	96	85	53
PF4,U	39.7	96	37	9.2
PF5,U	69.8	140	348	134

Table 3.2-3
Energy, Power and Temperature for the Divertor Discharge

Coil	$J_{env,pk}$ (MA/m^2)	T_{max} (K)	$E_{pk,req}$ (MJ)	P_{max} (MW)
PF1,U	66.1	221	72	20.9
PF2,U	79.4	317	229	64.1
PF3,U	88.8	254	369	80.4
PF4,U	75.4	163	386	122
PF5,U	25.7	86	70	35.5

the highly constricted envelope constraints. The highest coil temperatures occur in the central solenoids as well, both because of the high envelope current density and because the high stresses force the use of steel within the winding.. In the limiter discharge, the dominant requirements for energy and power are from the outside PF5 coil, because it is the largest of the PF coils and is providing most of the equilibrium field needed to restrain radial outward motion of the high pressure ignited plasma. In the divertor case, however, the dominant coils are PF3 and PF4, because of the high currents needed to form a separatrix inside the vacuum vessel.

The overall energy needs for the PF system are more demanding for the divertor case, requiring 2170 MJ, than for the limiter case, which requires only 1280 MJ, as shown in Figures 3.2-1 and 3.2-2. As shown in the two figures, the divertor coils PF3 and PF4 are the reason for the additional energy requirements.

For the limiter discharge, the power needed by the PF system from the power supplies is high at the end of coil precharge, the end of plasma current ramp-up and the end of burn, as shown in Figure 3.2-3. The most demanding requirement is at the end of current ramp-up, when 429 MW are required from the line. The requirements for PF5, which is the main equilibrium coil for the limiter discharge, totally dominate the system requirements at this point. The PF1 and PF2 solenoids have passed through zero, and are beginning to demand nonnegligible power at this point. For the divertor discharge, the divertor coils PF3 and PF4 dominate, as shown in Figure 3.2-4, and there are almost equally high power peaks at the end of current ramp-up and the end of auxiliary heating. The scenario-generating code was not provided with an adequate number of MHD equilibria for this case to determine whether the second peak would actually occur. The peak power required by the system is 497 MW. The TFTR generators have a peak power capability of 950 MVA, which corresponds to an ability to deliver approximately 700 MW to the load. The utility line at the TFTR site can be tapped up to 250 MVA, corresponding to approximately 175 MW of deliverable power. At the end of TF ramp-up, which would come fairly close to the time of plasma ramp-up in the current scenario, the TF coils require their peak power of 590 MW. This is based on a linear ramp-up and could probably be improved considerably by a better match to the existing generator capability. Under the worst set of assumptions, the existing generator and line would be marginally inadequate to provide all of the required PF power.

The peak currents and voltages in the coils for either scenario are required to design the winding, bus and ground insulation. The peak voltages and peak currents hardly ever have the same polarity, so they are not used directly in power supply sizing. Peak voltages

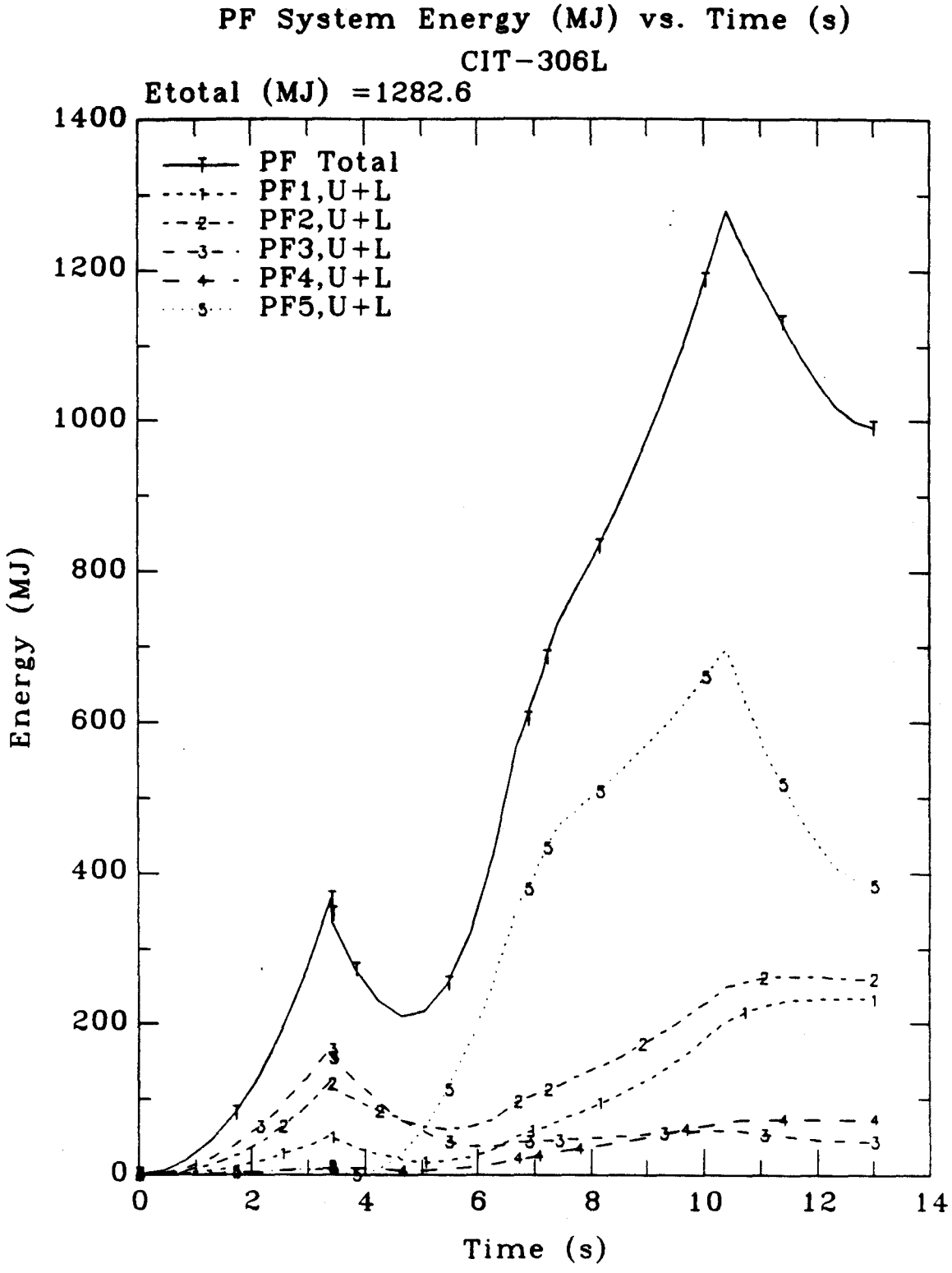

Figure 3.2-1
Energy Flow to the PF Coils for a Limiter Discharge

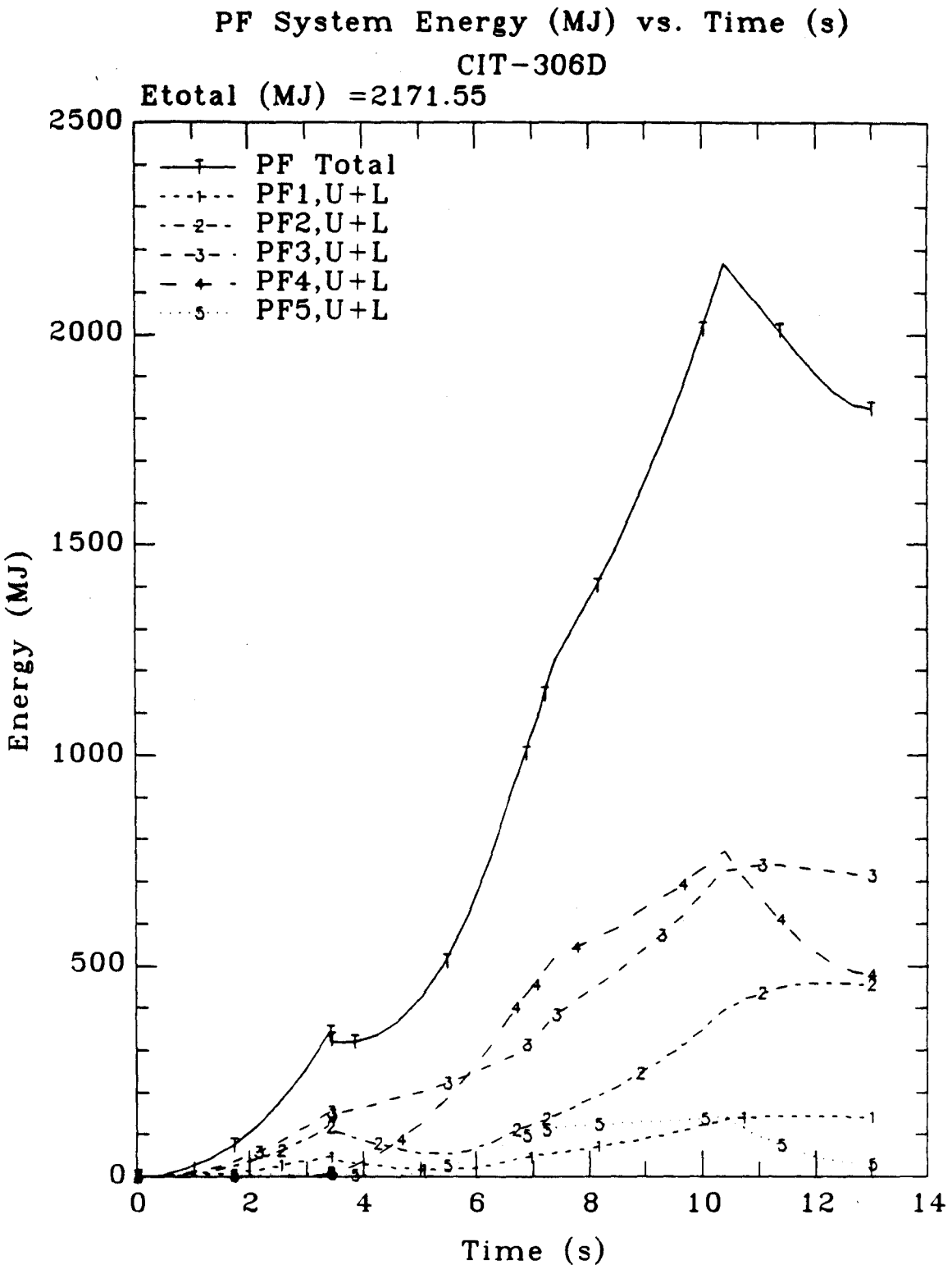

Figure 3.2-2
Energy Flow to the PF Coils for a Divertor Discharge

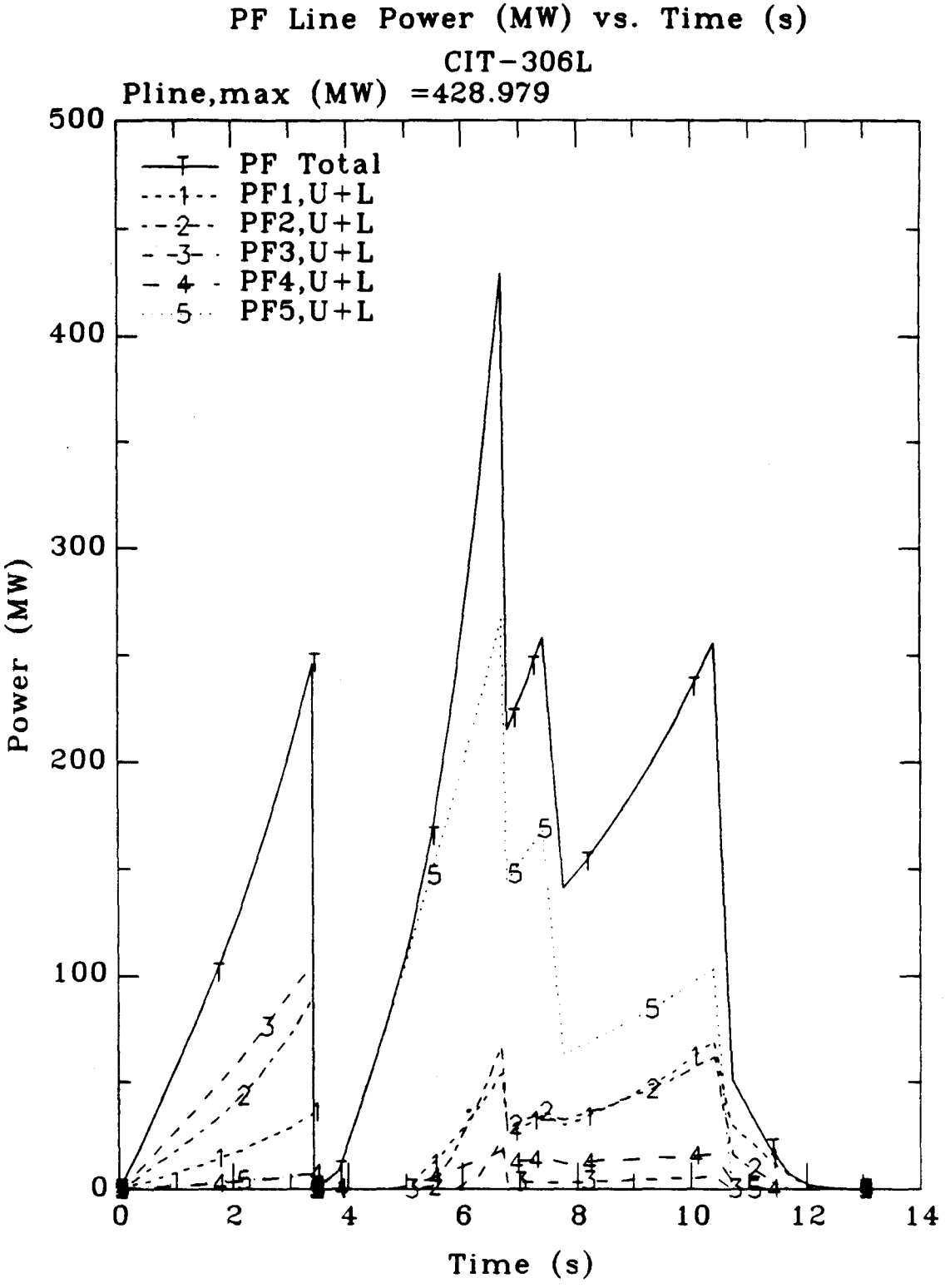

Figure 3.2-3
Positive Power Requirements of PF Coils During the Limiter Discharge

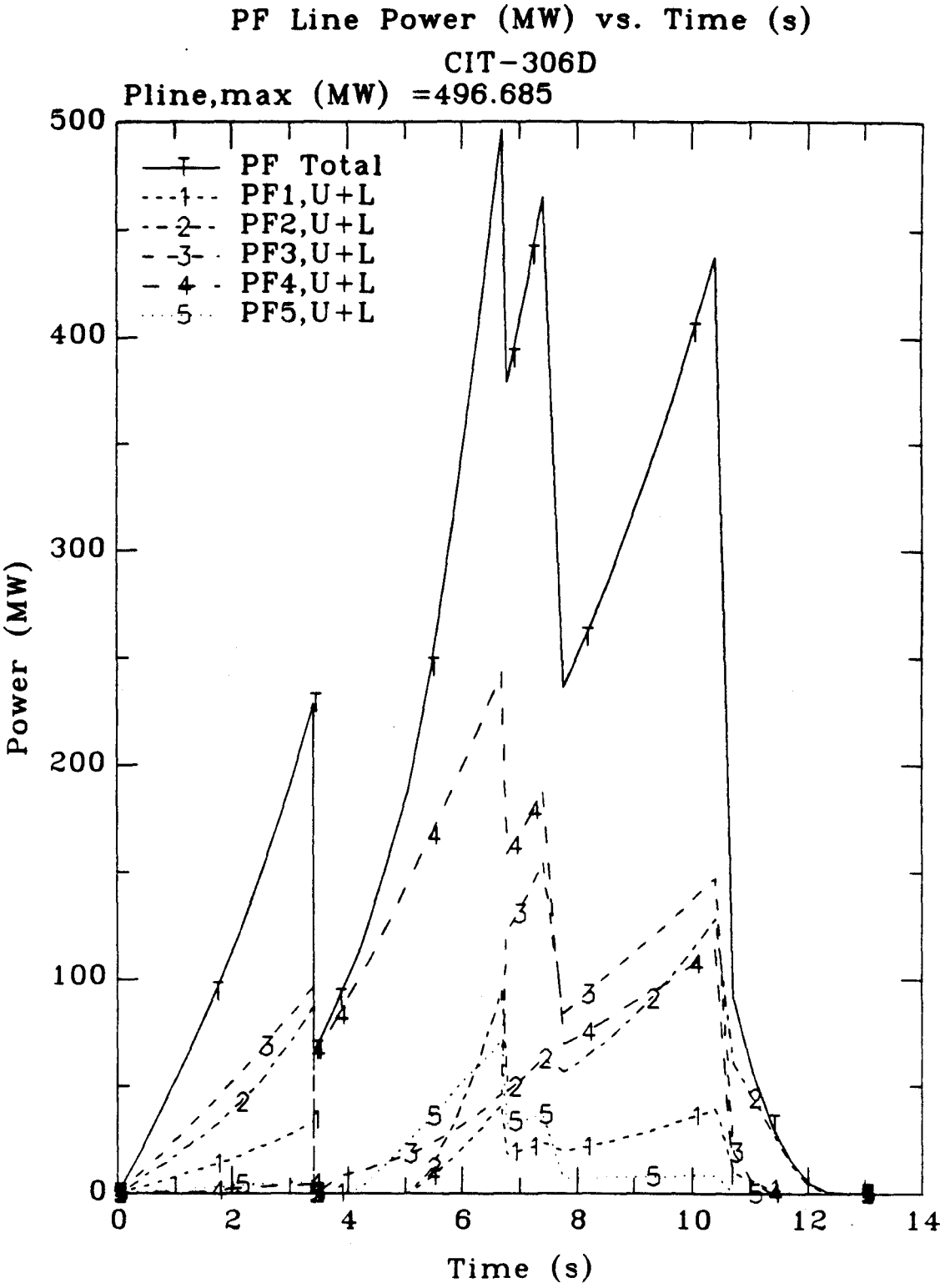

Figure 3.2-4
Positive Power Requirements of the PF Coil During the Divertor Discharge

and currents are listed for the divertor and limiter discharges in Tables 3.2-4 and 3.2-5.

The scenario generating code also calculates the radial and vertical forces and averaged winding pack stresses at each moment of time, as well as the forces on each coil after a flux-conserving disruption at any moment in time. The areas investigated in greater detail are those in which the averaged stress in a winding pack is a significant fraction of the yield stress of copper. These include the PF1 and PF2 coils, discussed above and in section 4, for which the solution was the use of the copper-Inconel laminate. The code also identified high stresses in PF4 during the divertor discharge, as shown in Figure 3.2-5. Unlike the two central solenoid coils, whose forces and stresses are quite similar for the two discharges, the forces on the PF4 coil are very scenario dependent, and are quite small for the limiter discharge. However, for the divertor discharge, PF4 has a high current density in order to form the plasma separatrix and the polarities of the currents are such that it is being pushed outward by the plasma and PF3 and pulled outward by PF5. The solution in this case, since the two PF4 coils already require a peak energy of 732 MJ energy and the structural envelope is less constrained than for the central solenoid's case, is to support the high hoop loads with a structural case around the winding pack. Fortunately, the total radial force and current in PF4 declines slightly after a flux-conserving disruption.

Another unique structural requirement identified by the code is that each PF5 coil experiences a large downward force of 85 MN at the end of the limiter burn. As shown in Figure 3.2-6, this does not lead to large axial bearing stresses, since the coils have very large bearing areas, but it does require a set of structural pillars to be added to the design to react the forces on the mirror image coils against each other.

3.2.2 Power Supply Interface

It is intended to use the extensive power supply capability at the Princeton Plasma Physics Laboratory to the maximum extent possible. After allocating adequate energy to supply the needs of the toroidal magnet system, the Princeton facility has a surplus of 2,300 MJ available from the pulsed motor-generator set. This might be marginal, as shown in Table 3.2-6, except that superpulsing the generator or drawing additional power from the line provides the PF system with adequate headroom, if needed. After allocating 21 rectifier modules for the TF system, 17 rectifier modules remain for use in the PF system. Each module consists of two seriesed, 12-pulse rectifiers, each with a nominal capability of providing 20 kA and 1 kV. Princeton has already developed techniques for bus-switching at current reversal, so it is not necessary to use separate power supply modules for positive and negative current. The reference energy allocations are shown in Table 3.2-6, including some of the options currently being considered.

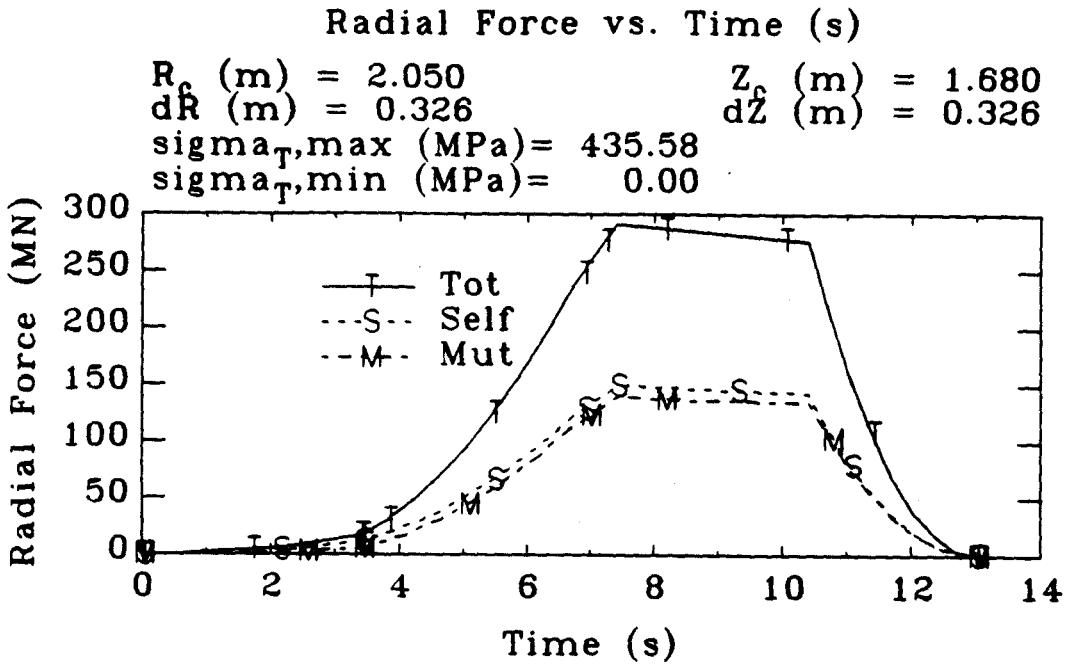

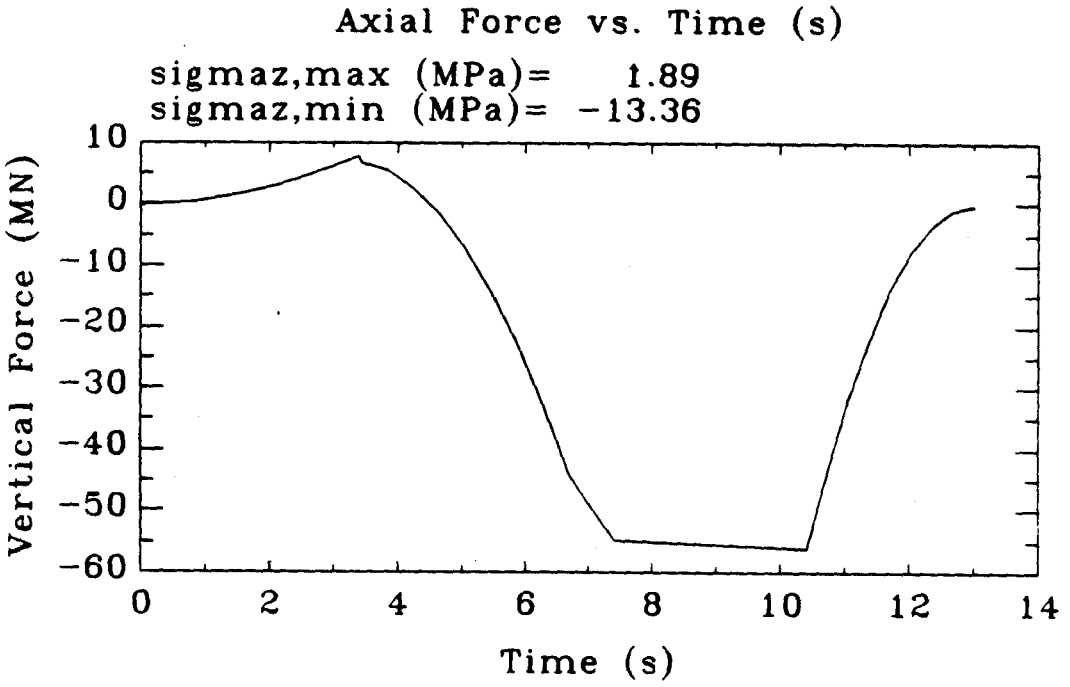

Figure 3.2-5
Hoop and Axial Forces in PF4 During the Divertor Discharge

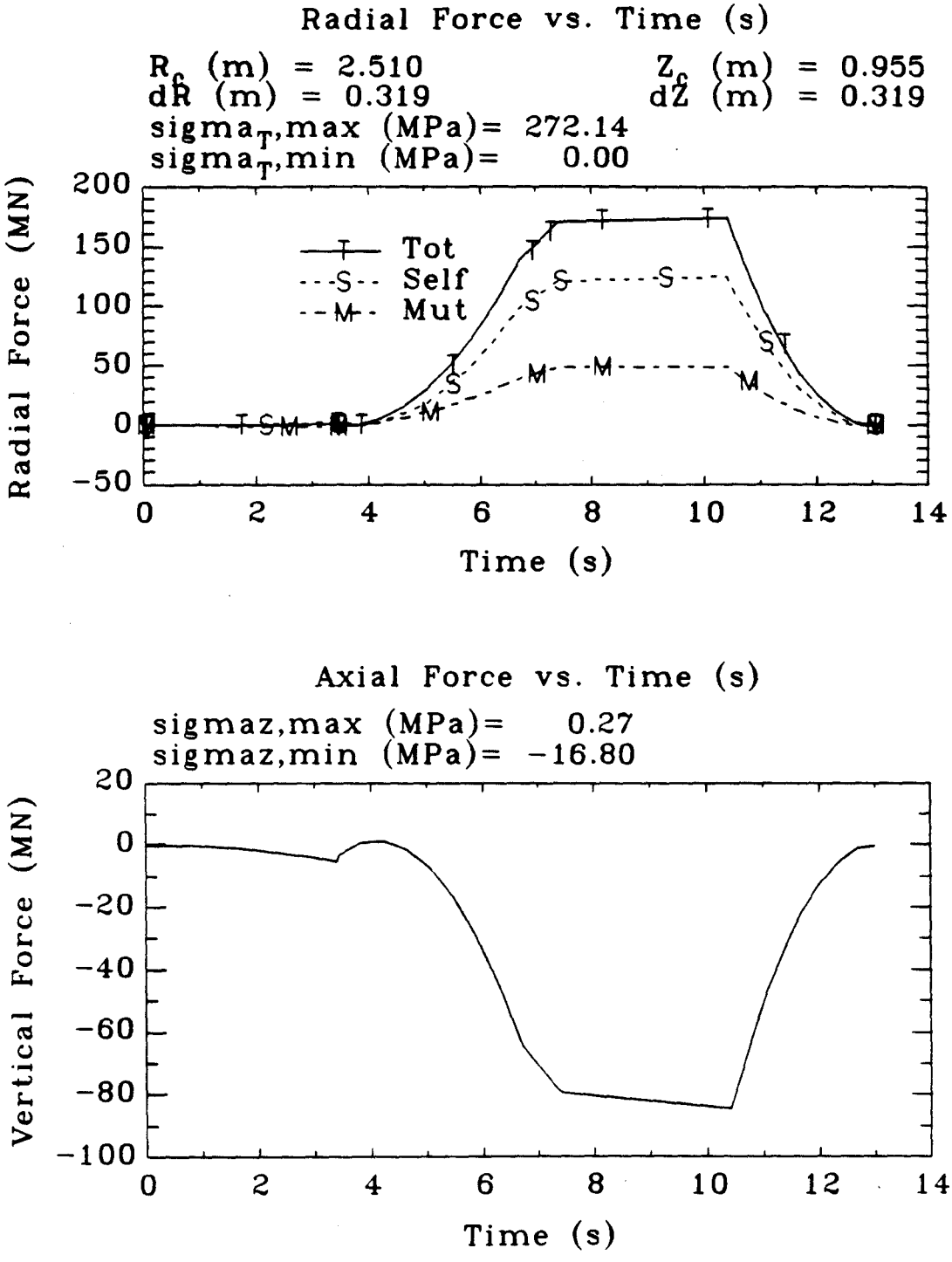

Figure 3.2-6
Hoop and Axial Loads on PF5 During the Limiter Discharge

Table 3.2-4
Peak Currents and Voltages on PF Coils for Limiter Scenario

Coil	$I_{cond,max}$ (kA)	$I_{cond,min}$ (kA)	$V_{term,max}$ (kV)	$V_{term,min}$ (kV)
PF1,U	29.300	-35.000	0.606	-2.786
PF2,U	78.750	-59.125	0.572	-2.062
PF3,U	25.533	-8.200	2.085	-9.196
PF4,U	37.679	-22.054	0.716	-0.156
PF5,U	5.750	-44.375	3.529	-12.986

Table 3.2-5
Peak Currents and Voltages on PF Coils for Divertor Scenario

Coil	$I_{cond,max}$ (kA)	$I_{cond,min}$ (kA)	$V_{term,max}$ (kV)	$V_{term,min}$ (kV)
PF1,U	28.550	-30.150	0.589	-3.491
PF2,U	77.813	-73.750	0.562	-2.214
PF3,U	38.090	0.000	2.065	-4.645
PF4,U	0.000	-71.554	2.226	-1.889
PF5,U	5.250	-16.375	2.705	-9.281

Table 3.2-6
Energy Requirements and Allocations

Energy Source/Load (MJ)	Requirement/Capability (MJ)
TFTR Generator-design value	4,500 × 0.9 = 4,050
TFTR Generator-superpulsed	5,500 × 0.9 = 4,950
Contribution from utility line	1,200 (6-8 s,equivalent)
TF Allocation	1,730
PF Requirement	2,170 (Divertor)
PF Available-Reference	2,320
PF Available-Maximum	4,420

References

[PI85A] R.D. Pillsbury,Jr. and R.J. Thome, "Compact Ignition Device Poloidal Field System Trade-Studies using an Equilibrium Field Expansion Technique," 11th Conference on Engineering Problems of Fusion Research, Austin, TX, 1985 b

[BO84] E.S. Bobrov, "Electrically Conducting Orthotropic Cylindrical Shell in Axial and Radial Magnet Fields," in The Mechanical Behavior of Electromagnetic Solid Continua", ed. G.A. Maugin, Proc of the IUTAM-IUPAP Symposium, Paris, France, 4-7 July, 1983, Elsevier Science Publishers (North-Holland), 1984.

[PI85B] R.D. Pillsbury,Jr., R.J. Thome, J.M. Tarrh and W.R. Mann, "Poloidal Field Coil System Design using a Field Expansion Technique," 9th International Conference on Magnet Technology (MT-9), Zurich, Sept 1985.

[SC86] J.H. Schultz, "A Poloidal Field Scenario Generating Code for Use in the Design and Operation of Tokamaks," M.I.T. Plasma Fusion Center Research Report, PFC/RR-86-10, May 1986.

4.0 Poloidal Field Coil Design

4.1 Summary

The system consists of five distinct coil sets identified as:

PF1 – the center sections of the central solenoid

PF2 – the end sections of the central solenoid

PF3 - 5 – three ring coil pairs

The principal design of PF1 and PF2 is based on composite plates of Inconel-copper-Inconel cut into spiral coils and joined inside and outside to adjacent coils. An alternative design, based on cowound strip, was also developed. The PF3 - 5 coils are wound from hard copper strip and sealed into stainless steel containers. An alternative concept based on hollow copper conductor has also been considered. All coils are liquid-nitrogen precooled.

4.2 General Description

4.2.1 Central Solenoid(PF1 andPF2)

The PF1 and PF2 systems are similar. The difference lies only in the number of pancake coils, the thickness of each pancake coil and the ratio of copper to Inconel. The radial build of each turn and the number of turns per pancake is identical in the two systems.

Figure 4.2-1 shows the PF1 and PF2 assembly while Figure 4.2-2 shows a single pancake. The base unit is the composite pancake coil having nine turns, of which eight are active. The coils are made by cutting a 2 mm curf on a stepped spiral pattern. All coils are cut identically but are stacked in alternating right hand and left hand sense. Adjacent coils are connected either at their inside or outside turns.

A tensile hoop stress of 465 MPa in the second turn of PF2 demands a strong interconnection. The radial width of the second turn increases to twice the normal value at the interconnection and is pinned to the adjacent turn by 8 pins of Inconel 718 maraging steel. See Figure 4.2-2. The Inconel is stripped from the inner part of the interconnection and replaced by copper which is soldered and pinned. The outer turn is not so highly stressed. Its construction is shown in Figure 4.2-3.

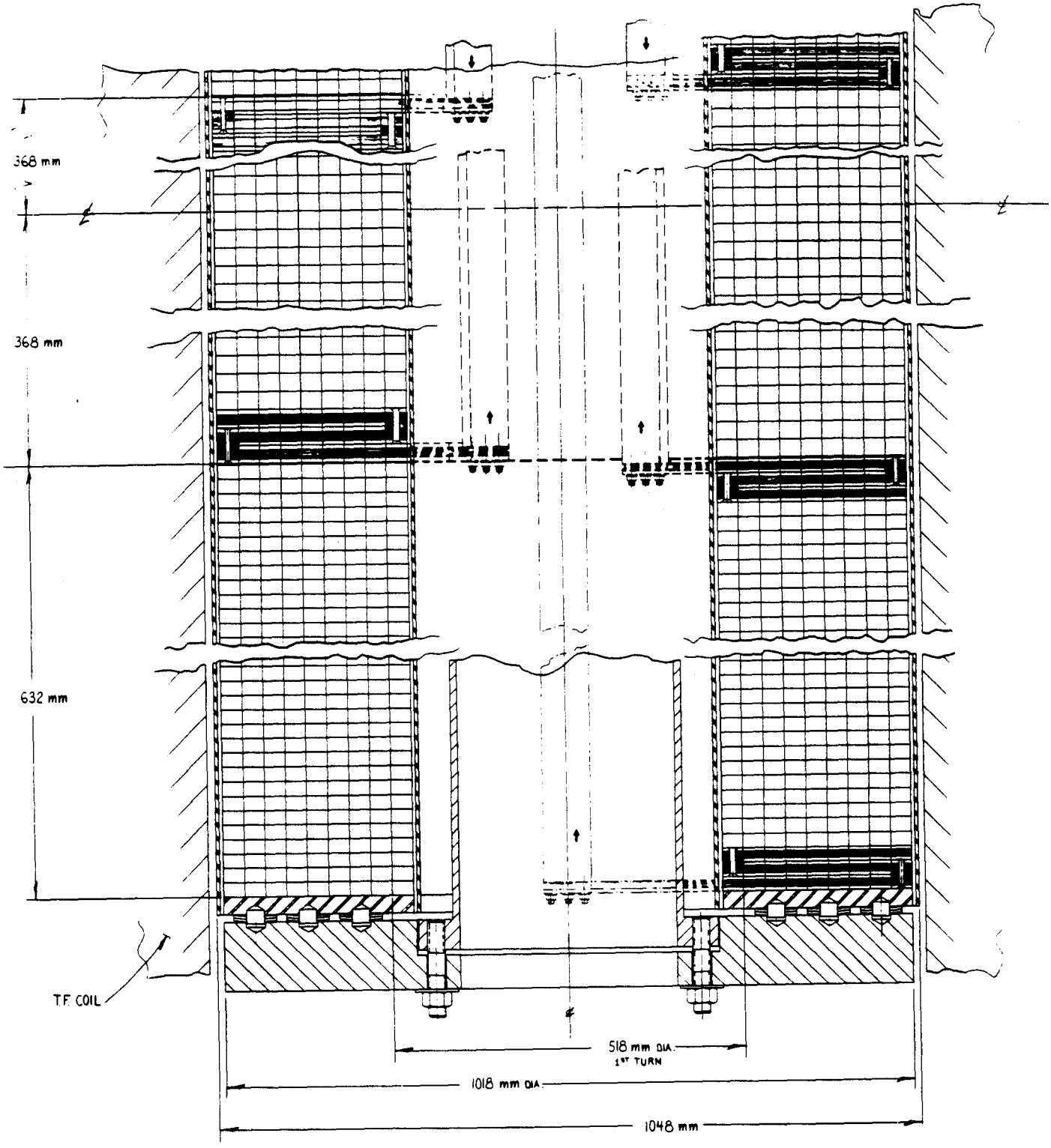

Figure 4.2-1
Assembly of PF1 and PF2 Central Cell Solenoid Coils
(Lower Half Only Shown)

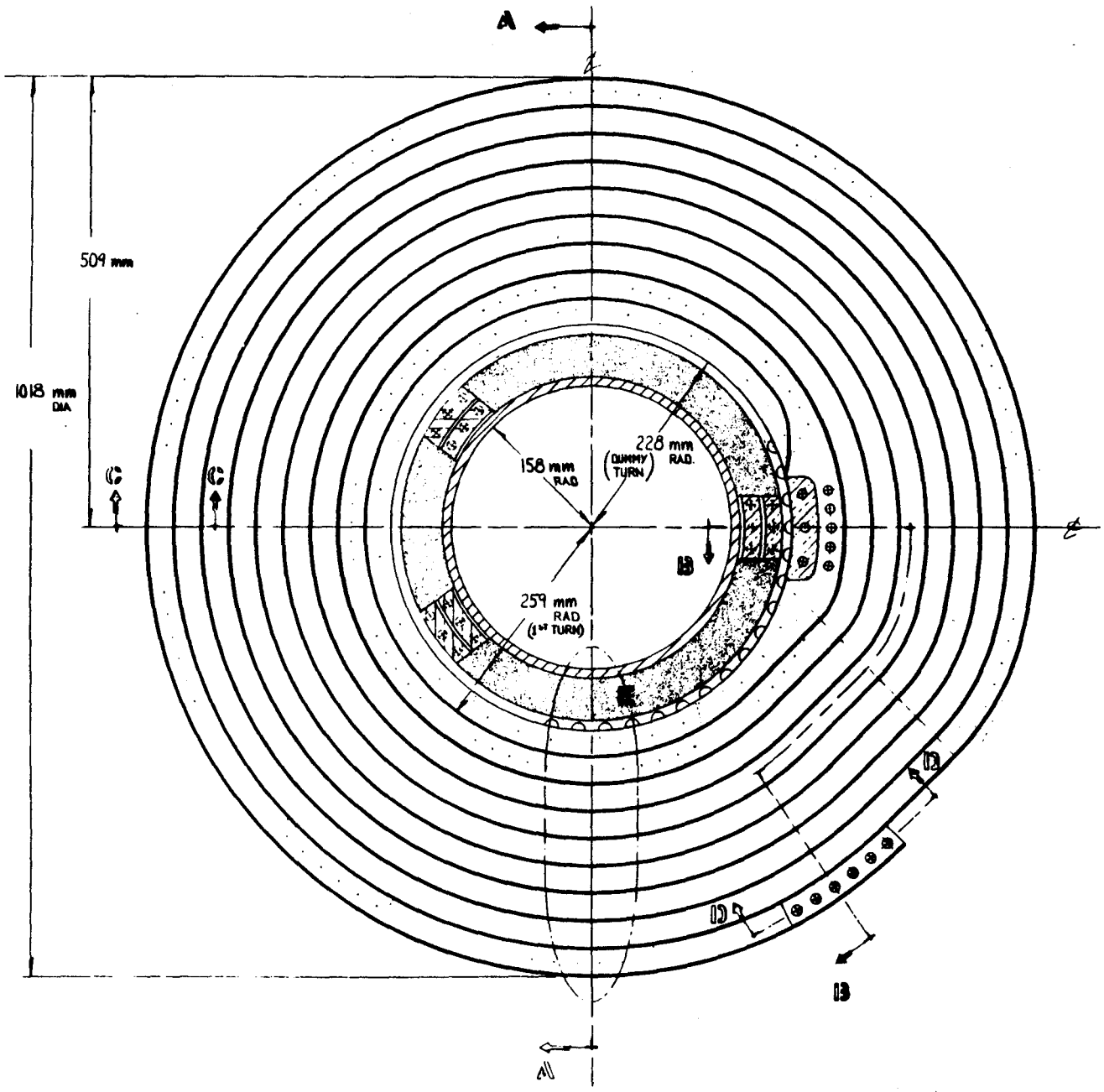

Figure 4.2-2
PF1 and PF2 Typical Pancake Coil
(Plan View)

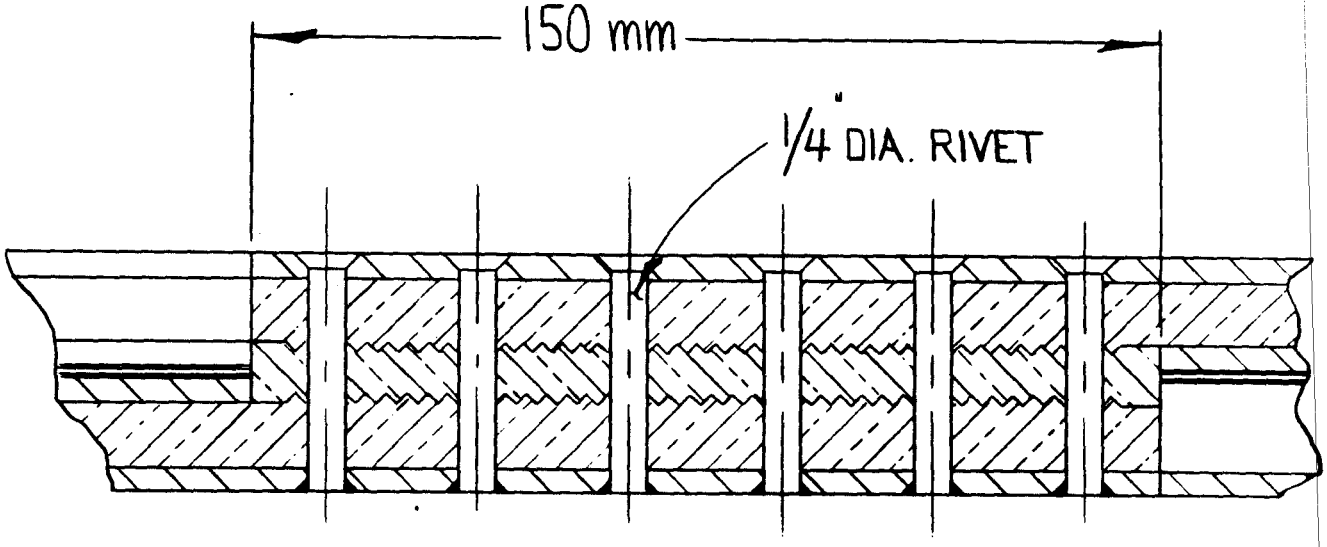

D - D

SCALE - FULL

Fig.4.2-3
PF1 and PF2 Outer Connection

The first turn of the pancake is a dummy, carrying no current. This turn is included to give an inside diameter without protruberances from the interconnections (except at terminations). This is necessitated by the liquid-nitrogen cooling scheme, described later.

It is proposed that the central solenoid stack should support part of the TF preload. This, together with thermal effects and the PF axial electromagnetic loads, causes axial contraction which requires that the six leads must be allowed to move at their external connections.

4.2.2 Ring Coils(PF3 - PF5)

All of these coils are wound from hard copper strips, cold welded and dressed during winding to form a continuous conductor. Figure 4.2-4 shows a section typical of all the ring coils.

The coils are edge cooled by liquid nitrogen flow and housed in welded stainless steel containers. For PF4 and PF5, this housing is integrated with external structure to support a substantial part of the hoop load. Manifolds at top and bottom of the steel housing direct nitrogen past the coil edges. The first and last turns of each pancake are shielded against face cooling. Figure 4.2-5 shows the plan view of a portion of a typical ring coil. Glass-epoxy wrap is used to define passages for coolant flow and to consolidate the turns of the coil.

4.3 Stresses

These have been calculated for the turns of the PF1 and PF2 coils. Estimates for PF3 through PF5 indicate that the copper in PF3 is sufficient for in-plane load support but that PF4 and PF5 require additional steel structure. Estimates have also been made of stresses in the interconnections of coil PF2 to show feasibility.

Table 4.3-1 gives the main stresses. Table 4.3-2 gives the assumed material properties for copper and Inconel and Table 4.3-3 gives typical winding properties.

The first three columns at the top of Table 4.3-1 give the hoop, axial and Tresca stresses for the inner layer at the worst axial location in each PF coil for the peak load condition in time and location. The next three columns give the same information, but averaged over the radial build at the worst axial location. These results are translated into the Tresca stresses in the Inconel and copper in the lower half of the table.

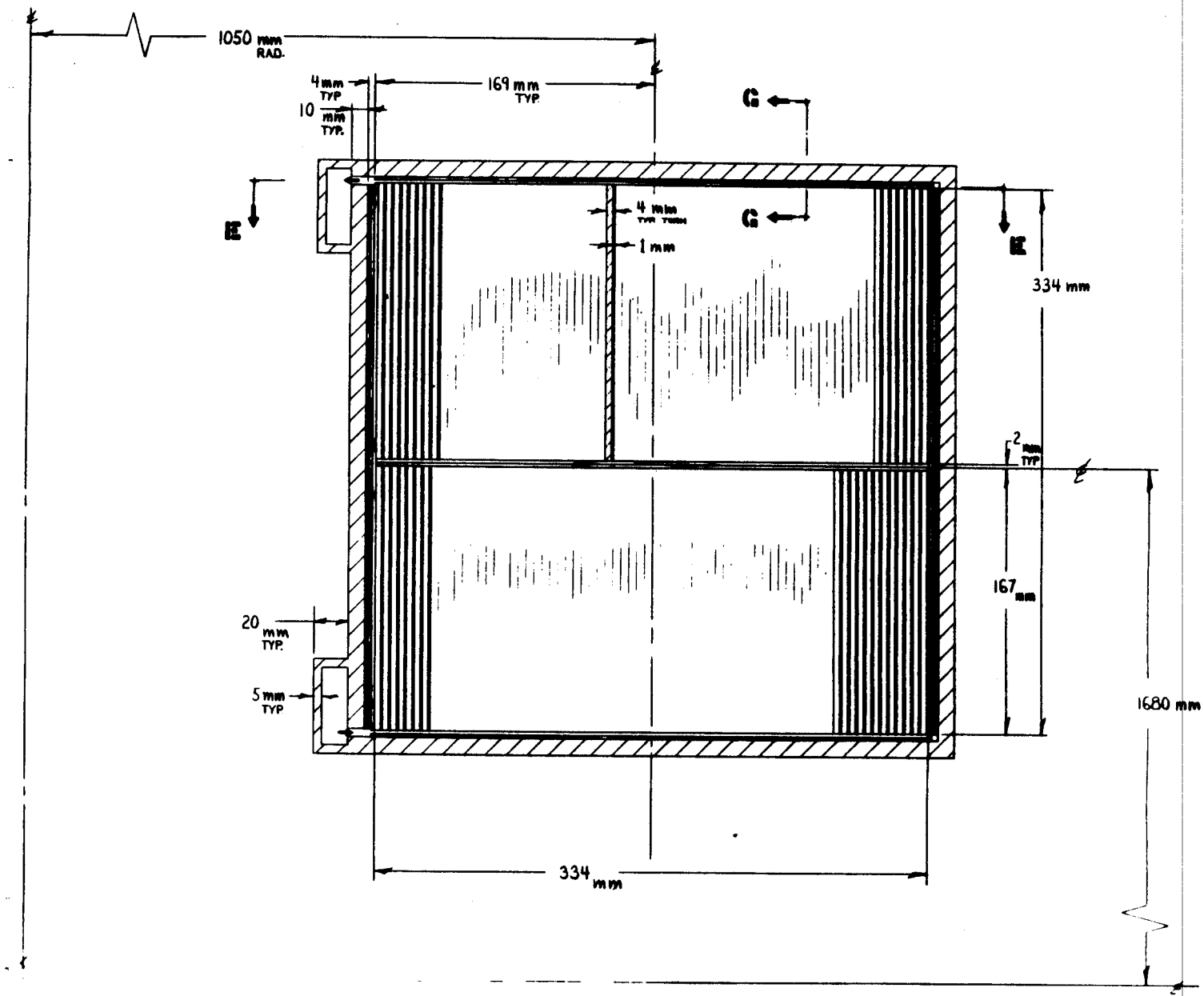

Figure 4.2-4
Section of Typical Ring Coil

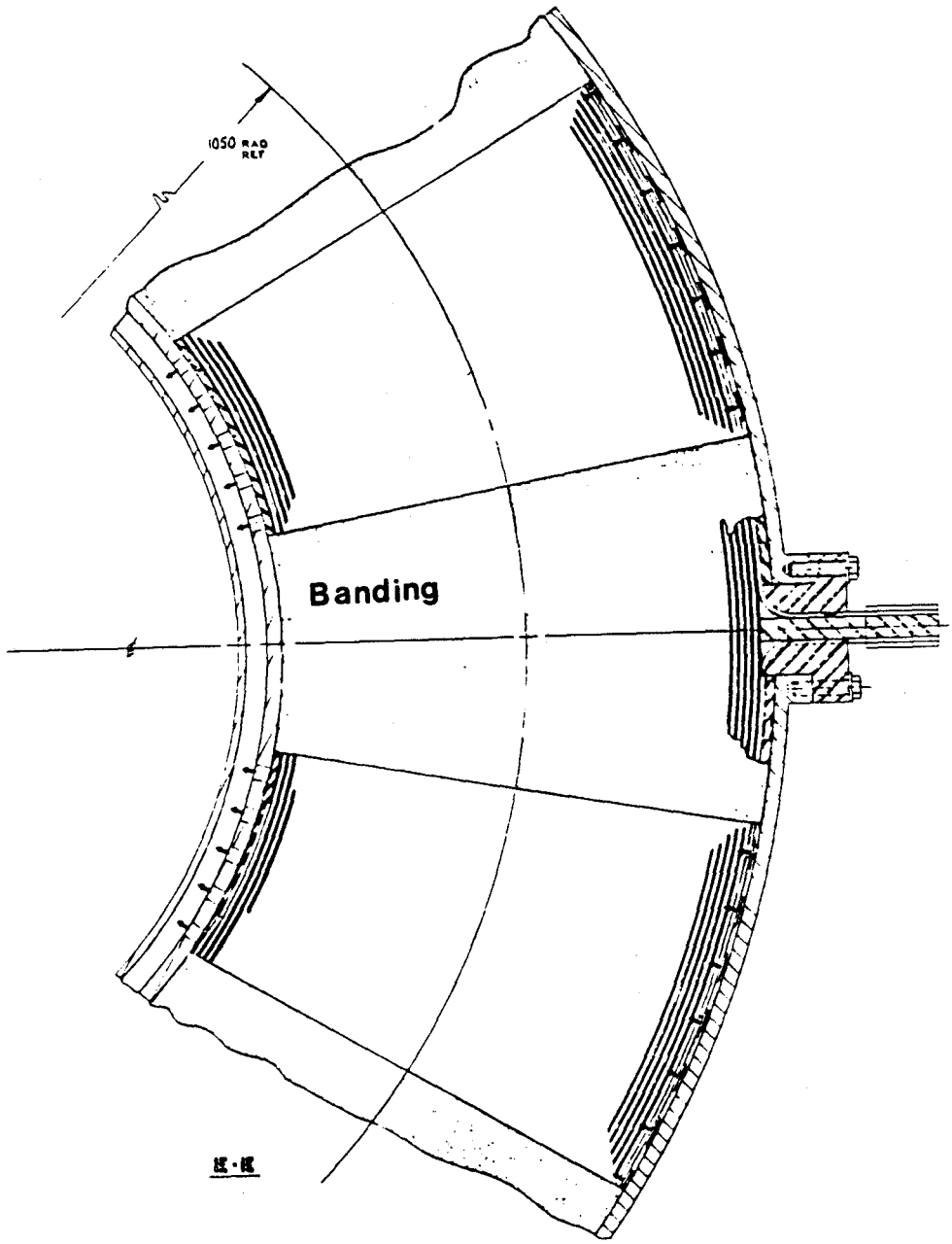

Figure 4.2-5
Plan View: Typical Ring Coil Showing Cooling Passages between Glass-Epoxy Bands and Direction of Coolant Flow into Manifolds

Table 4.3-1
Winding Stresses (MPa) – Peak Load Condition (Time and Location)

Coil	Average Stress Inner Layer σ_Θ	σ_z	σ_{Tresca}	Average Stress Coil Pack σ_Θ	σ_z	σ_{Tresca}
PF1	438	67	505	316	-78	394
PF2	465	-81.9	546	338	-85	423
PF3	–	–	–	106	-11	117
PF4	187	-42	229	161	-40	201
PF5	–	–	–	272	-17	289

Coil	Maximum Tresca Stress Cu	Inconel	Average Tresca Stress Cu	Inconel
PF1	308	896	308	565
PF2	308	868	308	579
PF3	–	–	138	NA
PF4	–	–	229	$\leq$ 812
PF5	–	–	$\leq$200	$\leq$ 812

Notes:

PF1, PF2: hydraulic press axial preload of 150 MPa not included.

PF3: Copper only, no steel.

PF4: External support to be integrated with out-of-plane structure; values assume 0.13 m^2 of steel support

PF5: Supported by case and to be integrated with out-of-plane structure.

Table 4.3-2
Assumed Material Properties

	E (GPa)	σ_{yield} (MPa)
Copper 102	124	308
Inconel 718	210	1218
G-10	9.5	

Table 4.3-3
Averaged Properties of Windings

Coil	Axial Modulus (GPa)	Circumf. Modulus (GPa)	Radial Modulus (GPa)
PF1	36.1	117	59.1
PF2	71.9	141	69.9
PF4	71.3	109	60.0

The table shows that PF1 and PF2 operate with the copper in yield at the inner turn and also when loads are averaged over the radial build. At the inner turn the Inconel is at 70-80 percent of yield; however, it is below two-thirds yield when averaged over the radial build. These levels are within the guidelines accepted for this phase of the conceptual design based on preliminary analyses and experimental data on laminates of this type. It is clear that an extensive analytical and experimental program is necessary to verify that operation at these levels is consistent with the expected machine lifetime and to develop the proper QC for the materials to be used in the device. These stress levels could be reduced with a modest increase in central solenoid outer diameter.

The ring coil PF3 is wound with unreinforced copper and is self supporting for its in-plane loads. No entries are given for the inner layer stresses because they are expected to be about the same as the average in this case. The coil is located within the structure indicated in Figure 2.1-1 to provide support for the out-of-plane loads it experiences through interaction with the radial fields from the other PF coils.

PF4 presents particular problems because of the large radial forces it experiences at the end of burn. Without support, the copper of PF4 within the present envelope suffers an average Tresca stress of 501 MPa, greatly exceeding its yield. Radial and hoop support for this coil will therefore be provided by the structure which also equilibrates the vertical loads between the PF coils. This is a structure which is integrated with the TF system.

PF5 is not as heavily loaded as PF4, but cannot be self-supporting for its in-plane loads if it is copper alone. It will be supported by the case shown in Figure 2.1-1 which will also be integrated into the system to provide out-of-plane support. Estimates indicate that a five centimeter case wall is sufficient to drop the Tresca stress in the copper to below two-thirds yield when averaged over the radial build.

Table 4.3-4 gives the stresses in various parts of the interconnector between inner turns of the PF2 pancakes. See Figure 4.2-2. The stresses are as follows:

i) Shear in pins. This is calculated as if all of the hoop tension in the first active turn (289 kN) were shared equally by the 8 pins with no other load path.

ii) The Inconel is removed from juxtaposed faces of the first (dummy) turn at the interconnection. It is replaced by copper soft soldered to exposed faces of the composite copper. Face shear would be the shear in this solder bond, if no other load path existed.

iii) The remaining copper-Inconel composite, after removal of the Inconel surface as

Table 4.3-4
Stresses in PF2 Interconnections

Shear in Pins	510 MPa
Face Shear In Copper	98.2 MPa
Edge Shear in Copper	203 MPa
Peak Tensile Stress in Composite	364 MPA
Stress Concentration Factor	2.0
Max. Avg. Metal Hoop Stress	364 MPa

Definitions (see drawing)

Pin Shear

shear stress in any of 8 pins joining the ends of the inside turns of adjacent pancakes

Face Shear

shear stress in the solder between the copper insert and conductor copper at the joint between inside turns

Edge Shear

average shear stress in the conductor copper and an Inconel sheet in a plane parallel to the coil axis where the interconnector extends radially inward from the turn end.

in (ii) above, is common with the rest of the turn through an imaginary surface oriented in a vertical plane and coincident with the boundary between the dummy and first active turns. The edge shear is the stress on this imaginary surface with no parallel load path.

The actual load path in the interconnector is shown in Figure 4.3-1. The division of loads between the elements requires a 3-D FE computation, but it will be noted that the edge shear is a critical component.

The interconnector is formed from the junction of the dummy turn and the first active turn by doubling the radial width at that point. Stress concentration in the composite around the pins doubles the local stress. This increased stress is given in Table 4.3-4. It appears that the stresses in the interconnector should be within allowables, but a detailed finite element analysis is required for verification.

4.4 Cooling

Forced liquid-nitrogen flow is used to cool or recool all coils. The longest allowable recool time is one hour. For the central solenoids, the recool time is dictated by the temperature gradients in the various parts of the thermal circuit.

4.4.1 Central Solenoids (PF1 and PF2)

Because of the high axial stresses imposed on the PF1 and PF2 coils, either by TF preload or by self radial fields, radial coolant flow is undesirable. Conduction cooling will therefore be used as shown in Figures 4.4-1 and 4.4-2. Copper plates interposed between pancakes and insulated by thin G-10 will conduct heat radially to fins located in axial channels formed in G-10 on the inner and outer diameters of the coil.

The equivalent circuit of cooldown is shown in Figure 4.4-3. Each C represents the thermal capacity of one turn of one pancake "charged" initially to 239 K. The temperature is actually 319 K; that is, 239 K above the assumed final condition of 80 K. G1 represents the interturn thermal conductance through G-10 or equivalent. G2 represents the conductance between the turn and the copper cooling plate and G3 is the radial conductance of that plate over a distance of one turn. G4 is the heat transfer coefficient between the fin at the edge of the plate and the coolant. Table 4.4-1 gives these conductances per turn.

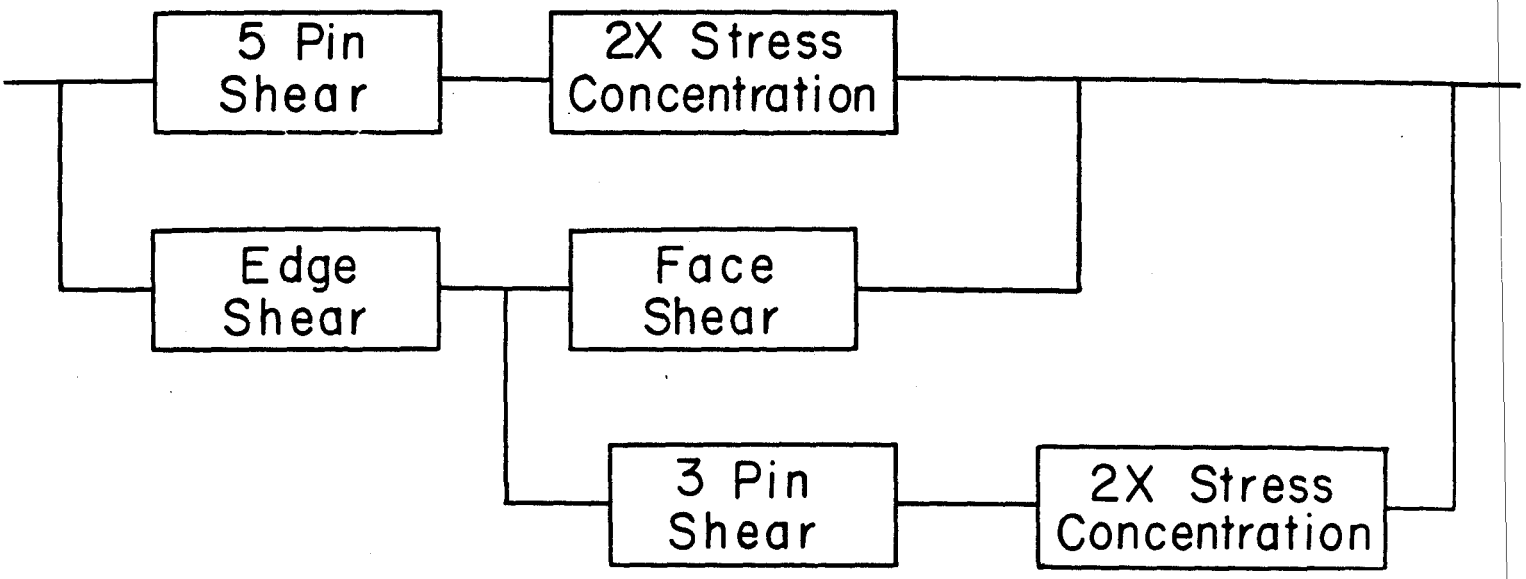

Figure 4.3-1
Approximate Paths of Tensile Load Through the Inside Interconnector
(See Table 4.3-4 for Definitions)

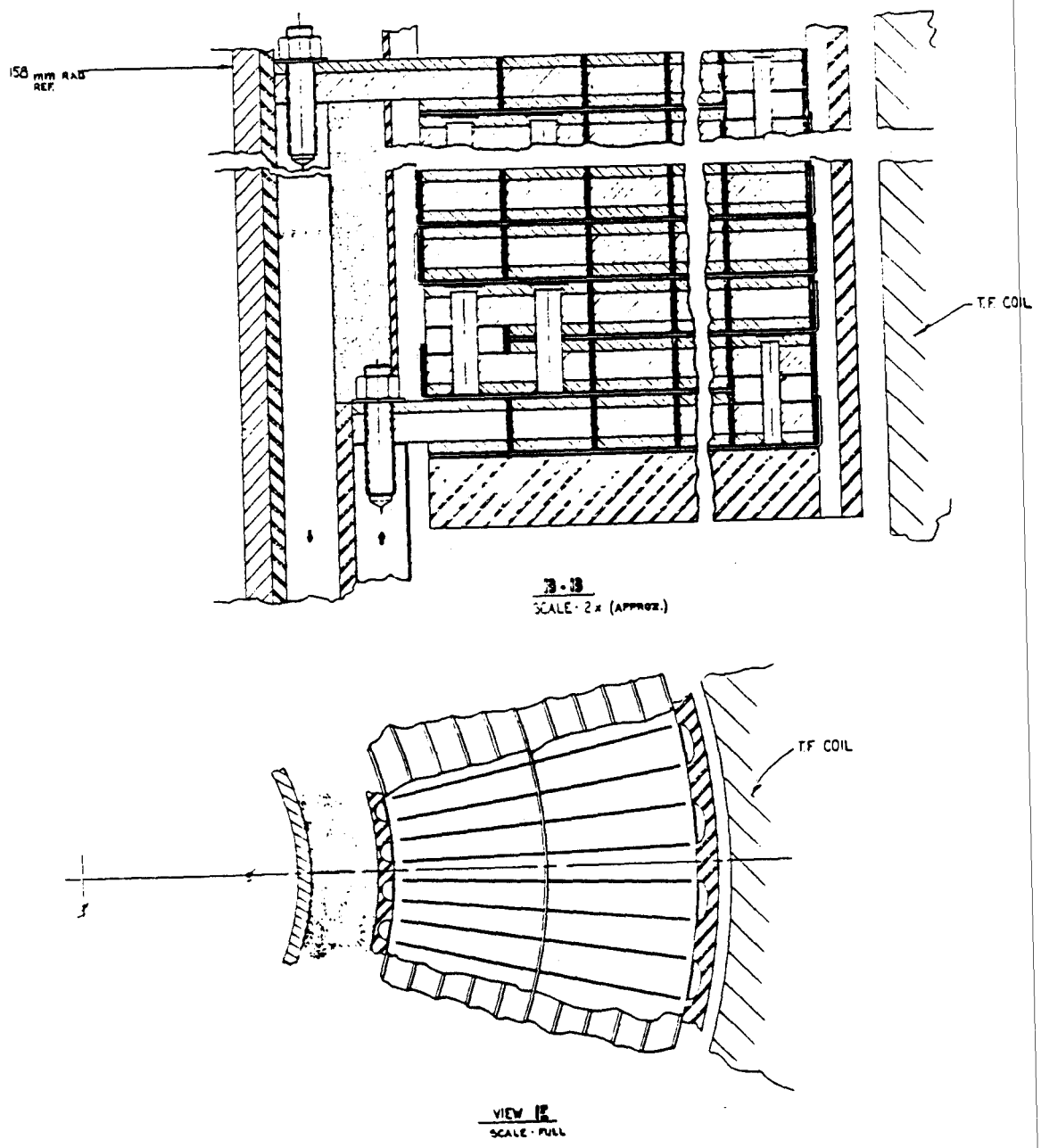

Figure 4.4-1
Top: Section View of PF2 Showing Leads , Inner and Outer Interconnectors, and Cooling Passages
Bottom: Section Showing Cooling Interplate and Coolant Passages

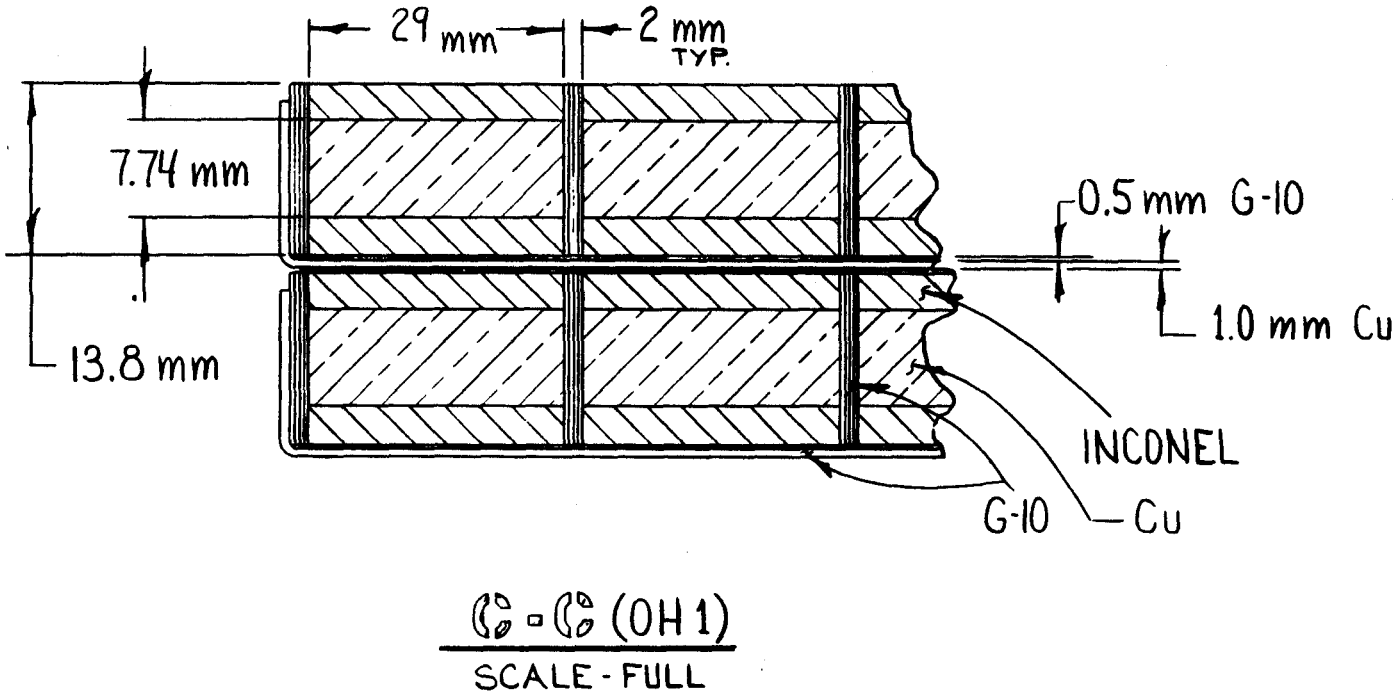

Figure 4.4-2
Detailed Section Showing Cooling Fin Projecting Into Cooling Passage and Occlusion of Turn 1 from Coolant

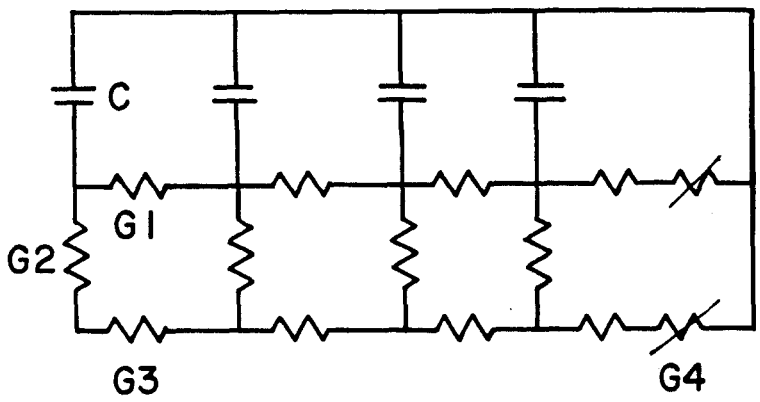

Figure 4.4-3
Equivalent Circuit of Cooldown

Table 4.4-1
Parameters for Circuit in Figure 4.4-3

C	0.005 MJ/K	5000 F
G1	11.5 W/K	0.087 Ω
G2	69.8 W/K	0.014 Ω
G3	15.5 W/K	0.065 Ω
G4	10 – 50 W/K	0.05 Ω
V_0	239 K	239 V

The thickness of the copper plate and the size of the tab are chosen so as to control the rate of cooldown and hence the radial and circumferential stress in the interturn insulation.

The network of Figure 4.4-3 has been solved using the values given in Table 4.4-1. Figure 4.4-4 shows the cooldown rate for four turns. Because there are two cooling paths, to the inside and to the outside channels, only four turn temperatures are shown. The maximum turn-to-turn difference is 25 K and the average absolute temperature after one hour is 120 K. (Figure 4.4-5 shows the cooldown curve for 2-mm thick copper interplates and the average temperature after one hour is 105 K.) In the analysis, no attempt was made to vary the conductance, G5. In fact, a fixed value of 20 W/K was assumed, whereas in fact it will vary between 10 and 50 W/K as the copper interplate temperature falls from 319 to 80 K. Furthermore, the effective capacitance C decreases as the temperature falls. Both of these effects decrease the cooling time constant.

For a temperature difference per turn of 25 K, the radial tension in the interturn insulation is 5.5 MPa.

4.4.2 Ring Coils (PF3 - PF5)

These are strip-wound copper coils cooled at one edge only with LN_2 forced flow between pulses. Figures 4.2-4 and 4.2-5 show the cooling arrangement for PF coils 3 through 5. The coils are 50% wrapped with glass. The edges of the conductors are exposed at the top and bottom of the coil pack. The inside face of the inner turn and the outside faces of the outer turns are occluded by G-10 to minimize cooling. Manifolds top and bottom of the steel container route the liquid nitrogen. Concepts for interfacing the wound coils with their cryogenic containers and support structure for in-plane and out-of-plane loads are in the process of being developed.

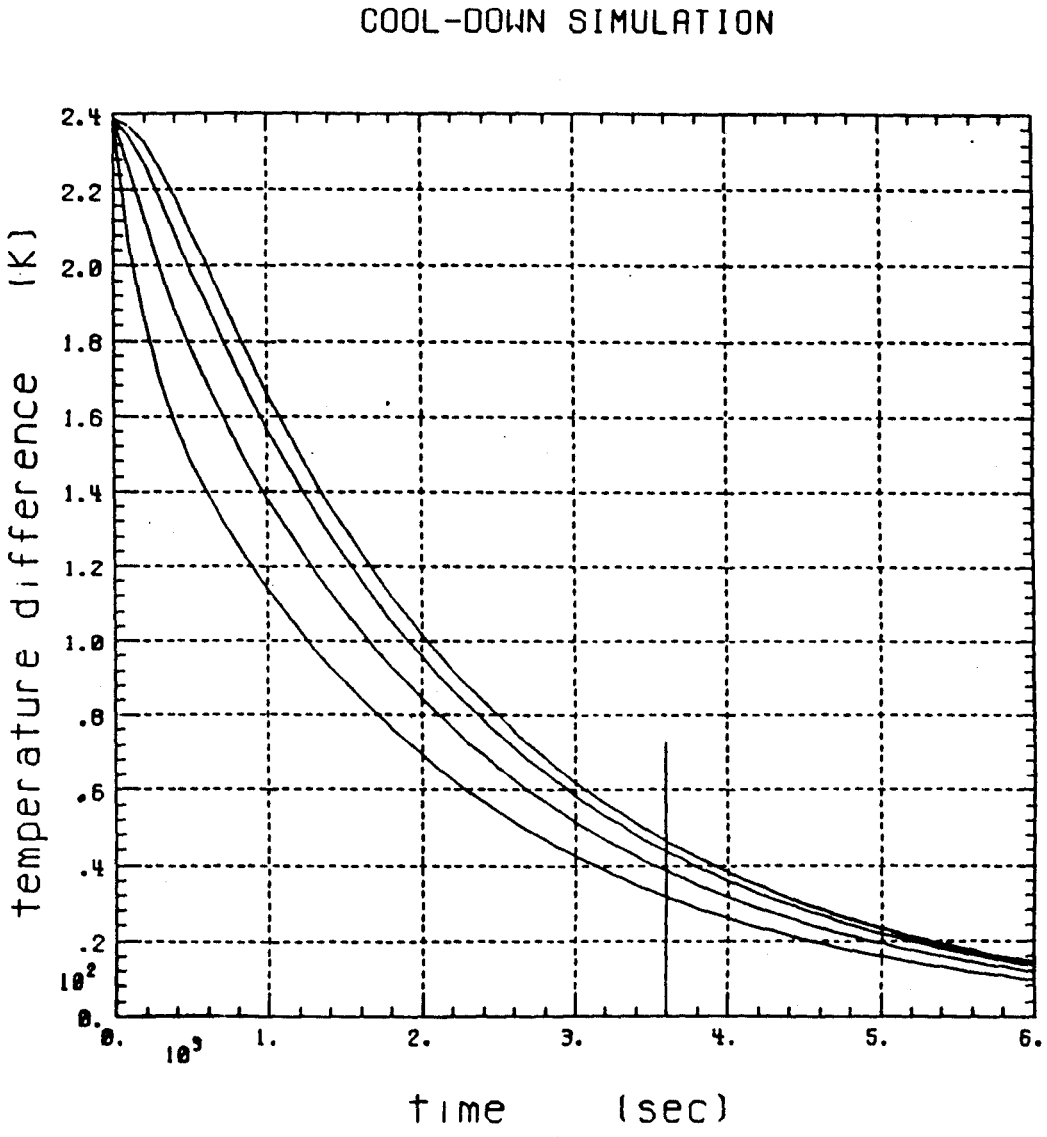

Figure 4.4-4

Cooling Curves for the Four Outermost Turns of PF1 or PF2

The Temperature Difference Shown is that Over 80 K

Same Curve for the Four Innermost Turns

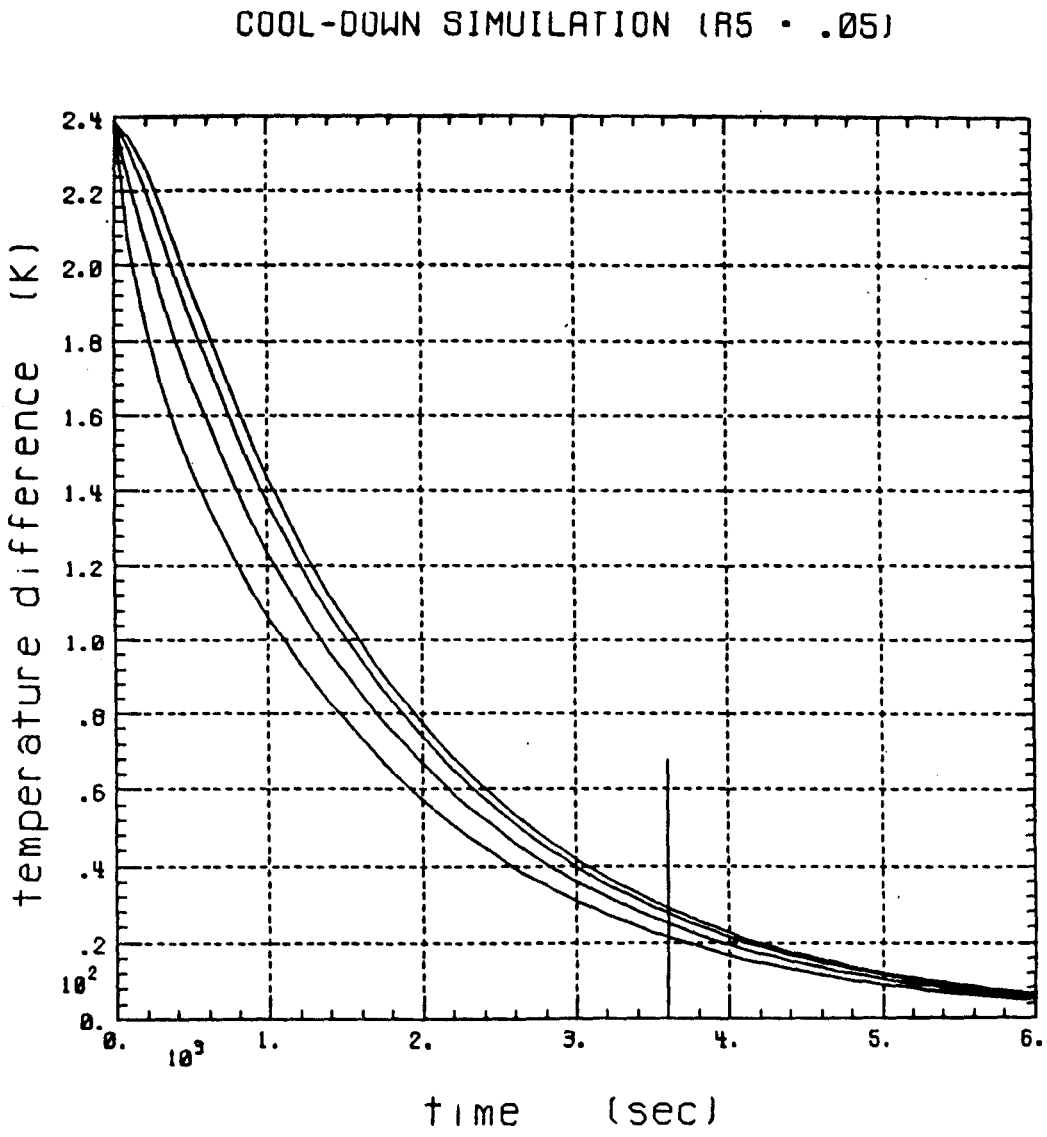

Figure 4.4-5
Cooling Curves for Four Adjacent Turns as in Figure 4.4-2 but for Copper Interplate Thickness of 2 mm

4.5 Alternate PF Designs

4.5.1 Central Solenoid (PF1 and PF2)

A possible alternative arrangement of material in a central solenoid turn would involve winding steel in parallel with the copper as shown in the lower sketch of Figure 4.5-1. The upper sketch shows the dimensions for a turn in the baseline design for comparison. The alternate design relies on the radial outward load from the copper to be reacted by the Inconel in pressure-vessel fashion. Figure 4.5-2 depicts a possible joint structure for the alternate conductor design.

4.5.2 Ring Coils (PF3 - PF5)

An alternate ring coil winding pack construction is under consideration. It is based on standard technology involving hollow copper conductors in vacuum impregnated winding packs. Each coil would be mounted in a steel case with ground insulation grooved on the inner and outer radius to form a plenum at these locations for the nitrogen feed and vent. Coils would be wound in double pancakes with nitrogen feed at the crossover between layers at the inner radius and nitrogen vent at the crossover between layers at the outer radius.

To shorten the coolant path length through the turns of the pancake, the pancakes would be wound with multiple conductors "in-hand" or in parallel. For example, if four conductors in-hand were used, the pancake to pancake crossover for each conductor would be ninety degrees out of phase with the previous and subsequent crossover. Turns could still be connected in series electrically, but would be in parallel hydraulically. Coils would be wound and vacuum impregnated. Coolant openings would then be formed by boring into the side of the conductor at each of the crossovers at the inner and outer radii. The coil would then be inserted into a steel container lined with the necesssary grooved insulation to provide the nitrogen plenum on the inner and outer surfaces. In-plane load support for PF4 and PF5 could be partially or totally supplied by winding steel in parallel with the copper or by the structural cases as in the baseline design.

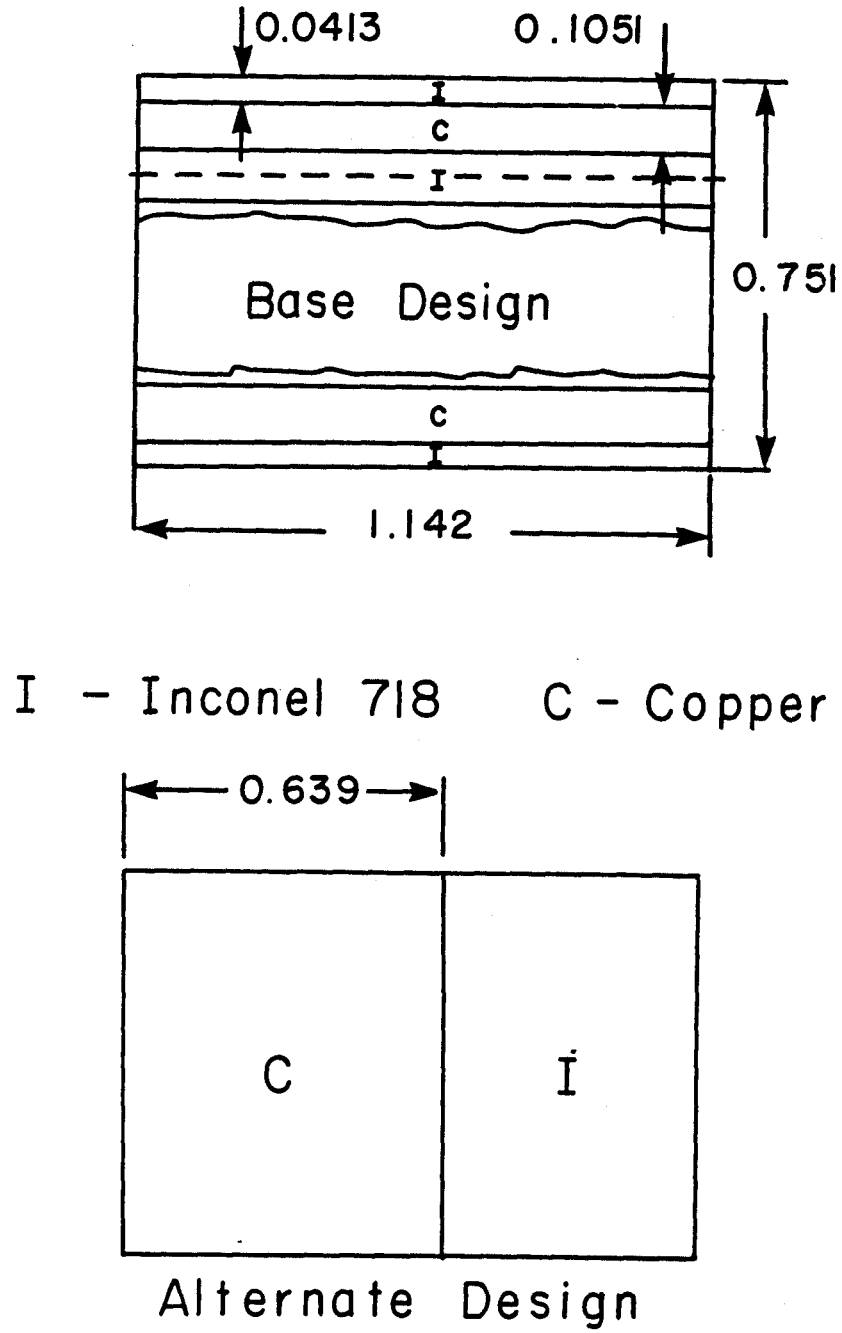

Figure 4.5-1
Dimensional Comparison of a Typical PF1 or PF2 Turn for the Baseline (top) or Alternate (bottom) Designs

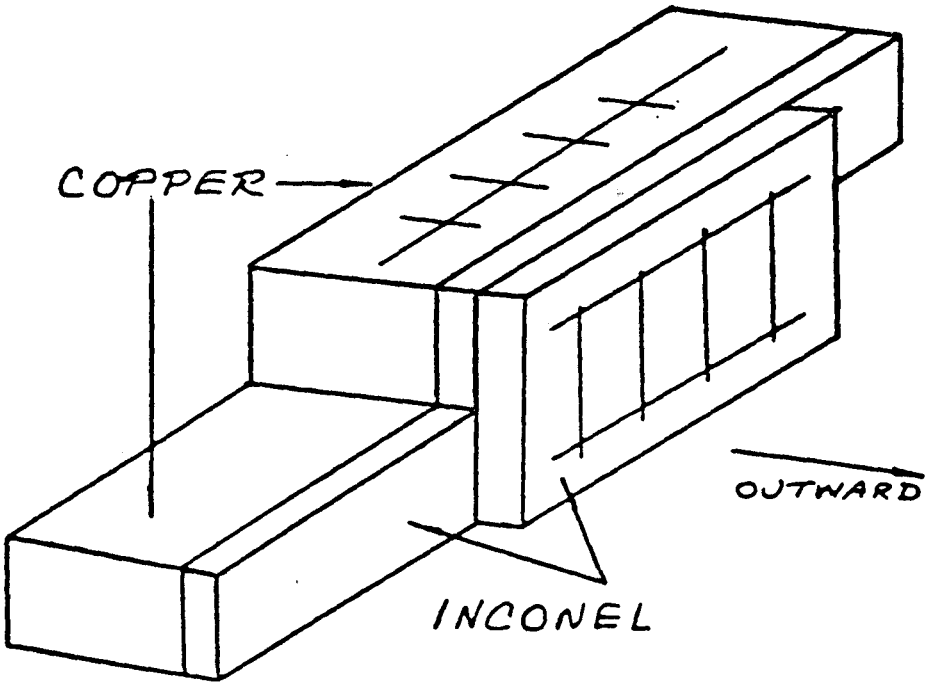

Figure 4.5-2
Illustration of Joint for Alternate PF1 or PF2 Winding

5.0 Divertor Plates

One of the tasks assigned to the PF system design team during this portion of the CIT conceptual design involved the determination of the profiles for the divertor plates. These profiles were then provided to the vacuum vessel design team (WBS D) for integration into the machine. This section outlines the physics requirements for these plates, the method for estimating the profiles, and results of preliminary one-dimensional thermal calculations on plate temperature rise during a pulse. More detailed calculations on temperature and stress during operation were performed under WBS B.

5.1 Physics Requirements

The divertor is required to absorb the incident rf and alpha particle power without contamination of the plasma by impurities and with an acceptable erosion rate. In CIT, a low-temperature, high particle density is desirable near the divertor plates. The low temperature reduces erosion while the high density results in high particle recycling and eliminates the need for active pumping. The temperature and density near the plates are determined by localized particle recycling coefficients and a high recycling rate is essential. More detailed calculations for estimates in this area are under way at Princeton. Meanwhile, estimates of plate profiles, heat loads, temperature profiles, and sensitivity to selected PF characteristics have proceeded on the basis of simplified assumptions.

The heat load, and one-dimensional temperature estimates reported below are acceptable at this stage of a preconceptual design, but indicate a strong sensitivity to plasma and flux profile details. It is clear that a concise definition of possible plasma variations during operation is needed because of their strong impact on maximum heat loads.

The following guidelines were provided for the initial calculations to be done for the CIT divertor plates:

a) The distance from the field null or "x-point" to the divertor plate should be at least 15 cm measured along the field line.

b) The total heat load is 60 MW of alpha power, of which 42 MW is absorbed by the divertor plates over a time of about 4 s.

c) The heat load will divide between inboard and outboard divertor plates. Two thirds of the total will be absorbed by the outboard plates and 1/3 by the inboard plates.

d) The radial scrape-off decay length ("e-folding") for energy at the midplane on the small major radius side will be 0.625 cm, with a possible variation of ± 0.125 cm.

e) A "box" type divertor chamber will be used.

f) Tile materials will be graphite or molybdenum.

5.2 Divertor Plate Profiles and Heat Loads

Preliminary divertor plate profiles have been determined for the 0306D double-null configuration. These are illustrated in Figures 5.2-1 and 5.2-2 for the inboard and outboard plates, respectively. Their relationship to the machine may be seen in Figures 2.1-1 and 2.1-4.

Plasma equilibria were analysed to determine power distributions at the midplane between flux surfaces and to obtain divertor profiles based on the flow between surfaces. The shape of the divertor plates was determined by adjusting the local tangent to the plate so that the incident heat load on a plate was constant in the high flux region.

A typical heat-load distribution and variation with radial scrape-off length for power at the midplane is shown in Figure 5.2-3 for the outboard plate. The flat profile denoted with a nominal heat-load value of 8 MW/m^2 is the baseline determined by adjusting the local plate tangent to maintain the incident heat flux constant. The curve with a maximum at about 10 MW/m^2 is the heat-load profile which occurs on the same plate if the e-folding length for power scrape-off at the midplane is changed from a nominal value at 0.625 cm to 0.50 cm. Similarly, the profile with a maximum at about 9.25 MW/m^2 is the heat-load distribution on the plate if the e-folding length changes to 0.75 cm. Similar profiles for the inboard plate are shown in Figure 5.2-4. They show that the heat load on the inboard plate is less severe.

5.3 Plate Temperature Profiles

A typical temperature profile determined on a one-dimensional basis is illustrated in Figure 5.3-1. The location of a 3 cm molybdenum tile and 0.5 cm stainless steel backing plate is shown along the abscissa. Each curve corresponds to an instant of time during heat cycling consisting of 2 s of rf heat load followed by 4 s of alpha heat load, followed by a cooling period. Note that the gap conductance has a strong influence on the temperature of the backing plate since it slows down the diffusion of heat into the plate.

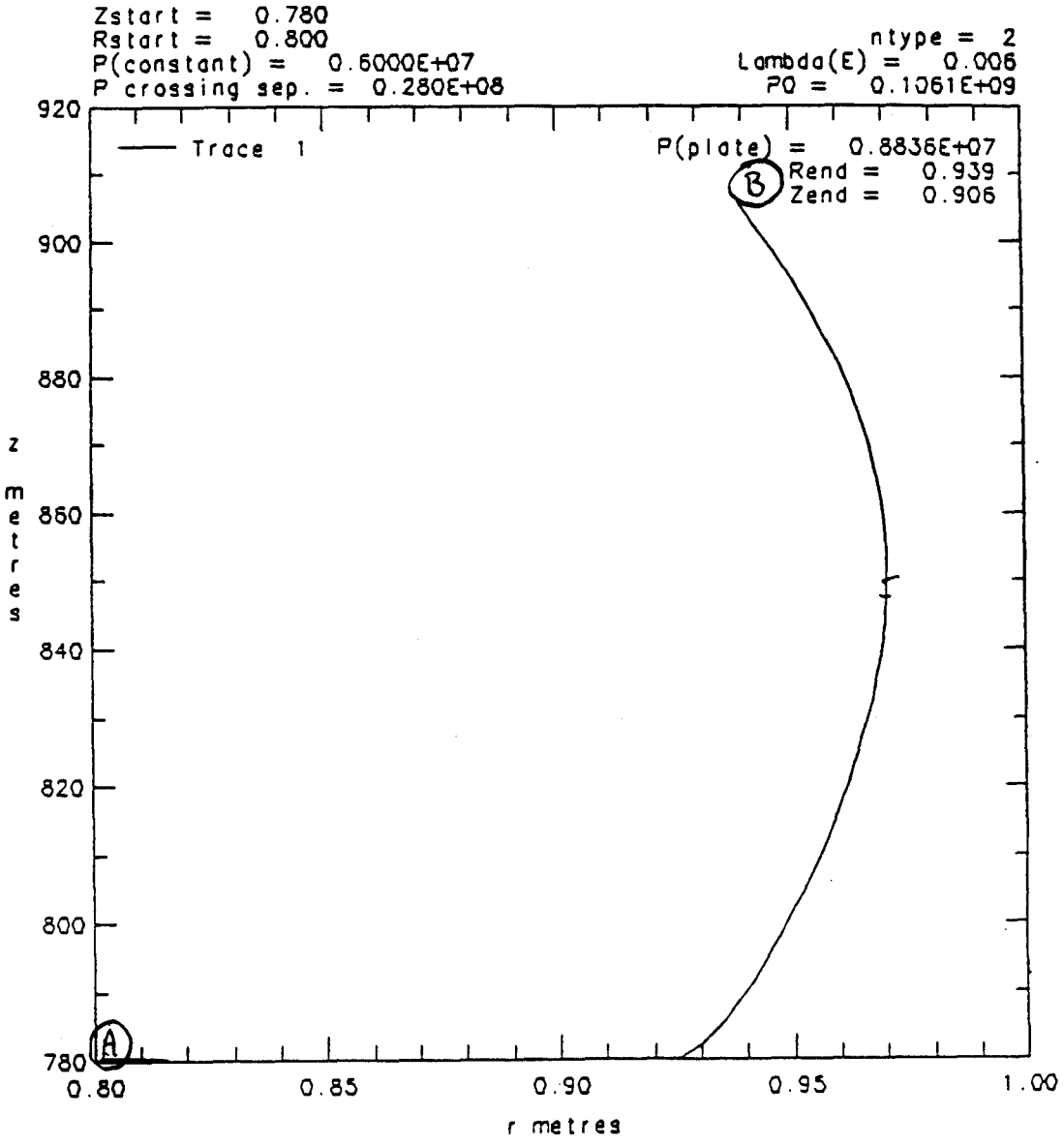

Figure 5.2-1
Inboard Divertor Plate Profile (MIT 0306D)

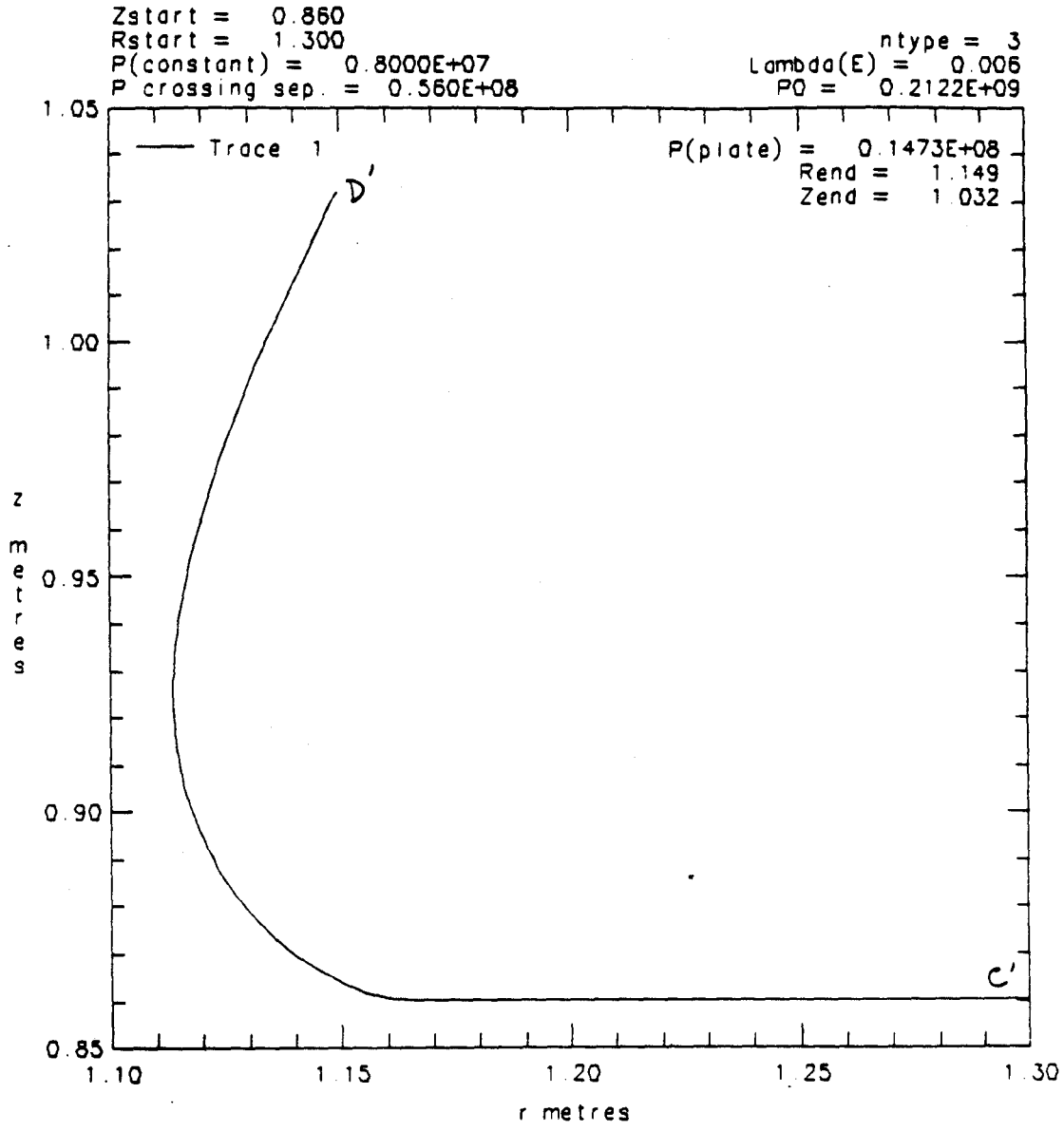

Figure 5.2-2
Outboard Divertor Plate Profile (MIT 0306D)

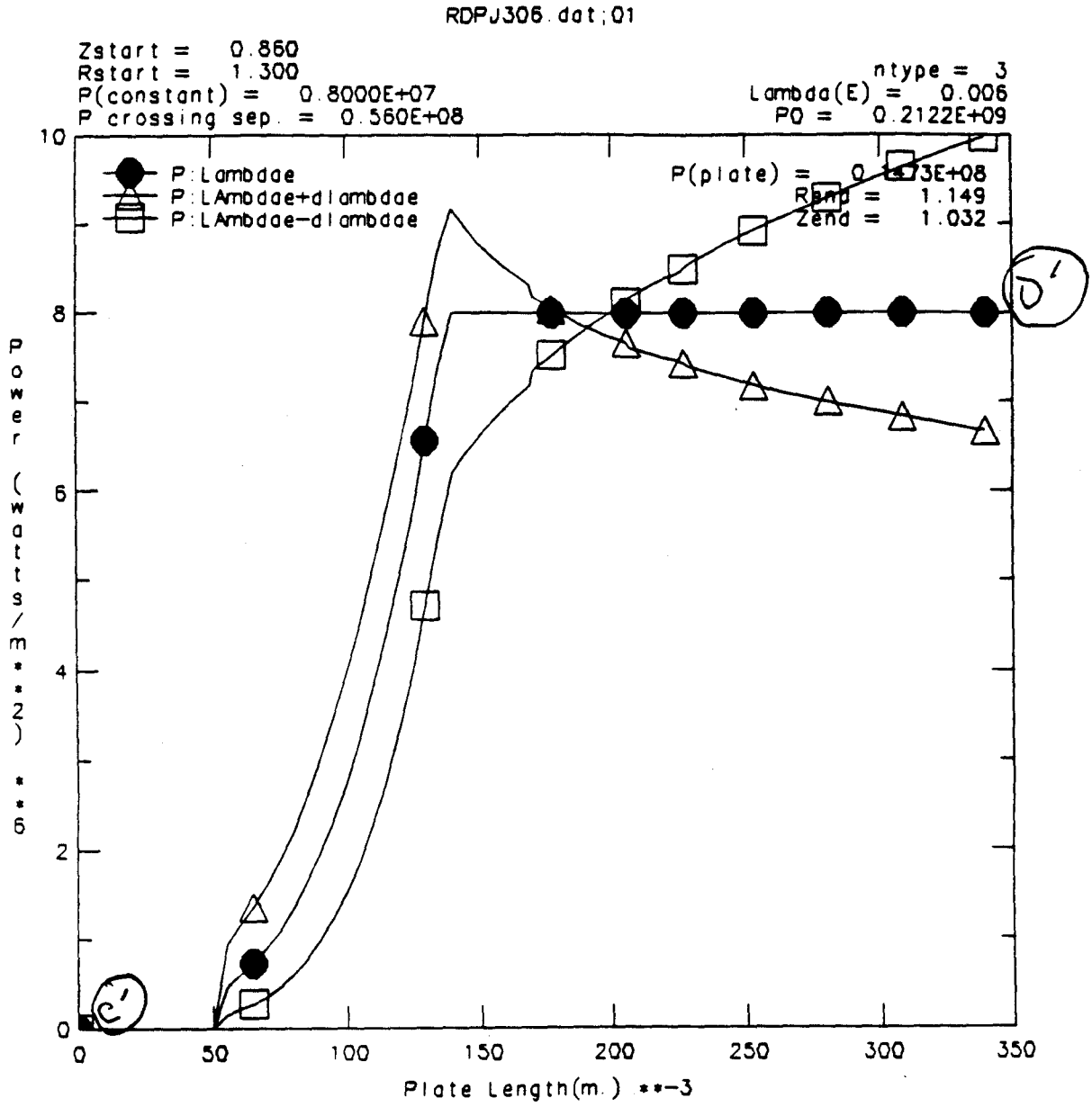

Figure 5.2-3
Outboard Plate Heat Flux (MIT-DIV 0306B)

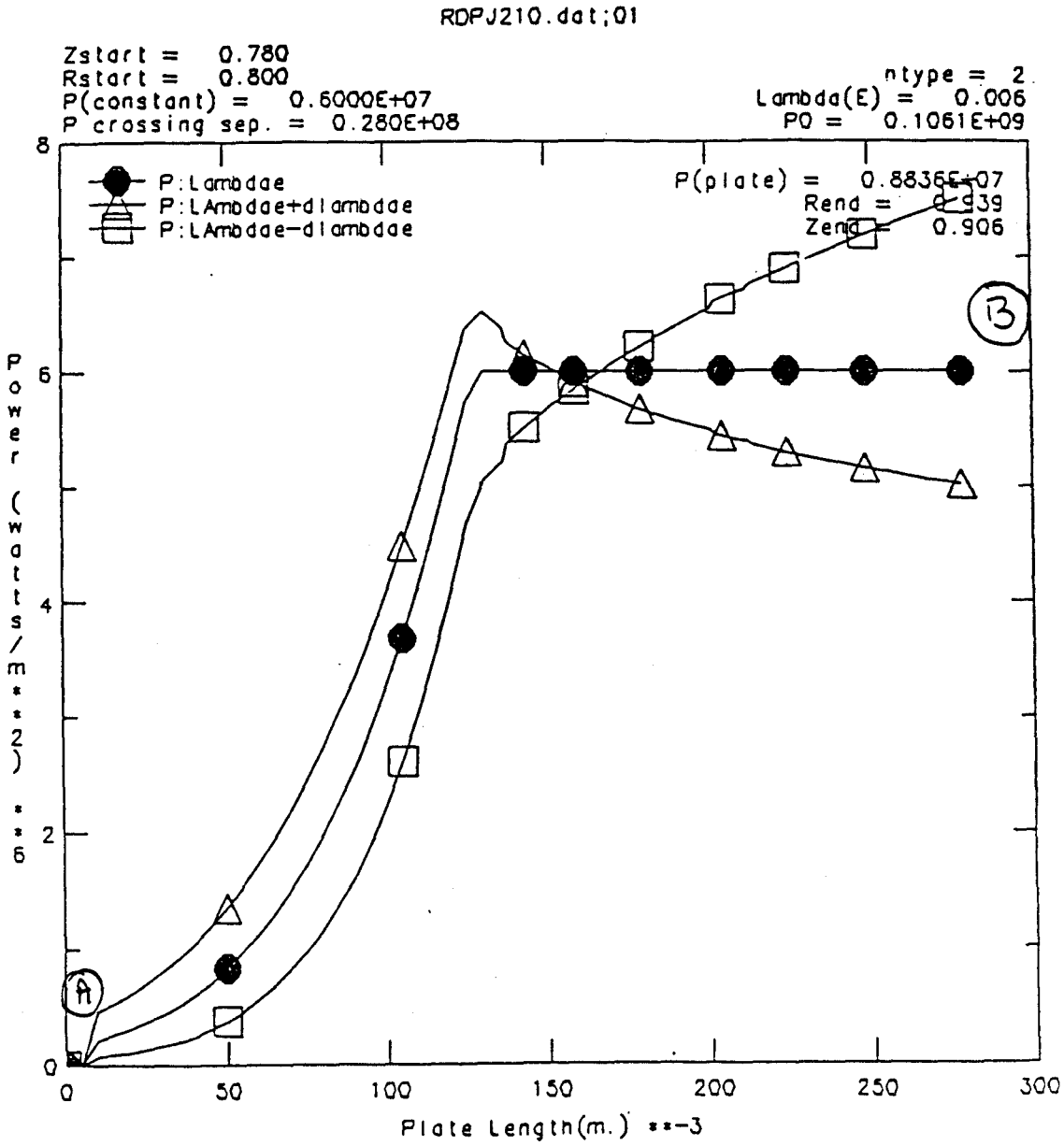

Figure 5.2-4
Inboard Plate Heat Flux (MIT-DIV 0306 = MIT 0228)

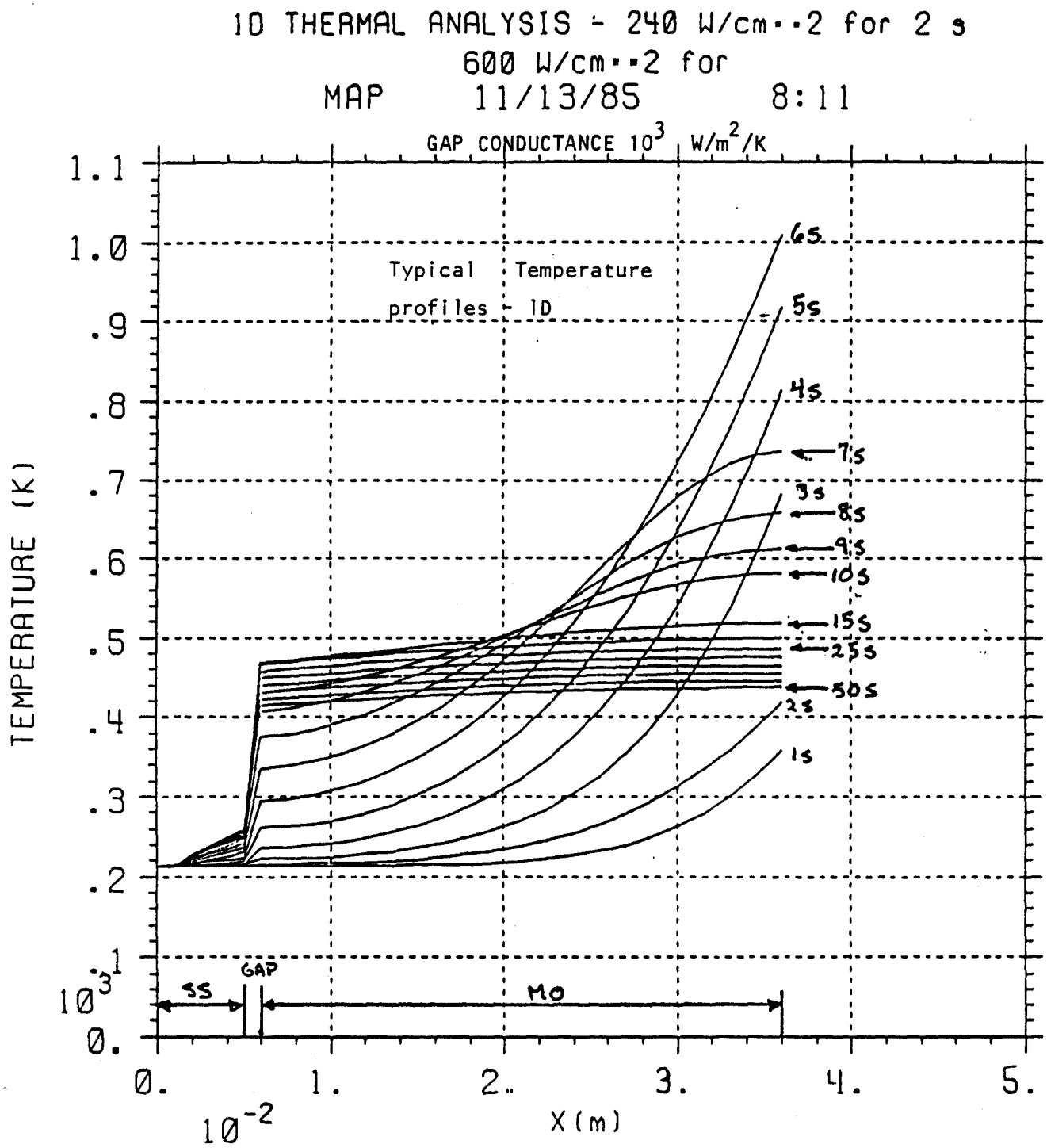

Figure 5.3-1
Typical 1D Temperature Profiles Through Molybdenum Tile with Stainless Steel Backing Plate

Table 5.3-1
CIT Divertor Plate Thermal Stress Analyses
One Dimensional

Mat'l	RF for 2s (MW/m^2)	α for 4s (MW/m^2)	Gap Conductance ($W/m^2/K$)	T_{max} (K)	T_{maxss} (K)
Moly	3.6	9.0	10^4	1407	419
Moly	3.6	9.0	10^3	1407	292
Moly	3.6	9.0	10^2	1407	224
Graphite	3.6	9.0	10^4	1502	359
Graphite	3.6	9.0	10^3	1502	274
Graphite	3.6	9.0	10^2	1502	221

Table 5.3-1 summarizes some results for a molybdenum/stainless steel and a graphite/stainless steel configuration at heat loads of 9 MW/m^2. Results show the strong influence of gap conductance on maximum temperature in the stainless steel and imply that it must be maintained below a certain level. The gap conductance has little influence on the surface temperature of the tiles since conditions are essentially adiabatic at that location. If an allowable temperature of about 2000 K is assumed for the tiles, the table implies that heat loads of up to about 12 MW/m^2 would be acceptable. This also assumes that gap conductance can be achieved at a reliably low level. More detailed calculations are underway under WBS B.

6.0 Plasma Shaping and Control

The baseline concept for CIT is for the main PF coils, PF1 through PF5, to provide the primary shaping and control function throughout the pulse. Because of the size of these coils, they are somewhat limited in their response time. As a result, smaller ring coils internal to the TF bore are provided for functions for which a rapid response is anticipated. These are coils I1 through I3 shown in Figure 2.1-1. Studies in this area have begun and preliminary results are summarized in this section.

6.1 Internal Coils

The three pair of internal coils are envisioned as being fabricated in two halves. This is consistent with the concept of creating two half machine subassemblies which are then assembled into one core. Each half of an internal coil would be mounted in its respective core half with its leads running to the outside of the TF coil system through the parting plane. This is illustrated in the elevation view in Figure 6.1-1 and the plan view of a single coil in Figure 6.1-2.

Each of the internal coils is mounted in the space between the vacuum vessel and the TF coil bore. It is supported by mounting fixtures attached to recesses in the bore side flange on the TF structure. Each coil consists of a single turn with a cross section of about 5×6 cm and is cooled between pulses by nitrogen flow through its hollow conductor. Present estimates indicate that a coil operating current of about 100 kA rms will be adequate for plasma separatrix control and vertical stability control. Coil center coordinates are given in the following table.

Table 6.1-1
Internal Coil Center Coordinates

Coil	r (m)	z (m)
I1	1.318	±1.013
I2	1.546	±0.841
I3	1.711	±0.569

Studies of separatrix control for the diverted plasma are under way, but preliminary estimates indicate that about 100 kA in coil I1 can shift the r-coordinate of the separatrix by about 2 cm.

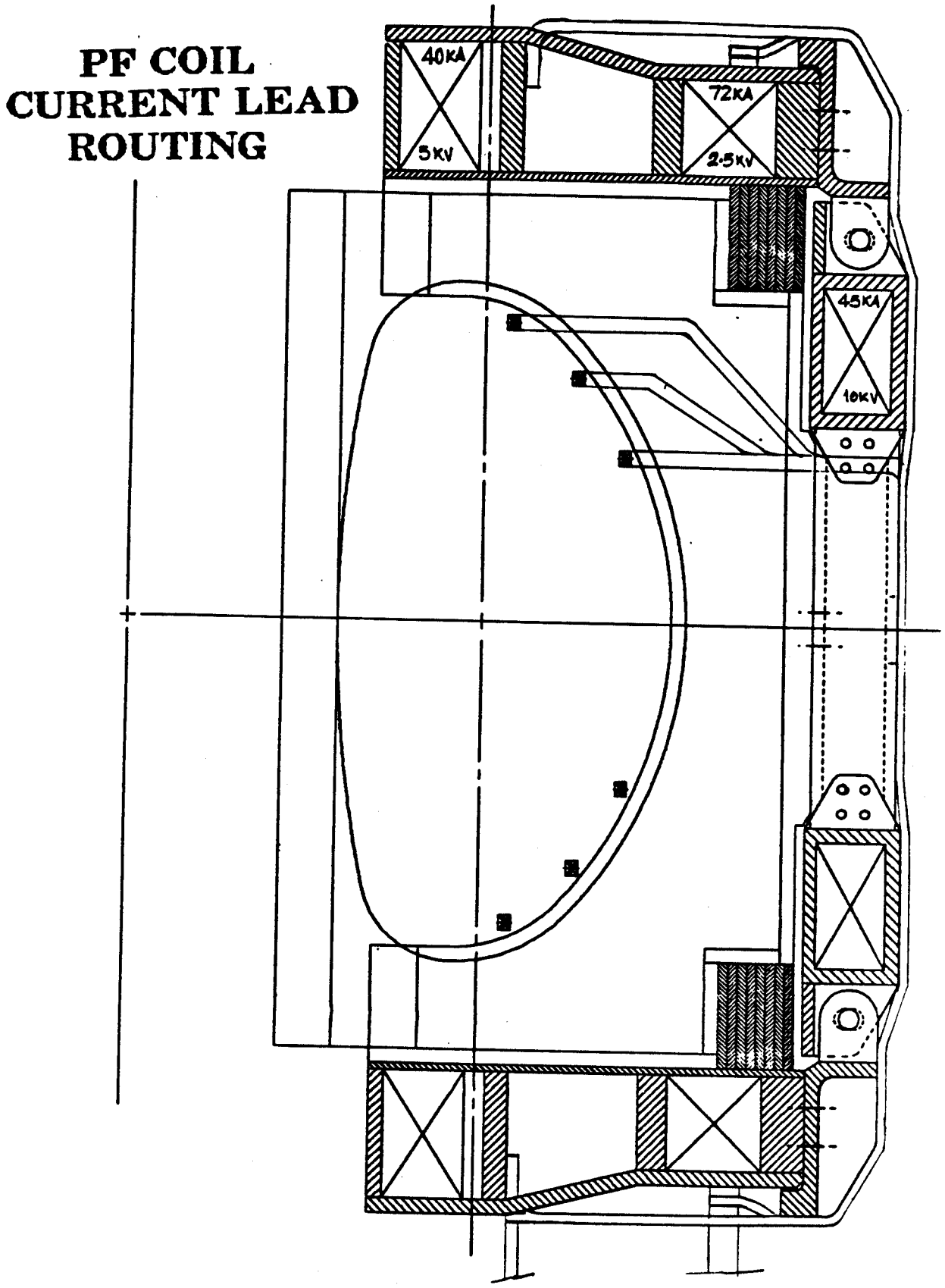

Figure 6.1-1
PF Coil Current Lead Routing, [FEDC]

CONTROL COIL CONFIGURATION

- **Six control coils are installed in the space between the vacuum vessel and the TF coils.**
- **Each coil has a single turn - each turn has a cross-section of 5 cm x 6 cm.**
  Current Rating = 100 kA (rms)
- **Coil conductor has a single hole for coolant flow.**
- **Each coil has an individual set of current leads. They are also internally cooled with liquid nitrogen.**
- **Cooling paths in the leads and the coil are connected in series to form a single cooling circuit.**

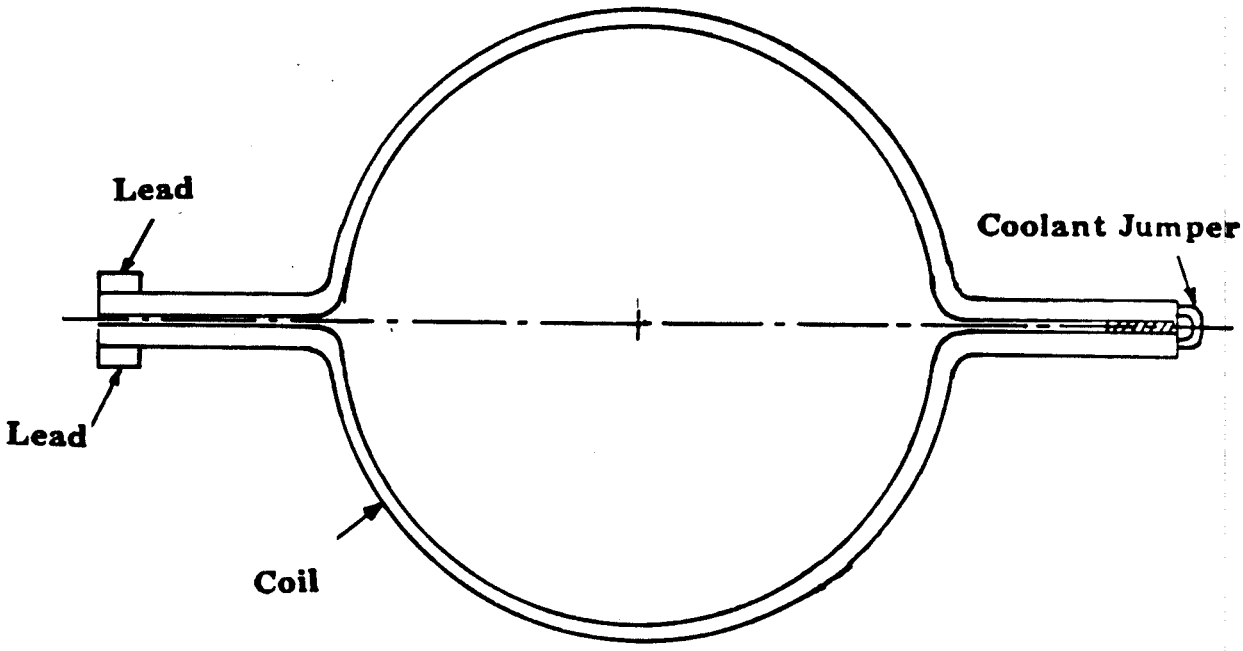

Figure 6.1-2
Control Coil Configuration, [FEDC]

6.2 Start-up and Vertical Stability

The plasma scenario and the requirements on the PF system are of prime concern and an area of on-going study. However, preliminary estimates of start-up have been performed with the TSC code (*op cit.*, Jardin) and also with successive static equilibrium code "snapshots" (using the FEDC code developed by Strickler).

The results of two simulations with the dynamic TSC code are shown in Figure 6.2-1. In the left figure, the plasma is limited on the inboard side and its current increases from 500 kA to 9.5 MA. The vacuum vessel is simulated by a large number of passive conducting loops of square cross section. The nested contours within the vessel are the outer flux surfaces of the plasma at successive times. The figure on the right is similar except that the plasma is bounded by the outboard limiter. In this case, the plasma current increases from 200 kA to 10 MA in three seconds.

The elongated plasma in CIT is vertically unstable with a displacement growth rate on the microsecond time scale if no passive or active stabilization measures are employed. The vacuum vessel (1.5 cm thick) alone has been shown to be able to provide sufficient passive stabilization to slow this growth rate to 16.7 ms. This is slow enough to allow control coils to be activated with reasonable power levels to control this unstable mode. Estimates indicate that coils I1 would require about 20 MVA to perform this function with current required in the range of 30 kA/cm of plasma displacement from the midplane. Note that coil excitation is antisymmetric with respect to the z=0 plane to perform this function.

No additional passive stabilizing plates are currently planned in the baseline design. However, some simulations for cases of this type have been performed. Figure 6.2-2 shows a case with aluminum stabilizing plates just outside the vacuum vessel. In this case, the growth rate is slowed to about 350 ms. This would allow a reduction of about a factor of 20 in the power used by the control coils since it relieves their response time requirement. If plates of this type are used they would probably have to be connected antisymmetrically to prevent their ability to shield the plasma from the symmetric field changes required for start-up.

Studies in this area are continuing. The availability of this code will not only allow adequate simulation of plasma development and control, but will allow better specifications to be developed for the PF current scenarios required. In a compact design of this type, this is of prime importance because the current profiles have a first-order impact on the primary PF coil design variables of stress and temperature.

CIT Current Start-up

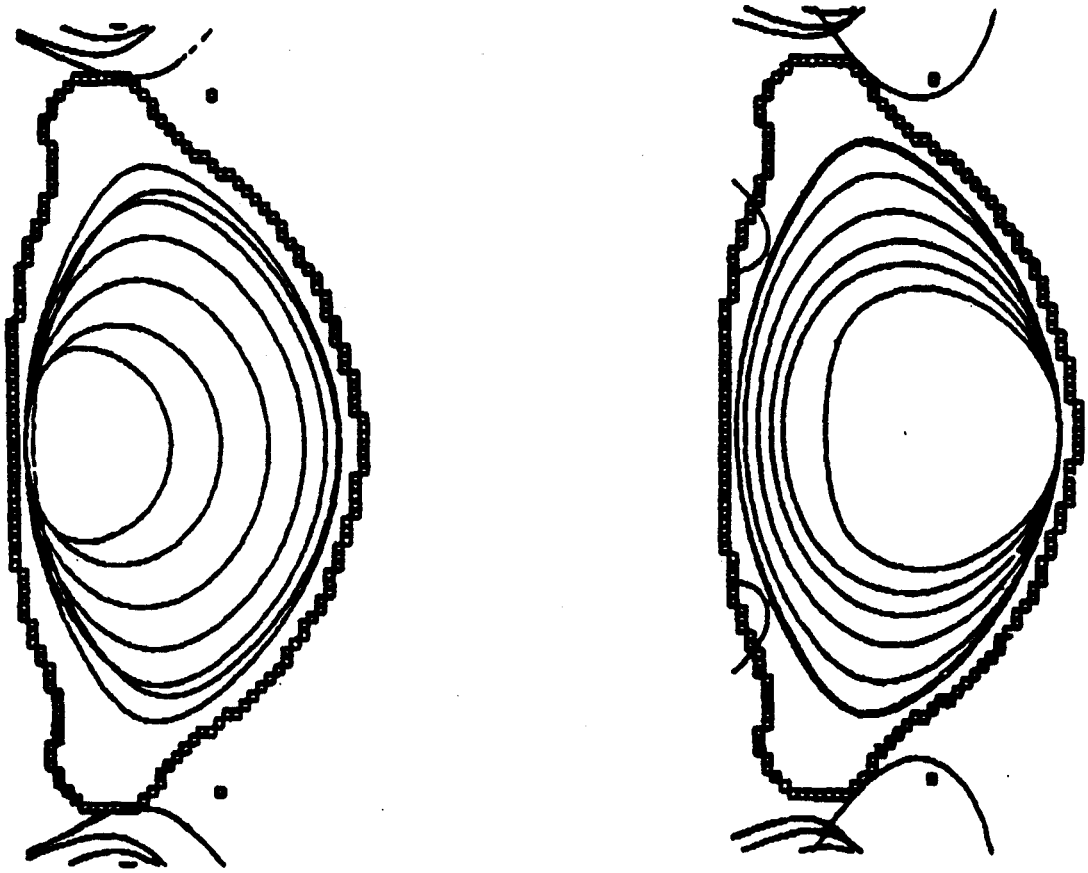

500 kA to 9.5 MA **200 kA to 10 MA**

Figure 6.2-1
CIT Plasma Start-up on either the Inboard or Outboard Limiter as Generated by the TSC Code, [PPPL]

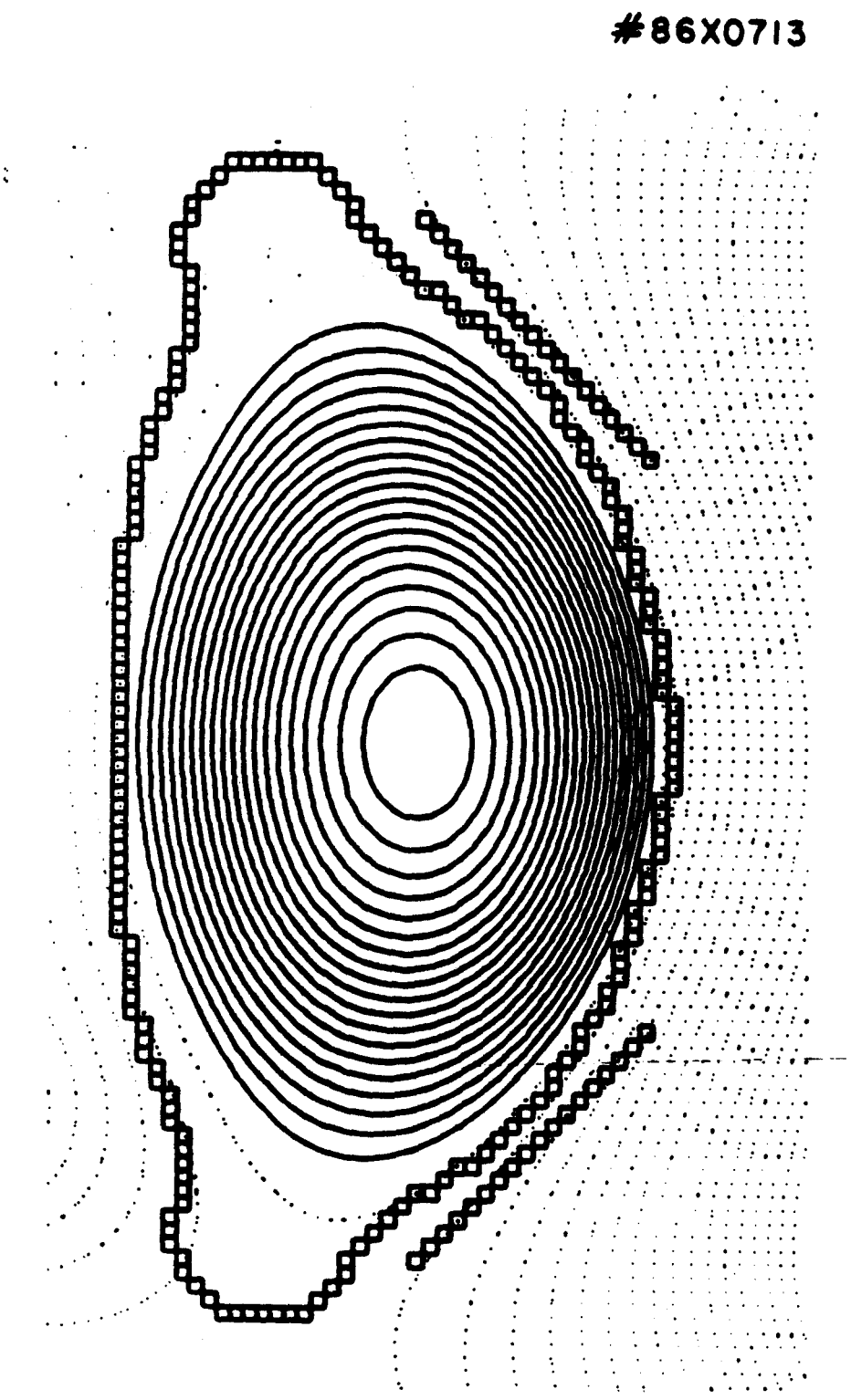

Figure 6.2-2
Simulation of Plasma Vertical Stability with Aluminum Plates Added to Slow Growth Rate, [PPPL]

Appendix A
R and D Requirements

This section presents an outline of seven areas in which R and D is required en route to final design of the CIT PF coil system.

1) Winding Component Tests

a) Brief Statement of Problem

The CIT PF coils will cycle from liquid nitrogen temperature to about 373 K. Cooling rate limitations will probably require a winding pack construction with an exposed conductor. The individual conductor and insulation (turn/turn and coil to ground) components as well as simulated winding packs must be tested to verify mechanical properties and electrical characteristics relative to design values. Because of the high mechanical loading, complex loading pattern, and difficulty of predicting mechanical performance of composites, an iterative process involving design evolution and data accumulation will be required.

b) Proposed R and D

Winding bundle components must be subjected to repeated mechanical loading to allow development of winding pack configurations which can simultaneously provide adequate mechanical support and voltage-withstand capability. A number of model variations will be necessary in relatively long duration tests to accumulate sufficient cycles to define design allowables. The tests must simulate loading, electrical and thermal characteristics in sufficient detail to confirm expected performance within operating limits, as well as test to failure to determine relative safety.

2) Central Solenoid Leads

a) Brief Statement of Problem

The central solenoid leads will be required to carry currents in the range of 20,000 to 100,000 amperes and operate in a pulsed mode with essentially twice the number of cycles experienced by the TF coils. They will cycle between liquid nitrogen temperature (80 K) and about 373 K for each pulse. Furthermore they must carry these high currents in the presence of about 23 T since they will run in the bore of the central solenoid stack. The solenoid is expected to have two separately excited sections; hence, four leads are required.

b) Proposed R and D

Perform electrical and mechanical tests on four lead configurations. Establish static and fatigue load-carrying ability under simulated full-load conditions. Establish operating limits in terms of full current, simulated voltage conditions. Confirm expected temperature rise and cooldown performance. Modify leads as required and retest. Analyze results and relate to performance specifications for leads to verify final design.

3) PF Ring Coil Leads

a) Brief Statement of Problem

The PF ring coil leads will be required to carry currents in the range of 20,000 to 100,000 amperes and operate in a pulsed mode with essentially twice the number of cycles experienced by the TF coils. They will cycle between liquid-nitrogen temperature (80 K) and about 373 K for each pulse. They will be external to the TF coils, but may be expected to have circuitous paths to reach the main buswork because of restrictions from other components. They are often subject to large deflections during machine operation and are typically one of the weak links in machine availability.

In addition there will be control coils (e.g., for vertical stabilization or separatrix control) within the TF coil bore. The leads to these coils will experience the TF of up to 11 T and are, therefore, highly loaded.

b) Proposed R and D

Perform electrical and mechanical tests on six lead configurations. Establish static and fatigue load-carrying ability under simulated full-load conditions. Establish operating limits in terms of full current, simulated voltage conditions. Confirm expected temperature rise and cooldown performance. Modify leads as required and retest. Analyze results and relate to performance specifications for leads to verify final design.

4) Central Solenoid Joints

a) Brief Statement of Problem

The central solenoid will have a bore of about 0.5 m diameter and will be repeatedly cycled between about +23 T and -22 T. It will be cooled to liquid nitrogen temperatures between pulses. It will use a developmental conductor consisting of a copper/steel laminate.

A pancake type of winding configuration is envisioned and will require two different types of joints: one at the inner radius and one at the outer. The mechanical and electrical performance of these joints is critical to the mechanical integrity and energy dissipation in this system.

b) Proposed R and D

Perform electrical and mechanical tests on candidate joint configurations. Establish static and fatigue load carrying ability under simulated full load conditions. Establish operating limits in terms of full current, simulated voltage conditions. Confirm expected temperature rise and cooldown performance. Modify joints as required and retest. Analyze results and relate to performance specifications for joints to verify final design.

5) PF Ring Coil Joints

a) Brief Statement of Problem

The PF ring coils will be the largest liquid nitrogen coils constructed to date. There will be at least three different types of conductor/winding configurations. A high strength copper or reinforced copper conductor is envisioned. Materials will not be available in sufficient lengths to allow coil fabrication without joints, hence a joint development program is essential.

In addition there will be control coils (e.g., for vertical stabilizaton or separatrix control) within the TF coil bore. These coils will also require joint development and design verification.

b) Proposed R and D

Perform electrical and mechanical tests on candidate configurations. Establish static and fatigue load carrying ability under simulated full load conditions. Establish operating limits in terms of full current, simulated voltage conditions. Confirm expected temperature rise and cooldown performance. Modify joints as required and retest. Analyze results and relate to performance specifications for joints to verify final design.

6) Central Solenoid Prototype

a) Brief Statement of Problem

The central solenoid has an inherently less complex shape than the TF coils, but

is more highly loaded because of the 23 T operating point and is subjected to cyclic operation. It will have about a 0.5 m bore and will be the largest coil ever built at this field level. It will require an advanced conductor configuration consisting of a steel-reinforced copper laminate. This will require development and verification of fabrication and assembly methods followed by verification of expected performance.

b) Proposed R and D

The prototype coil will be scaled in height and diameter (not necessarily in the same proportion) in a manner which will allow testing with existing power supplies and which will maximize manufacturing experience and test data. The goals will be to demonstrate manufacturability, tolerances, reliability, electrical performance, thermal performance, and QC techniques. In so far as possible the coil will operate at the operating current and field level, perhaps with a reduced pulse length. A test schedule with a reasonably large number of operations will be selected to demonstrate satisfaction of specifications.

7) PF Ring Coil Prototype

a) Brief Statement of Problem

The PF ring coils will be large diameter, pulsed, liquid nitrogen cooled coils wound with a high strength or reinforced copper conductor. Cooldown limitations will require an open winding configuration with some direct exposure of conductor to coolant. The winding, QC, and testing of coils of this type is essential to design verification.

The system will also use control coils internal to the TF. Because they are "trapped" in this fashion, fabrication of a prototype to test manufacturing methods and verify performance is necessary.

b) Proposed R and D

The prototype coils will be scaled in height and diameter (not necessarily in the same proportion) in a manner which will allow testing with existing power supplies and which will maximize manufacturing experience and test data. The goals will be to demonstrate manufacturability, tolerances, reliability, electrical performance, thermal performance, and QC techniques. In so far as possible the coil will operate at the operating current and field level, perhaps with a reduced pulse length. A test schedule with a reasonably large number of operations will be selected to demonstrate satisfaction of specifications.

Appendix B
Impact of Selected Changes in Machine Characteristics

In this section, the results of a sensitivity study of the volt-seconds requirements for the PF system and the characteristics of the overall system are discussed. The purpose of the study is to gain insight into the tradeoffs between the different systems.

The engineering and the physics constraints are kept constant in the parametric study. The average stresses and the peak temperatures, the gaps, the plasma current and the figure of merit for ignition ($B^2a/q^* = 25$ T^{2}m) are held constant unless otherwise specified. With these parameters specified, the machine is well determined. Only by changing some of the specifications can the machine be varied. Results imply that:

1. Changing from a TF coil design with a press to one with a self-supported TF system requires a major radius increase of about 14 cm.

2. Central solenoid stresses can be decreased by 10% or 20% with a net major radius change of about 3 cm or 5 cm, respectively.

3. Additional volt seconds (beyond the change required for increased plasma inductive V·s) of 1.1 and 2.3 V·s can be achieved with a net major radius change of 3 cm and 5 cm, respectively (note: no change in solenoid stress).

4. Pulse length flattop times can be increased by 1.4, 3.3, and 5 s with an increase in major radius of about 3, 5, and 9 cm, respectively.

Table B-1 shows the present baseline case (press) for the CIT. R is the plasma major radius, B_T is the field on axis, n_o is the plasma density, E_{TF}, P_{TF}, W_{TF} and j_{throat} are the stored energy, the power required at 80 K, the weight of the toroidal field magnet and the current density in the toroidal field magnet; T_{peak}, σ_{hoop} and $F_{Inconel}$ are the peak temperature, the compressive hoop stresses and the ratio of Inconel to copper in the toroidal field coil; E_{OH}, P_{OH} and σ_{OH} are the stored energy, resistive power and stresses in the central solenoid stack; and E_{EF}, P_{EF}, W_{EF} and MA_{EF} are the energy, power, weight and MA-turn of the ring coils. The hoop stresses in the composite in the throat of the toroidal field magnet (σ_{hoop}) are estimated to be 440 MPa, which result in a Inconel/copper ratio of about 0.4 in the throat. The ratio between the copper and the Inconel is calculated using an approximate approach that includes the plastic behavior of the copper. More detailed calculations indicate that the hoop stresses are 550 MPa, and the Inconel/copper ratio may have to increase further. The stresses in the central solenoid

(σ_{OH}) do not include the vertical component. It should be noted that the purpose of the parametric code is not to calculate the numbers with great accuracy, but to be precise enough to show trends.

Also shown in Table B-1 is the effect of completely removing the press. This space may then be occupied by the poloidal field coils. The net effect of removing the press and relying on a self-supported TF magnet is an increase in size of about 14 cm. The consequences of removing the press on the poloidal field system, in particular with respect to the divertor coils, needs to be explored.

Table B-2 shows the variation of the baseline design when the stresses of the central solenoid are decreased. The stresses can be decreased by 10% with a net increase in machine size of 3 cm and by 20% with an increase of 5 cm. It should be noted that the stresses have been reduced by increasing the size of the central solenoid without varying the copper/steel ratio, thus resulting in lower temperatures (and also lower current density). If the temperature limit were to be fixed, the increase in machine size would be 2 cm for a 10% decrease in stress. This results in an increase in the inconel/copper ratio in the central solenoid.

The plasma volt-second requirement is discussed next, followed by the estimated impact of additional volt seconds on machine size. The plasma current is 10 MA at full β. It is, however, only 9.8MA at the lower β, but same $q(a)$. The external volt seconds are calculated using Hirshman and Neilson (Phys Fluids **29** 3 (1986)):

$$L_{external}(\epsilon) = \mu_o R_o \frac{a(\epsilon)(1-\epsilon)}{1-\epsilon+b(\epsilon)\kappa}$$

$$a(\epsilon) = (1 + 1.81\sqrt{\epsilon} + 2.05\epsilon)\log\left(\frac{8}{\epsilon}\right) - (2 + 9.25\sqrt{\epsilon} - 1.21\epsilon)$$

$$b(\epsilon) = 0.73\sqrt{\epsilon}\left(1 + 2\epsilon^4 - 6\epsilon^5 + 3.7\epsilon^6\right)$$

For CIT, $\Phi_{external} = L_{external} I_p = 10.9$ Vs.

The internal volt seconds, on the other hand, depend on the current profile of the plasma. The current profile depends on the time history. Estimates for the internal inductance vary from $l_i = 1.15$ through $l_i = 1.5$, the larger value for peak current profiles

(just prior to a sawtooth). Then the estimate of the internal volt seconds ranges from $\Delta\Phi_{Internal} = 8.85$ to $\Delta\Phi_{internal} = 11.5$ Vs.

The resistive volt second requirements are harder to determine, but fortunately are a relatively small part of the total volt second requirement. Using approximations, the V·s for start-up and heating is 3.1 V·s. This estimate could vary, specially if sawtooth activity is included in the model. W. Houlberg's code estimates that about $3.8 - 4$ V·s are required for the plasma current start-up (without heating phase).

From all the requirements, it can then be seen that for the high beta plasma, the requirement is 25.5 V·s (10.9 + 11.5 + 3.1), leaving 0.7 V·s for the heating phase and burn (assuming the baseline specification of 26.2 V·s). This is likely to be inadequate; hence it will be necessary to increase the volt-second capability of the PF system in order for the machine to fulfill the physics mission. Table B-3 shows the estimated variation in the machine design if the volt-second requirement increases. The increase in machine size with each additional volt second provided is about 3 cm. It should be noted that the incremental volt-second increase is beyond the increase necessary for the change in plasma inductive volt seconds; that is, in the second column there is 1 volt second provided beyond what the unaltered parametric code would predict as necessary for the inductive and resistive volt seconds. The extra drive may be required to provide additional resistive volt seconds, or to produce a full current, low beta plasma, when the contribution of the vertical field to the plasma current is smaller. If the requirement of a full plasma current at low plasma beta is insisted upon, then the required drive from the PF system increases by an estimated 2 volt seconds. Table B-3 shows that an additional 1.1 V·s could be achieved with a major radius increase of 3 cm and that an additional 2.3 V·s could be provided with an increase of 5 cm.

Table B-4 shows the variation in machine size as the pulse length of the machine is increased. This is accomplished by both decreasing the average current density and by increasing the copper/inconel ratio in the throat of the toroidal field coil. This tradeoff is important for the poloidal field system in that it shows the consequence of increased time for start-up, decreasing the ramp rates and the power supply requirements.

Table B-1. CIT- Inconel TF Coil; Press vs Self-supported TF Coils

	press	self-supported
A	2.7	2.81
R (m)	1.22	1.36
B_f (T)	10.4	10.1
I_p (MA)	10.2	10.1
$n_{o,M.}$ (10^{20} m^{-3})	9.0	7.82
τ_e (s)	0.333	0.384
E_{TF} (GJ)	0.9	1.06
$P_{TF,dis}$[††] (MW)	69	86
W_{TF} (ktonnes)	0.193	0.237
j_{throat} (kA/cm^2)	8.39	5.72
τ_{flat} (to 350 K; s)	3.76	4.15
T_{peak} (12 τ_e; K)	348	345
$\sigma_{vertical}$ (MPa)	0.0	255
σ_{hoop} (MPa)	442	327
$f_{Inconel}$	0.397	0.687
$E_{OH,max}$ (GJ)	0.513	0.623
$P_{OH,max,dis}$[†††] (MW)	265	292
$\sigma_{OH,max}$ (MPa)	0.342	0.356
E_{EF} (GJ)	0.695	0.652
$P_{EF,dis.}$[†††] (MW)	0.116	0.112
W_{EF} (ktonnes)	0.226	0.218
MA_{EF} (MA turns)	35.1	31.9

[††] At liquid nitrogen temperature.

[†††] At room temperature.

Table B-2. CIT- Inconel TF Coil; Stress Variation in Central Solenoid

$\kappa = 1.8$, $I_p = 10$ MA

A	2.7	2.72	2.74
R (m)	1.22	1.25	1.28
B_f (T)	10.4	10.3	10.3
$n_{o,M.}$ (10^{20} m^{-3})	9.0	8.77	8.53
τ_e (s)	0.333	0.342	0.352
E_{TF} (GJ)	0.90	0.93	0.95
P_{TF} †† (MW)	81	81	81
W_{TF} (ktonnes)	0.193	0.199	0.205
j_{throat} (kA/cm^2)	8.39	8.26	8.14
τ_{flat} (to 350 K; s)	3.93	4.06	4.18
T_{peak} (12 τ_e; K)	348	346	345
$\sigma_{vertical}$ (MPa)	0.0	0.0	0.0
σ_{hoop} (MPa)	431	432	432
$f_{Inconel}$	0.375	0.377	0.377
$E_{OH,max}$ (GJ)	0.521	0.506	0.496
$P_{OH,max,dis}$ †††(MW)	269	242	222
$\sigma_{OH,max}$ (GPa)	0.347	0.31	0.28
E_{EF} (GJ)	0.694	0.678	0.663
$P_{EF,dis}$ †††(MW)	116	114	113
W_{EF} (ktonnes)	0.225	0.222	0.22
MA_{EF} (MA turns)	35.0	34.2	33.4

†† At liquid nitrogen temperature.

††† At room temperature.

Table B-3 CIT- Inconel TF Coil; Effect of Additional Volt Seconds

$\kappa = 1.8$, $I_p = 10$ MA

$\Delta\Phi_{add'l}$ (Vs)	0	1.1	2.3
A	2.7	2.72	2.74
R(m)	1.22	1.25	1.28
B_f (T)	10.4	10.3	10.3
$n_{o,M.}(10^{20}$ m$^{-3})$	9.0	8.77	8.53
τ_e(s)	0.333	0.342	0.352
MI_{MIRNOV}	3.58	3.53	3.5
E_{TF} (GJ)	0.90	0.93	0.95
P_{TF}[††] (MW)	81	81	81
W_{TF} (ktonnes)	0.193	0.199	0.205
j_{throat} (kA/cm^2)	8.39	8.26	8.14
τ_{flat} (to 350 K;s)	3.93	4.06	4.18
T_{peak} (12 τ_e; K)	348	346	345
$\sigma_{vertical}$ (MPa)	0.0	0.0	0.0
σ_{hoop} (MPa)	431	432	432
$f_{Inconel}$	0.375	0.377	0.377
$E_{OH,max}$ (GJ)	0.521	0.555	0.605
$P_{OH,max,dis}$[†††](MW)	269	266	270
$\sigma_{OH,max}$ (GPa)	0.347	0.347	0.347
E_{EF} (GJ)	0.694	0.678	0.663
$P_{EF,dis}$ [†††](MW)	116	114	113
W_{EF} (ktonnes)	0.225	0.222	0.22
MA_{EF} (MA turns)	35.0	34.2	33.4

[††] At liquid nitrogen temperature.

[†††] At room temperature.

Table B-4. CIT- Inconel TF Coil; Size vs Change in Pulse Length

$\kappa = 1.8$, $I_p = 10$ MA

A	2.7	2.72	2.75	2.76
R (m)	1.22	1.25	1.28	1.31
B_f (T)	10.4	10.3	10.3	10.2
$n_{o,M.}$ (10^{21} m^{-3})	6.01	5.83	5.69	5.51
τ_e (s)	0.333	0.342	0.353	0.367
E_{TF} (GJ)	0.9	0.93	0.96	0.99
P_{TF} †† (MW)	75	67	62	59
W_{TF} (ktonnes)	0.193	0.204	0.208	0.216
j_{throat} (kA/cm^2)	8.38	7.77	7.13	6.68
τ_{flat} (to 350 K; s)	3.95	5.35	7.24	8.94
T_{peak} (12 τ_e; K)	347	264	207	180
$\sigma_{vertical}$ (MPa)	0.0	0.0	0.0	0.0
σ_{hoop} (MPa)	431	404	376	357
$f_{Inconel}$	0.375	0.319	0.261	0.221
$E_{OH,max}$ (GJ)	0.521	0.534	0.556	0.574
$P_{OH,max,dis}$ ††† (MW)	271	272	275	274
$\sigma_{OH,max}$ (MPa)	348	346	349	344
E_{EF} (GJ)	0.694	0.677	0.663	0.65
$P_{EF,dis}$ ††† (MW)	116	114	113	111
W_{EF} (ktonnes)	0.225	0.222	0.22	0.217
MA_{EF} (MA turns)	35.0	34.2	33.3	32.5

†† At liquid nitrogen temperature.

††† At room temperature.